

# Open Research Online

---

The Open University's repository of research publications and other research outputs

## An electrophysiological study of the hyperstriatal visual projection area in the young chicken.

### Thesis

How to cite:

Denton, Christopher John (1979). An electrophysiological study of the hyperstriatal visual projection area in the young chicken. PhD thesis The Open University.

For guidance on citations see [FAQs](#).

© 1978 The Author

Version: Version of Record

Link(s) to article on publisher's website:  
<http://dx.doi.org/doi:10.21954/ou.ro.0000fc7d>

---

Copyright and Moral Rights for the articles on this site are retained by the individual authors and/or other copyright owners. For more information on Open Research Online's data [policy](#) on reuse of materials please consult the policies page.

---

[oro.open.ac.uk](http://oro.open.ac.uk)

D 38919/82

UNRESTRICTED

AN ELECTROPHYSIOLOGICAL STUDY OF THE HYPERSTRIATAL  
VISUAL PROJECTION AREA IN THE YOUNG CHICKEN.

Christopher John Denton, BSc. (Hull)

Submitted in part fulfilment of the requirements for the degree of Doctor of Philosophy at the Open University.

Discipline : Biology      Date of submission : 18 December 1978

Date of submission: 10-7-78

Date of award: 28-2-79

ProQuest Number: 27777458

All rights reserved

INFORMATION TO ALL USERS

The quality of this reproduction is dependent on the quality of the copy submitted.

In the unlikely event that the author did not send a complete manuscript and there are missing pages, these will be noted. Also, if material had to be removed, a note will indicate the deletion.



ProQuest 27777458

Published by ProQuest LLC (2020). Copyright of the Dissertation is held by the Author.

All Rights Reserved.

This work is protected against unauthorized copying under Title 17, United States Code  
Microform Edition © ProQuest LLC.

ProQuest LLC  
789 East Eisenhower Parkway  
P.O. Box 1346  
Ann Arbor, MI 48106 - 1346

ABSTRACT

The structural organisation of avian visual pathways is discussed, and particular reference is made to the retino-thalamo-hyperstriatal projection.

The appearance of the young (1-2 week old) chicken forebrain in Nissl-stained transverse sections is discussed, and an interpretation of the structure and nomenclature of the hyperstriatal complex is presented and compared with the interpretations found in the literature.

An analysis is then presented of field and single unit potentials recorded from the hyperstriatal complex of the 1-2 week old chicken following electrical stimulation of the contralateral and ipsilateral retina and optic papilla. The retino-hyperstriatal projection was found to be topographically organised - thus, the inferior retina was found to project to the posterior regions of the Wulst, and the superior retina to anterior regions of the Wulst.

A complex dorsoventral lamination of visual inputs to the hyperstriatum was revealed. Stimulation of the contralateral anterior retina resulted in early field potentials (mean peak latency, MPL:  $14.3 \pm 0.7$  mS) located in the hyperstriatum intercalatus accessorium (IHA), followed by later activity spreading throughout superficial regions of the hyperstriatum accessorium (HA) (MPL:  $18.5 \pm 1.6$  mS). Similarly, stimulation of the contralateral posterior retina resulted in early potentials (MPL:  $14.9 \pm 1.0$  mS) in IHA, and late potentials

(MPL:  $17.2 \pm 0.9$ ms) spreading throughout deep regions of HA. It was concluded that IHA was the main visual thalamo-receptive lamina within the hyperstriatal complex.

Stimulation of the ipsilateral optic papilla resulted in a single field potential response (MPL:  $21.8 \pm 3.0$ ms), located in ventral HA, overlapping ventral areas of the contralaterally responsive region of HA.

The responses of 220 single cells recorded from the hyperstriatum following electrical stimulation of the contralateral and ipsilateral optic papilla were analysed. 123 (56%) of these cells responded to the stimulation. Within the responsive sample, four classes of cell were identified: 85% responded exclusively to contralateral stimulation; 3% responded exclusively to ipsilateral stimulation; 8% responded to both contralateral and ipsilateral stimulation with different latencies (independent binocular); and 4% responded to both contralateral and ipsilateral stimulation with identical latencies (coincident binocular). The single cell responses showed excellent spatiotemporal correlation with the evoked field potentials.

Comparison of these results with those obtained by other workers from the owl and pigeon indicated some similarities between the organisation of the thalamofugal pathway in chicken and owl, but also that at present, no single species should be assumed to be typical of the avian class.

DECLARATION

None of the material contained in this thesis has been previously submitted for a degree or other qualification to this or any other university or institution.

The experimental work and its interpretation in this thesis are entirely my own.

## ACKNOWLEDGEMENTS

I should like to thank my supervisor, Dr G.S.Einon (Lecturer, Biology Department, O.U.) for his many helpful comments and suggestions regarding the draft of this thesis; and Professor S.P.R.Rose (Biology Department, O.U.) for his encouragement during the completion of the written work.

I am deeply indebted to Mr H.Parkin (Technician, Biology Department, O.U.) for constructing and programming the Motorola G6800 microprocessor; for developing programmes for use with the Nova 820 minicomputer; and for general technical assistance and many hours of discussion around matters mathematical, physical and mystical pertaining to the nature and occurrence of voltage gradients and surfaces within biological tissue.

I should also like to express my gratitude to Mr N.Heap (Scientific Officer, Electronics Department, O.U.) for assisting myself and Mr Parkin with computing problems, and for the many hours of use of the Hewlett Packard Graphic Plotter.

Finally, a few inadequate words to thank Mr T.Cassidy (Technician, Biology Department, O.U.) for many things, not least his moral and technical support during the arduous initial task of constructing a neurophysiological laboratory at the Open University.

<u>CONTENTS</u>	<u>PAGE</u>
<u>SECTION A : INTRODUCTION</u>	1
CHAPTER A1: PREVIEW	4
CHAPTER A2: AVIAN VISUAL PATHWAYS	8
CHAPTER A3: THE THALAMOFUGAL PATHWAY	13
<u>SECTION B : EXPERIMENTAL PREPARATION</u>	27
CHAPTER B1: ANESTHESIA AND PARALYSIS	29
CHAPTER B2: GENERAL SURGERY	33
CHAPTER B3: STEREOTAXIS	38
CHAPTER B4: PREPARATION FOR STIMULATION AND RECORDING	44
<u>SECTION C : HISTOLOGY</u>	47
CHAPTER C1: METHODS	50
CHAPTER C2: THE CHICKEN FOREBRAIN IN NISSL SECTIONS	52
<u>SECTION D : ELECTRICALLY EVOKED FIELD POTENTIALS</u>	72
CHAPTER D1: INTRODUCTION	76
CHAPTER D2: METHODS	81
CHAPTER D3: GENERAL PROPERTIES OF FIELD POTENTIALS	89
CHAPTER D4: DORSOVENTRAL LAMINATION OF FIELD POTENTIALS	105
CHAPTER D5: SPATIOTEMPORAL PATTERN OF FIELD POTENTIALS	122
CHAPTER D6: DISCUSSION	149
<u>SECTION E : ELECTRICALLY EVOKED SINGLE UNITS</u>	156
CHAPTER E1: INTRODUCTION	159
CHAPTER E2: METHODS	161
CHAPTER E3: SINGLE UNIT POTENTIALS	164
CHAPTER E4: DISCUSSION	182
<u>SECTION F : OVERVIEW</u>	187
<u>SECTION G : REFERENCES</u>	199



<u>LIST OF ILLUSTRATIONS</u>	<u>PAGE</u>
FIGURE A1 : EXTERNAL MORPHOLOGY OF THE CHICKEN BRAIN	5
A2 : T.S. CHICKEN HYPERSTRIATUM	7
A3 : PRIMARY RETINAL PROJECTIONS	11
A4 : SECONDARY TECTAL PROJECTIONS	11
A5 : SECONDARY THALAMIC PROJECTIONS	16
A6 : EFFERENT PROJECTIONS OF THE WULST	16
A7 : SUMMARY OF THALAMO-HYPERSTRIATE RELATIONSHIPS	19
A8 : PIGEON HYPERSTRIATUM	23
A9 : OWL HYPERSTRIATUM	23
 FIGURE B1 : DRIFT OF TECTAL RECEPTIVE FIELD	 31
B2 : PHYSIOLOGICAL RECORDS	36
B3 : HEAD OF CHICKEN IN HOLDER	39
B4 : EXPERIMENTAL ARRANGEMENT	39
B5 : ORIENTATION OF HEAD IN STEREOTAXIC FRAME	40
B6 : STEREOTAXIC COORDINATES	42
 FIGURE C1 : T.S. GENERALISED AVIAN FOREBRAIN	 53
C2 : THE NOMENCLATURE OF HYPERSTRIATAL LAMINAE	56
C3 : T.S. CHICKEN WULST AT ANTERIOR 6.0	58
C4 : T.S. CHICKEN WULST AT ANTERIOR 4.0	59
C5 : CHICKEN IHA	60
C6 : THE CHICKEN FOREBRAIN IN SERIAL T.S.	63
 FIGURE D1 : TECTAL FIELD POTENTIALS	 78
D2 : LOCALISATION OF TECTAL FIELD POTENTIALS	80
D3 : BIPOLAR STIMULATING ELECTRODE	82
D4 : STIMULUS PLACEMENTS	82
D5 : PONTAMINE SKY BLUE LESIONS	85
D6 : BLOCK DIAGRAM OF STIMULATION AND RECORDING ARRANGEMENTS	88
D7 : EFFECTS OF AVERAGING	90
D8 : CONTRALATERAL FIELD POTENTIALS	94
D9 : IPSILATERAL FIELD POTENTIALS	97
D10 : DISTRIBUTION OF CONTRALATERAL RESPONSES	99

<u>LIST OF ILLUSTRATIONS (CONTINUED)</u>	<u>PAGE</u>
FIGURE D11: DISTRIBUTION OF IPSILATERAL RESPONSES	102
D12: RESPONSIVE AREA OF FOREBRAIN	103
D13: AVERAGED POTENTIALS AND DVT CONTOUR PLOT	109
D14: DVT 2309H1 DIRECT STIMULATION OF OPTIC PAPILLA	111
D15: DVT 2309H1 RETINAL STIMULATION	113
D16: DVT 0706H2 RETINAL STIMULATION	116
D17: RANGE AND MEAN PEAK LATENCY (MPL) FOR CONTRALATERAL AND IPSILATERAL POTENTIALS	118
D18: DATA OBTAINED FROM TYPICAL TRANSVERSE RECORDING GRID	124
D19: ISO CONTOUR MAP	126
D20: 7JH2 LOCATION OF TRANSVERSE GRID	129
D21: 7JH2 ISO CONTOURS GRID 2 ANTERIOR RS BIN 48-71	131
D22: 7JH2 ISO CONTOURS GRID 2 ANTERIOR RS BIN 48-92	136
D23: 7JH2 ISO CONTOURS GRID 2 POSTERIOR RS BIN 48-92	138
D24: 1605H2 LOCATION OF TRANSVERSE GRID	141
D25: 1605H2 ISO CONTOURS IPSILATERAL STIMULATION	142
D26: 2111H2 LOCATION OF SAGITTAL GRID	144
D27: 2111H2 ISO CONTOURS GRID 2 ANTERIOR RS	145
 FIGURE E1 : SAMPLE POPULATION OF UNITS	 165
E2 : FIRST SPIKE LATENCY RANGE (mS)	165
E3 : CONTRALATERAL UNIT RESPONSES	167
E4 : IPSILATERAL UNIT RESPONSES	169
E5 : FREQUENCY ATTENUATION OF CONTRALATERAL UNIT POTENTIAL	170
E6 : INDEPENDENT BINOCULAR UNIT RESPONSE	172
E7 : COINCIDENT BINOCULAR UNIT RESPONSE	172
E8 : CONTRALATERAL FIELD AND UNIT POTENTIALS	173
E9 : IPSILATERAL FIELD AND UNIT POTENTIALS	175
E10: INDEPENDENT BINOCULAR FIELD AND UNIT POTENTIALS	175

<u>LIST OF ILLUSTRATIONS (CONTINUED)</u>	<u>PAGE</u>
FIGURE E11: CORRELATION OF CONTRALATERAL FIELD AND UNIT POTENTIALS	177
E12: CORRELATION OF IPSILATERAL FIELD AND UNIT POTENTIALS	179
E13: CORRELATION OF BINOCULAR FIELD AND UNIT POTENTIALS	180
E14: PERCENTAGE OF CELL TYPES ISOLATED FROM CHICKEN, PIGEON AND BARN OWL WULST	184
FIGURE F1 : SUMMARY OF THE SPATIAL ORGANISATION OF VISUAL INPUTS TO THE AVIAN WULST	195

SECTION A : INTRODUCTION

CONTENTS OF SECTION A

CHAPTER A1 : PREVIEW

CHAPTER A2 : AVIAN VISUAL PATHWAYS

A2.1 : PRIMARY VISUAL PROJECTIONS

A2.2 : SECOND ORDER VISUAL PROJECTIONS

A2.2.1 : Accessory optic system

A2.2.2 : Tectofugal pathway

A2.2.3 : Thalamofugal pathway

CHAPTER A3 : THE THALAMOFUGAL PATHWAY

A3.1 : THE RETINO-THALAMO-HYPERSTRIATE PROJECTION

A3.2 : EFFERENT PROJECTIONS OF THE WULST

A3.3 : THALAMO-HYPERSTRIATE ORGANISATION

A3.3.1 : Anatomical studies

A3.3.2 : Physiological studies

A3.3.3 : Discussion

LIST OF ILLUSTRATIONS FOR SECTION A

- FIGURE A1 : EXTERNAL MORPHOLOGY OF THE CHICKEN BRAIN
- A2 : T.S. CHICKEN HYPERSTRIATUM
- A3 : PRIMARY RETINAL PROJECTIONS
- A4 : SECONDARY TECTAL PROJECTIONS
- A5 : SECONDARY THALAMIC PROJECTIONS
- A6 : EFFERENT PROJECTIONS OF THE WULST
- A7 : SUMMARY OF THALAMO-HYPERSTRIATE RELATIONSHIPS
- A8 : PIGEON HYPERSTRIATUM
- A9 : OWL HYPERSTRIATUM
-

## CHAPTER A1 : PREVIEW

This thesis reports the results of an experimental project designed to examine the nature and extent of the visual projection areas in the forebrain hyperstriatum of the young domestic chicken (Gallus domesticus). This area of the avian forebrain is often referred to in the literature as the visual Wulst. The chicken has been used by a number of laboratories for biochemical and behavioural experiments involving visual stimulation and the forebrain (eg. Horn et al, 1973; Rose et al, 1974; Bateson et al, 1974; Salzen et al, 1975). The precise extent of the hyperstriatal visual area, however, remains to be completely documented for this species.

The birds used for the present study were 1-2 week old, 90-110g chickens (Ross Chunky) reared normally on a 12 hour light - 12 hour dark cycle.

The data consist of electrically evoked field potential and single unit responses, recorded extracellularly from the hyperstriatum after bipolar stimulation of the contralateral and ipsilateral retinae or optic papillae.

Figure A1 illustrates the external morphology of the brain taken from a 100g chicken. Note the large, almost completely smooth forebrain hemispheres, and the laterally situated optic tecta. The approximate area sampled by electrode

penetrations is outlined on the left hemisphere of the dorsal view; the Wulst is labelled on the right hemisphere. The Wulst consists of the anterior, dorsal swelling of the forebrain hemispheres, limited medially by the midline, and laterally by a vascular channel, the vallecule. In transverse section, the Wulst includes the hyperstriatal laminae down to the lamina frontalis superior (LFS).

Vertical recording electrode penetrations were made through the hyperstriatal laminae of the Wulst, as shown diagrammatically in Figure A2. (The appearance of the chicken hyperstriatum in Nissl stained sections, and the nomenclature used in this study, are discussed in detail in Section C). Responses to stimulation of the retina or optic papilla were recorded at 0.2mm intervals along the electrode penetrations.

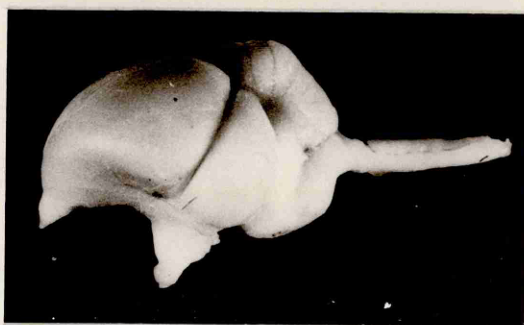
The following two chapters provide a brief review of the organisation of the avian visual system, with particular emphasis given to the thalamofugal pathway which projects to the hyperstriatum. The majority of data from the literature included in this account has been obtained from the adult pigeon (Columba livia). The anatomical nomenclature used throughout the thesis is that of Karten and Hodos (1967), unless stated otherwise. The polarity convention used in all electrical records is negative down.



FIG A1    EXTERNAL MORPHOLOGY OF THE CHICKEN BRAIN

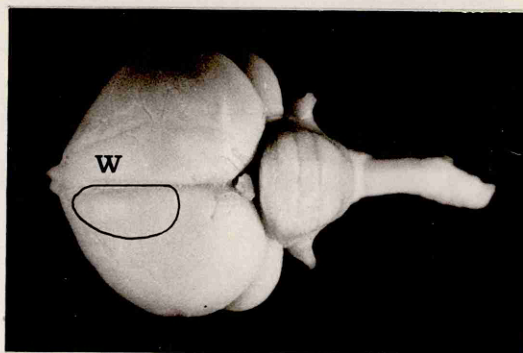
A

LATERAL



B

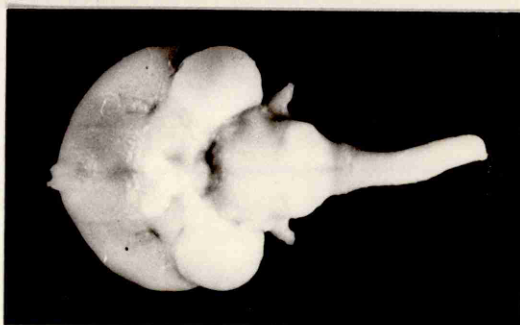
DORSAL



W - WULST

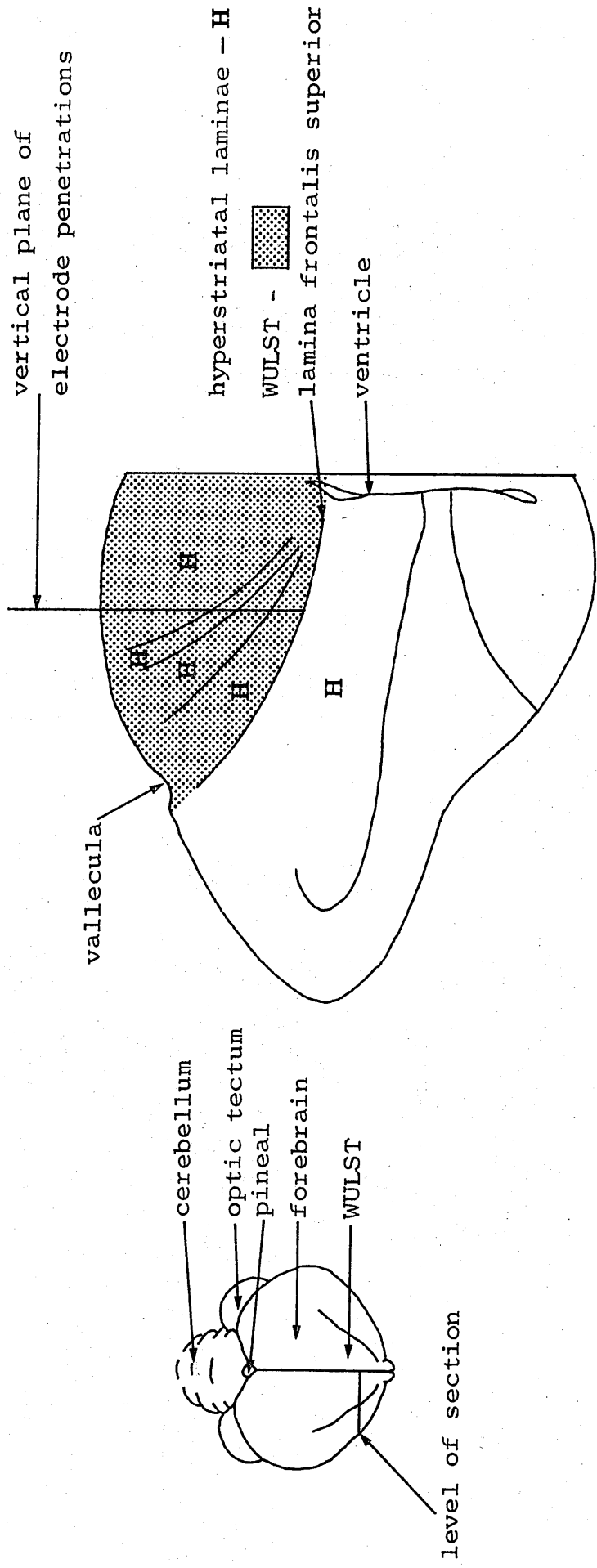
C

VENTRAL



1 cm

FIGURE A2 T.S. CHICKEN HYPERSTRIATUM



## CHAPTER A2 : AVIAN VISUAL PATHWAYS

### A2.1 PRIMARY RETINAL PROJECTIONS

The structural organisation of the avian visual system has recently been concisely documented by Cohen and Karten (1974), who remark upon the similarity of the primary retinal projections to comparable mammalian pathways (see also Karten, 1969; Webster, 1974).

The primary avian retinal projections terminate contralaterally in the area pretectalis (AP); nucleus lentiformis mesencephali (LMmc, LMpc = nucleus superficialis synencephali, Cowan et al, 1961); nucleus geniculatus pars ventralis (GLv); nucleus ectomamillaris (EM = nucleus of the basal optic root); the dorsolateral thalamic area (OPT - see A3.1); and most extensively within the tectum opticum (TeO) (Cowan et al, 1961; Karten and Nauta, 1968). (See Figure A3).

Knowlton (1964) maintained that some uncrossed fibres probably exist in the retinotectal projection, and Hunt (1974) reports the variable appearance of a few degenerating fibres in the ipsilateral thalamus after unilateral enucleation in the pigeon. Karten and Nauta (1968), however, found a total decussation in the pigeon and owl; LaVail et al (1973) could find no evidence of an ipsilateral retinotectal projection in the chicken; and Meier et al (1972) and Mihailovic et al (1974) found no evidence of ipsilateral projections to the pigeon

dorsolateral thalamus.

Anatomical (Cohen et al, 1961; DeLong and Coulombre, 1965; McGill et al, 1966a; LaVail et al, 1973) and physiological (Hamdi and Whitteridge, 1954; Bilge, 1971) studies have revealed a point to point representation of the retina upon the optic tectum in both the pigeon and chicken. There is, however, no data available for the spatial organisation of the retinal projection to the dorsolateral thalamus.

The existence of a direct retinal projection to the avian hypothalamus remains unresolved (see Cowan et al, 1961; Blumcke, 1961; Okshe, 1970; van Tienhoven, 1970; Meier, 1973). Substantial evidence, however, now exists for a topographically organised centrifugal pathway from the tectum to the retina via the nucleus isthmo opticus (ION) (Cowan et al, 1961; Cowan and Powell, 1963; McGill, 1964; McGill et al, 1966b; Holden, 1968c,d; Miles, 1970, 1971, 1972a,b,c,d; Holden and Powell, 1972; LaVail and LaVail, 1972; see Cowan, 1970, for a review). The functional significance of the centrifugal pathway remains obscure (Holden, 1966; Rogers and Miles, 1972).

## A2.2 SECOND ORDER PROJECTIONS

Three second order ascending visual projections have been described in the avian brain. These are 1. the accessory optic system, involving an efferent projection from the nucleus ectomamillaris; 2. the tectofugal pathway, involving

an efferent projection from the tectum opticum; and 3. the thalamofugal pathway, involving an efferent projection from the dorsolateral thalamus. The remainder of this chapter provides a brief introduction to the anatomical organisation of these projections.

#### A2.2.1 Accessory optic system

The ectomamillary nucleus projects bilaterally to the vestibulo-cerebellum (uvula and flocculus) (Cowan et al, 1961). This pathway constitutes the accessory optic system, and may provide a source of visual input to portions of the cerebellum involved in oculomotor control (Karten and Finger, 1976; Brauth and Karten, 1977).

#### A2.2.2 Tectofugal pathway

The efferent tectal cell layer (stratum griseum centrale, SGC) projects to the ipsilateral diencephalic nucleus rotundus (NR) (Huber and Crosby, 1929; Karten and Revzin, 1966) which in turn projects to the core of the ectostriatum of the telencephalon (Revzin and Karten, 1967; Karten and Hodos, 1970) (see Figure A4). The GLv also receives a tectal input (Karten and Revzin, 1966), but no efferents have been described for this nucleus. The ectostriatum projects to the superficial area corticoidea dorsalis (ACD) and the neostriatum (N) (Nauta and Karten, 1970); Karten (1969) and Nauta and Karten (1970) also describe a projection from the ectostriatal core to a surrounding layer of cells, the periectostriatal belt (Ep), although no details are given.

FIGURE A3 : PRIMARY RETINAL PROJECTIONS

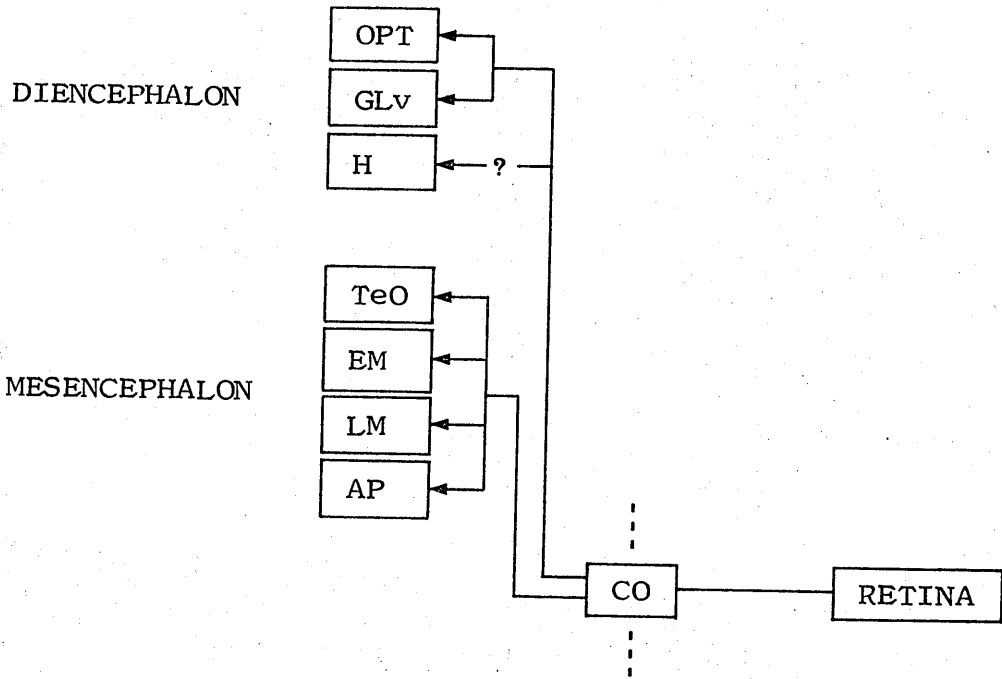
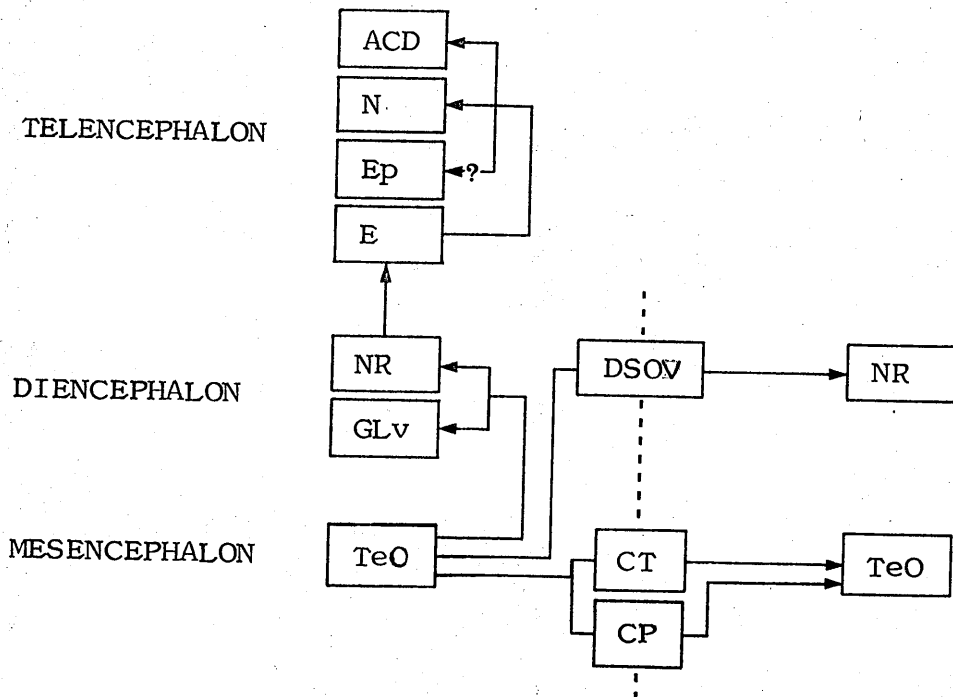


FIGURE A4 : SECONDARY TECTAL PROJECTIONS



See text for details of nomenclature

Visual cells recorded from both the NR and ectostriatum have very large receptive field sizes, ranging from 140 to 180 degrees of visual arc in diameter (Revzin, 1970; Kimberley et al, 1971), and it therefore seems unlikely that the topography of the retinotectal projection is maintained at the highest level of the tectofugal pathway (see Webster, 1974).

Inter-tectal visual fibres cross the midline (represented by the broken line in Figure A4) via the tectal and posterior commissures (CT, CP) (Karten, 1965; Robert and Cuenod, 1969a,b; Voneida and Mello, 1975). A small tectal projection to the contralateral NR has also been described (Hart, cited in Webster, 1974).

### A2.2.3 Thalamofugal pathway

The second major ascending visual pathway which projects to the telencephalon in birds consists of a bilateral projection of the dorsolateral thalamus (OPT) to the hyperstriatum of the Wulst (see Figure A5) (Powell and Cohen, 1961; Karten and Nauta, 1968). The research presented in this thesis describes the complete topography of the visual projection upon the hyperstriatum of the young chicken. The following chapter discusses the organisation of the thalamofugal projection in detail, and provides the background and rationale of the research.

## CHAPTER A3 : THE THALAMOFUGAL PATHWAY

### A3.1 THE RETINO-THALAMO-HYPERSTRIATE PROJECTION

After enucleation of the eye in the pigeon, Cowan et al (1961) traced degeneration from the optic tract to the contralateral thalamic nucleus lateralis anterior (LA); the lateral geniculate (= nucleus geniculatus lateralis pars ventralis, GLv; Karten and Hodos, 1967); and the nucleus superficialis synencephali (= nucleus lentiformis mesencephali pars magnocellularis, LMmc; Karten and Hodos, 1967). Subsequent studies revealed a more direct and extensive retinal projection to the dorsal thalamus in the pigeon and burrowing owl (Karten and Nauta, 1968; Karten et al 1973). Karten et al (1973) designated this dorsal thalamic terminal field the nucleus opticus principalis thalami (OPT). In the pigeon, several nuclei are subsumed under this heading by these authors, including the nucleus dorsolateralis anterior (DLA), nucleus dorsolateralis anterior pars lateralis (DLL), nucleus lateralis anterior (LA), and the nucleus dorsolateralis anterior pars magnocellularis (DLAmc).

Webster (1974) discusses the cytoarchitecture of the pigeon dorsolateral thalamic complex (OPT) in detail. Due to difficulties of identifying nuclear boundaries in this area, and to the lack of a complete understanding of the afferent and efferent connections of the complex, he suggests that the entire area should be divided into three regions only:



a dorsomedial complex (DM); a dorso-intermediate complex (DI); and a dorsolateral complex (DL), which may be subdivided into three fields. DL lies in the anterior region of the thalamus, and constitutes the visual thalamic area. Field 1 of DL, in Webster's analysis, is the retino-receptive area of the complex, and thus corresponds to the DLAmc of Karten et al (1973) (= dorsolateral optic nucleus, DLO, Ebbesson 1972; nucleus suprarotundus, Hirschenberger 1967).

In the owl, the OPT group reaches massive proportions, but the precise correspondence of the nuclear masses with those of the pigeon remains unclear.

The various cellular groups of OPT have been found to project to the ipsilateral Wulst via the lateral forebrain bundle (= fasciculus prosencephali lateralis, FPL; Karten and Hodos, 1967) in both the pigeon and owl (Powell and Cohen, 1961; Karten and Nauta, 1968; Karten et al, 1973), and bilaterally, via the decussatio supraoptica dorsalis (DSOD) to the contralateral Wulst (Perisic et al, 1971; Karten et al, 1973).

Electrophysiological studies recording from the hyperstriatum have confirmed this thalamofugal pathway to the Wulst, using both single unit (Revzin, 1969a,b; Perisic et al, 1971; Pettigrew and Konishi, 1976a,b) and evoked potential (Adamo and King, 1967; Perisic et al, 1971; Parker and Delius, 1972; Mihailovic et al, 1974) techniques in the pigeon and owl.

### A3.2 EFFERENT PROJECTIONS OF THE WULST

Efferent visual projections of the Wulst have been found to terminate in the ipsilateral hyperstriatum ventrale (HV) of the pigeon (Karten and Hodos, 1970) and chicken (Bradley and Horn, 1978), and in the neostriatum and Ep in the pigeon and owl (Karten and Hodos, 1970; Karten, 1971). The Ep is a source of visual evoked potentials in the pigeon (Parker and Delius, 1972). Extratelencephalic efferents project via the tractus septomesencephalicus (TSM) to the ipsilateral OPT, pretectal nuclei and TeO (Karten and Hodos, 1970; Bagnoli et al, 1977), and bilaterally to the GLv (Karten et al, 1973) in the pigeon and owl. (See Figure A6).

Thus, in the pigeon and owl, connections of the visual Wulst of the thalamofugal pathway to the periestriatal belt and optic tectum suggest the capacity for reciprocal relationships with the tectofugal pathway. However, Mark (personal communication) has been unable to demonstrate the hyperstriatal - TeO pathway in the chicken.

### A3.3 THALAMO-HYPERSTRIATE ORGANISATION

Recent anatomical and physiological studies of the visual nuclear groups of the pigeon dorsolateral thalamus, and their projections to the hyperstriatal laminae of the Wulst,

FIGURE A5 : SECONDARY THALAMIC PROJECTIONS

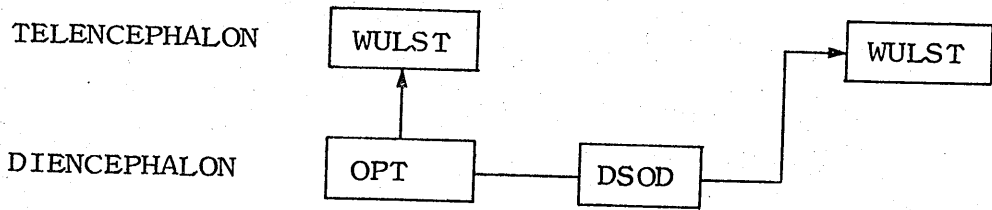
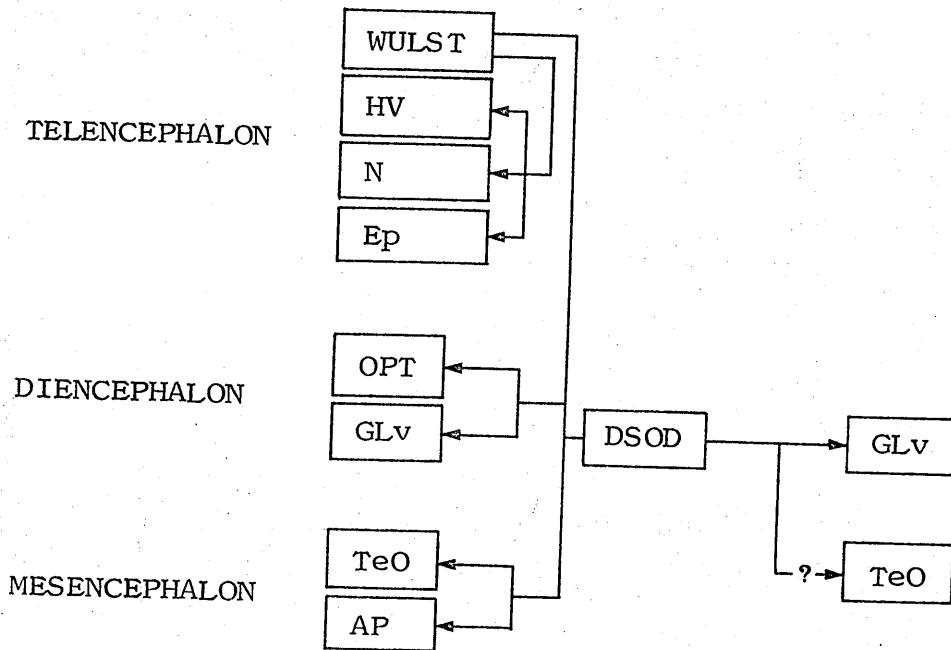


FIGURE A6 : EFFERENT PROJECTIONS OF THE WULST



See text for details of nomenclature.

have revealed a complexity of inter-relationships which exceeds that reported by Karten et al (1973). Unfortunately, division of the dorsolateral thalamus into cytologically distinct nuclear groups is difficult, and has led to possible confusions of terminology and loci. Also, as Webster (1974) points out, the phenomenon of 'sustaining collaterals' may hinder the interpretation of degeneration patterns which follow experimental lesions. (That is, a cell whose axon terminates within the region of a lesion, but which also possesses a collateral branch which terminates outside of the lesioned area, may be sustained by that same branch, and not exhibit degeneration). Thus, the relationships so far revealed between the avian thalamus and hyperstriatum may themselves be simplifications of the true networks.

#### A3.3.1 Anatomical studies

An important and relatively consistent finding has been that DLL may be functionally divided into two portions, the pars dorsalis (DLLd) and the pars ventralis (DLLv). DLLv projects to the ipsilateral Wulst via the FPL, whilst DLLd projects bilaterally to the Wulst via the FPL and DSOD (Hunt and Webster, 1972; Hunt, 1974; Meier et al, 1974; Miceli et al, 1975). Further bilateral projections were found by Hunt and Webster (1972) to arise from the nucleus of the septomesencephalic tract (nTSM = nucleus superficialis parvocellularis, SPC; Karten and Hodós, 1967). The bilaterally projecting thalamic groups may consist of two neuronal populations, one purely crossed, and the other

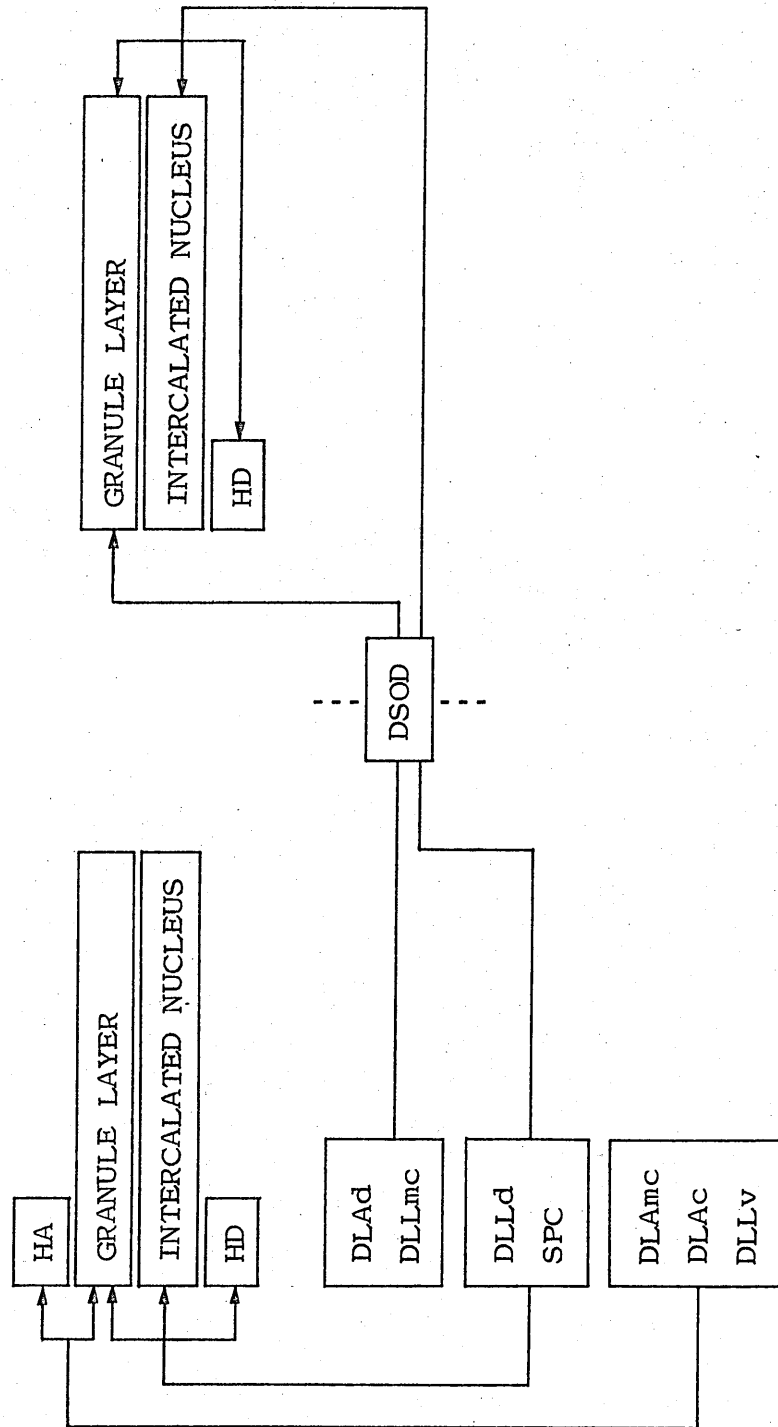
sending collateral branches via DSOD (Meier et al, 1974). In addition to the bilateral projections, ipsilateral fibres have been reported to originate in DLAmc (Hunt, 1974; Miceli et al, 1975) and caudal regions of DLA (Hunt, 1974), whilst predominantly contralateral projections arise from dorsal DLA (Hunt, 1974), DLLmc (pars magnocellularis) and dorsal DLLd (Miceli et al, 1975).

Brief mention of the cytoarchitecture of the Wulst should be made at this point, although this is discussed in detail in Section C. In transverse section, the Wulst includes three of the classically identified hyperstriatal nuclei : the superficial hyperstriatum accessorium (HA); an intercalated nucleus associated with the lamina frontalis suprema (LFM), and generally referred to as the hyperstriatum intercalatus superior (HIS); and lying below HIS, the hyperstriatum dorsale (HD).

There are conflicting reports in the anatomical literature as to the precise location of the visual terminal fields within the Wulst complex. Contrary to the findings of Karten et al (1973), which showed OPT to project only to HD and the intercalated nucleus in the pigeon and owl, Hunt and Webster (1972), Hunt (1974), and Miceli et al (1975) consider the pigeon HA to also receive ipsilateral visual thalamic input (but not contralateral) (see Figure A7).

Hunt and Webster (1972) and Webster (1974) report a rostro-

FIGURE A7 : SUMMARY OF THALAMO-HYPERSTRIATE RELATIONSHIPS



caudal topographic relationship between thalamus and Wulst, but Miceli et al (1975) found little evidence of this in the pigeon. It should be noted that these latter authors reported finding no essential differences in the thalamo-hyperstriate projections of four other species; chicken, duck (Anas platyrhynchos), herring gull (Larus argentatus), and jackdaw (Corvus monedula).

### A3.3.2 Physiological studies

Electrophysiological data confirming the primary retinal projection to the dorsal thalamus have been reported by Mihailovic et al (1974), who recorded short latency evoked potentials to electrical or photic stimulation of the contralateral eye in LA, DLAmc, DLLd and DLLv. Extracellular single unit responses to visual stimuli have been recorded from DLLd, DLLv, DLAmc (Jassik-Gerschenfeld et al, 1975, 1976) and from the general region of OPT (de Britto et al, 1975).

Recordings of single visual units have been made from the hyperstriatum of the pigeon (Revzin 1969a) - visually responsive cells were isolated in the intercalated nucleus and HA, and appeared to be orientated in columns perpendicular to the border between these two nuclei. No responses, however, were obtained from HD, although it is not clear from the report whether this nucleus was extensively sampled or not. Perisic et al (1971), recording field and unit potential responses to optic papilla

stimulation in the pigeon, provide data which confirm the existence of a bilateral visual projection to the hyperstriatum, as indicated by the anatomical studies outlined in A3.3.1. Thus, two groups of units were isolated: the first group showed response latencies of 7-39mS, and responded exclusively to stimulation of the contralateral optic papilla; the second group showed latencies of 10-86mS, and responded exclusively to stimulation of the ipsilateral optic papilla. The latencies of the latter group reflect the longer pathway recrossing the midline via DSOD. Furthermore, the units were found to show a functional lamination along vertical electrode tracks: contralateral and binocular units were isolated in HA, whilst ipsilateral units were isolated in ventral HA, the intercalated nucleus and dorsal HD. (See Figure A8).

Although Hunt (1974) found no indication of overlap of hyperstriatal inputs to account for the binocular HA region reported by Perisic et al (1971), he suggests that intratelencephalic collaterals may exist to provide such a cellular field. The available evidence does suggest that the hyperstriatal terminal field consists of a laminar organisation of thalamic inputs - Parker and Delius (1972) found a range of increasing complexity in photically evoked contralateral potential waveforms from deep to surface layers in the pigeon hyperstriatum, which they suggest are indicative of multi-layer terminations.

A complex pattern of hyperstriatal visual units was found



by Pettigrew and Konishi (1976a) in the barn owl. Binocular units predominated, and were found throughout the depth of HA. The owl intercalated nucleus contains a predominant granular layer, the nucleus intercalatus hyperstriatum<sup>o</sup> accessorium (IHA). This is a bilaminar structure, divided into the IHA externus (IHAex) and internus (IHain) (see Karten et al, 1973). Monocular units only were found in IHA, ipsilateral in IHAex, and contralateral in IHain. (See Figure A9). Further, a definite retino-Wulst topography was established. Thus, the area of the contralateral visual field sampled by the superficial retina was represented upon the anterior Wulst, whilst the area sampled by the inferior retina was represented upon the posterior margin of the Wulst; they describe a similar relationship to exist between the nasal retina and the medial Wulst, and between the temporal retina and the lateral Wulst.

Different results, however, were obtained from the burrowing owl by Revzin (1969b). Firstly, he reports visual cells to be located only in the granule layer and ventral HA. Secondly, he partially describes a topographic retino-Wulst relationship in which the inferior retina was projected upon the anterior Wulst, whereas "lateral points (of the visual field) projected to medial Wulst areas.

### A3.3.3 Discussion

Both anatomical and physiological studies clearly indicate that the hyperstriatum of the pigeon and owl contain visual

FIGURE A8 : PIGEON HYPERSTRIATUM

(AFTER PERISIC ET AL, 1971)

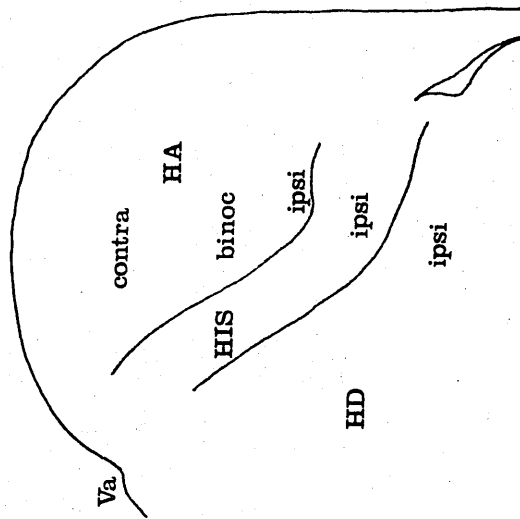
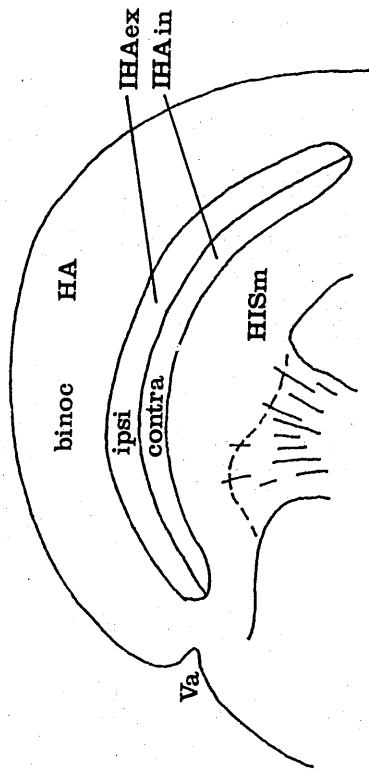


FIGURE A9 : OWL HYPERSTRIATUM

(AFTER PETTIGREW AND KONISHI, 1976)



contra : AREA OF CONTRALATERAL VISUAL INPUT

ipsi : AREA OF IPSILATERAL VISUAL INPUT

binoc : AREA OF BINOCULAR VISUAL INPUT

projection areas which receive information from both eyes, and which therefore presumably are capable of some form of binocular integration - indeed, units selective for binocular disparity have been found in the Wulst of the barn owl (Pettigrew and Konishi, 1976a,b). The precise locations of the hyperstriatal visual terminal fields, however, remain inconclusively resolved. The spatial organisation of hyperstriatal visual cells reported for the pigeon by Revzin (1969a) is not identical to that proposed by Perisic et al (1971). Revzin does not distinguish between contralateral and ipsilateral responses - and, as only one eye was stimulated, by images upon a tangent screen, one has to consider the reported visual cells as being driven by contralateral stimulation only. This may account, therefore, for the lack of visual responses in HD inferred from Revzin's study, compared to the exclusively ipsilateral characterisation of HD made by Perisic et al (1971). If there is a real lack of visual responsiveness in HD, this would suggest that its thalamic input (Karten and Nauta, 1968; Hunt, 1974; Webster, 1974) may arise from a non-visual thalamic nucleus such as the dorsolateralis anterior pars medialis (DLM), although most of the anatomical studies have suggested HD to receive visual thalamic efferents. However, a further important difference exists between the two studies: Revzin (1969a) found the major concentration of (contralateral) visual cells to be located in the intercalated nucleus, whereas Perisic et al (1971) characterised this nucleus as an exclusively ipsilateral area.

It does appear, therefore, that each investigation of the

avian hyperstriatum has suggested a different spatial organisation of the visual inputs to this region, not only between widely different species (the pigeon and owl), but also between similar (the barn owl and burrowing owl; see page 22) and identical (pigeon) experimental species. Furthermore, there exists no complete description of the topography of the visual input to the Wulst of any avian species other than Pettigrew and Konishi's study of the barn owl (and this description is not in agreement with the partial description of the visual topography of the burrowing owl Wulst provided by Revzin (1969b)). In view of the loss of topographic specificity at the telencephalic level of the tectofugal pathway, it seems likely that the telencephalic Wulst, in receipt of thalamofugal fibres, should exhibit a more well defined spatial organisation of visual input than has yet been described for the pigeon, or indeed investigated for the chicken.

Against this somewhat confusing and eclectic background of results, the research reported in this thesis was conducted in an attempt to investigate the following:

1. the identification of the visually responsive laminae of the chicken hyperstriatal complex;
2. the monocular and/or binocular organisation of the visual input to the chicken hyperstriatum;
3. the complete topography and extent of the chicken 'visual Wulst';
4. a comparison of the results obtained from the chicken with those reported in the literature for the pigeon and owl, and the nature of the inter-species differences

and/or similarities that such a comparison may reveal between the organisations of the visual input to the hyperstriatum of these species.

SECTION B : EXPERIMENTAL PREPARATION

CONTENTS OF SECTION BCHAPTER B1 : ANESTHESIA AND PARALYSIS

- B1.1 : PREMEDICATION
- B1.2 : GENERAL ANESTHESIA
- B1.3 : LOCAL ANESTHESIA
- B1.4 : PARALYSIS

CHAPTER B2 : GENERAL SURGERYCHAPTER B3 : STEREOTAXISCHAPTER B4 : PREPARATION FOR STIMULATION AND RECORDING

- B4.1 : PREPARATION OF THE EYE
- B4.2 : EXPOSURE OF THE BRAIN

LIST OF ILLUSTRATIONS FOR SECTION B

- FIGURE B1 : DRIFT OF TECTAL RECEPTIVE FIELD
- B2 : PHYSIOLOGICAL RECORDS
- B3 : HEAD OF CHICKEN IN HOLDER
- B4 : EXPERIMENTAL ARRANGEMENT
- B5 : ORIENTATION OF HEAD IN STEREOTAXIC FRAME
- B6 : STEREOTAXIC COORDINATES

## CHAPTER B1 : ANESTHESIA AND PARALYSIS

### B1.1 PREMEDICATION

Atropine sulphate was routinely administered to alleviate respiratory wetness. 24 $\mu$ g atropine sulphate/100g body weight were injected into the left pectoral muscle, as 0.1ml of a 20% solution of 0.6mg/ml atropine sulphate (Macarthys Limited).

### B1.2 GENERAL ANESTHESIA

The data reported in this thesis was obtained from birds anaesthetised with a mixture of chloral hydrate, magnesium sulphate and sodium pentobarbital (previously marketed as 'Equithesin' by Jensen-Salsbery Laboratories Incorporated). The solution was prepared using a vehicle of 20% propane-1,2-diol in 9% ethyl alcohol as follows (see Lumb and Jones, 1973; Soma, 1971):

- 42.6mg/ml - chloral hydrate
- 21.2mg/ml - magnesium sulphate
- 9.6mg/ml - sodium pentobarbital

0.3ml of this solution/100g body weight was injected into the right pectoral muscle to provide a surgical depth of anaesthesia which lasted about 1 hour. During experiments, anaesthesia was maintained by injections of 0.1ml/100g body weight every 1-2 hours.



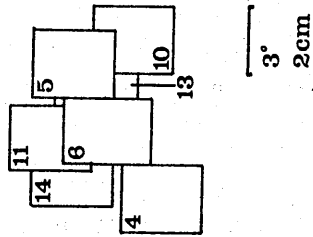
### B1.3 LOCAL ANESTHESIA

Local anesthesia of all pressure and incision points was achieved by the application of Xylocaine spray (100mg/g lignocaine, Astra Chemicals Limited). Local anesthesia of the eye lids, nictitating membrane and eye was effected by eye drops of 1% w/v amethocaine hydrochloride (Evans Medical Limited).

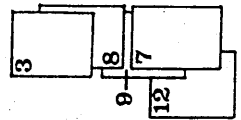
### B1.4 PARALYSIS

Techniques required for the systemic introduction of paralyzing agents were developed during preliminary experiments involving the mapping of single unit receptive fields. Drifts of up to 27 degrees of visual arc over a time of 30 minutes, including rapid movements of 10 degrees, were observed during receptive field mapping of tectal units in non-paralysed preparations. Figure B1 illustrates typical movements of a tectal field, plotted upon a tangent screen. The field position was mapped at 0.5 minute intervals over a total time of 33.5 minutes. The column of figures on the right hand side of the diagram gives the duration of the plotted positions in minutes. Ocular movements of this order of magnitude were thought to be sufficient to disturb the retinal electrode placements in the present experiments. Consequently, routine use was made of a mixture of gallamine triethiodide and d-tubocurarine hydrochloride found to effectively control eye movements by Miles (1972a). The injection was made up in 0.75% sodium chloride as follows,

FIGURE B1 : DRIFT OF TECTAL RECEPTIVE FIELD RECORDED FROM A NON-PARALYSED CHICKEN



3°  
2cm



DURATION OF FIELD POSITION (MIN)

- 1 : 2.0
- 2 : 3.0
- 3 : 1.0
- 4 : 0.5
- 5 : 2.0
- 6 : 3.0
- 7 : 1.5
- 8 : 2.0
- 9 : 2.5
- 10 : 1.5
- 11 : 4.0
- 12 : 5.0
- 13 : 2.5
- 14 : 3.0

33.5 MINUTES TOTAL

and administered intravenously:

10.00mg/ml gallamine triethiodide (Flaxedil, May and Baker Limited)

0.75mg/ml d-tubocurarine chloride pentahydrate (Sigma Chemical Company)

Single unit recordings made from both the tectum and hyperstriatum of animals paralysed with the above mixture showed no appreciable receptive field drifts over periods of up to 60 minutes.

CHAPTER B2 : GENERAL SURGERY

During surgery, the birds were kept warm by a thermostatically controlled electric underblanket (C.F. Palmer Homeothermic Blanket B140), cotton wool pads and an overhead hospital inspection lamp.

Overlying feathers were removed from the external auditory meatus to facilitate placement of the stereotaxic ear bars.

Artificial ventilation was administered routinely, whether paralyzing agents were used or not, in order to reduce brain movements. This procedure also eliminated the necessity to continue the administration of atropine sulphate to control the often profuse production of mucus in the respiratory tract. Regardless of controversy over the direction of air-flow through the parabronchi of the avian respiratory system (see Hughes, 1963), a unidirectional method of artificial ventilation has been found to be effective in adult chickens (Burger and Lorenz, 1960). A modification of this method was used in the present experiments, involving the following procedures. An incision of approximately 1cm in length was made between the last two ribs on the left flank. The posterior thoracic air sac was punctured with curved forceps introduced through the incision, and a 2cm length of plastic tubing (o.d. 5mm) inserted into the air sac. A plastic cannula (Portex PP90) was then inserted about 1cm into the trachea and gently taped to the lower beak. A

gas mixture of 95% O<sub>2</sub> - 5% CO<sub>2</sub> was passed via a reduction valve and flowmeter through the tracheal cannula. When the gas was turned on, respiratory movements were immediately reduced, or ceased altogether. The flowmeter was set to pass between 190 and 210ml/min for 90-110g birds.

Attempts were made to monitor the CO<sub>2</sub> concentration in the gas flow from the air sac, but the small volumes of gas involved made this impossible with the equipment available. Endogenous CO<sub>2</sub> build-up, however, seemed to pose no problem with the unidirectional system, and preparations remained stable for periods of 10-15 hours with no further adjustments to the ventilating flow.

The femoral vein was exposed in the left leg by either reflecting or parting the tensor faciae latae muscle (= ilio-tibialis; Saunders and Manton, 1969) of the thigh from the lateral aspect. The vein was cannulated with Portex PP25 tubing, and the paralysis mixture delivered as a continuous infusion at a rate of 0.2ml/hour for a 90-110g bird.

The monitoring of core temperature via the cloaca and rectum was achieved either by insertion of a thermistor probe connected to a chart recorder (Beckman Dynograph R411), or by insertion of a probe connected to a galvanometer display on the electric blanket control unit. The core temperature was maintained at 40-42 degrees C by adjustment of the underblanket control. (At about two weeks of age, the deep

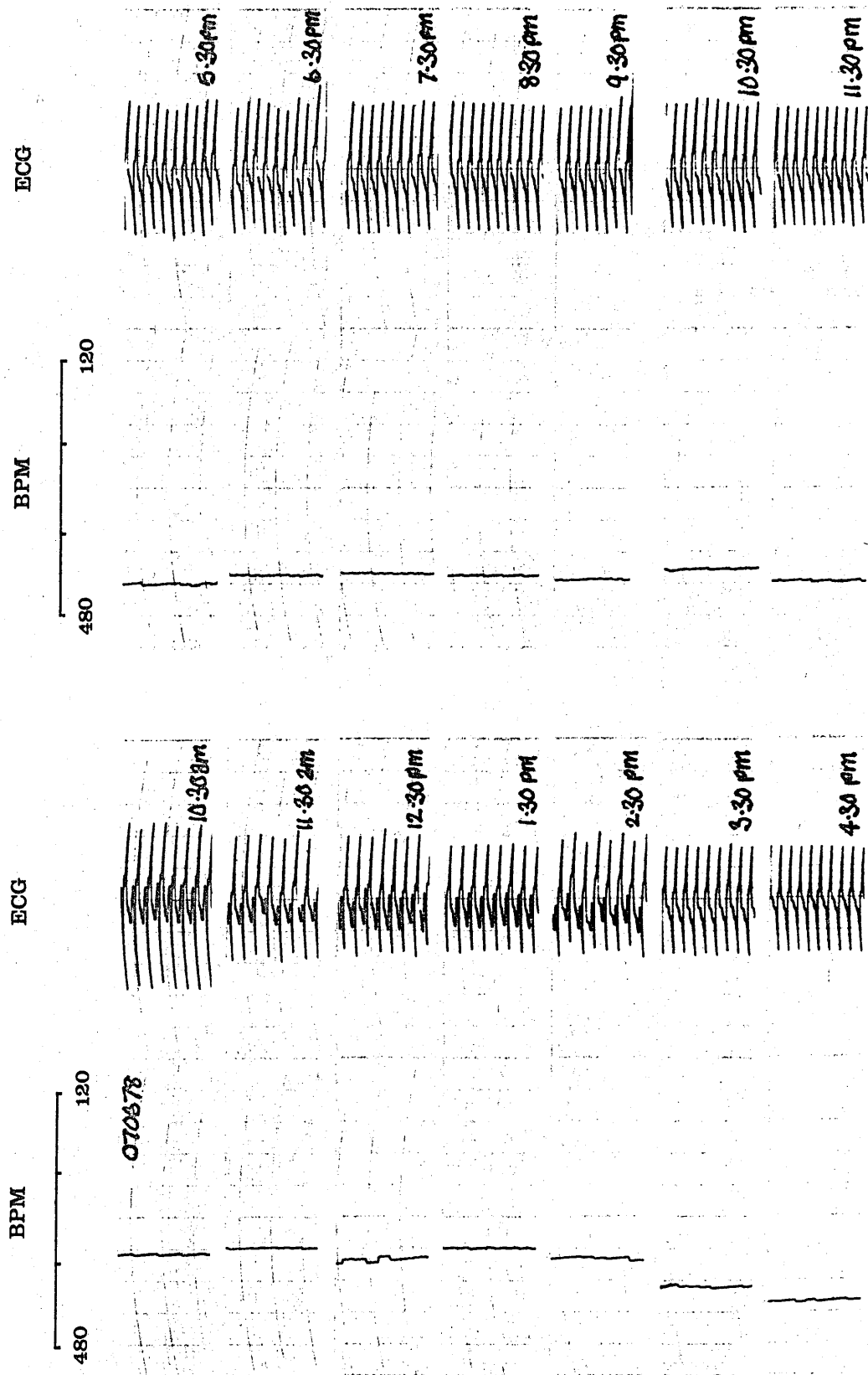
body temperature of chickens approaches the adult mean of 41.9 degrees C; Whittow, cited in Sturkie, 1963). During experiments, the birds were also covered with a cotton wool pad and warmed from above by the hospital inspection lamp if necessary.

An electrode made from a 26 gauge hypodermic needle was inserted through the skin flap at the posterior axis of both wings for recording the ECG. The ECG waveform was continuously monitored by the chart recorder and an audio unit. A direct write-out of heart rate was provided by a tachometer module connected to the ECG amplifier, and was typically between 300 and 400 beats/minute. Figure B2A shows records of the temperature, heart rate and ECG taken at hourly intervals during a typical experiment. Figure B2B shows similar records from another experiment, but in this case the temperature was monitored on the blanket control unit, and does not appear on the recorder chart.



FIGURE B2. PHYSIOLOGICAL RECORDS

B. HEART RATE AND ECG DURING 13 HOUR RECORDING PERIOD



070578



### CHAPTER B3 : STEREOTAXIS

After the initial surgery outlined in Chapter B2, the birds were placed in a modified small animal head holder on a Baltimore Universal stereotaxic frame (Model L). Very little pressure was applied during the insertion of the ear bars, as the young chicken skull is very flexible and fragile. The upper beak rested upon a 1mm diameter silver steel rod which could be raised or lowered through 15mm. Extra rigidity of the skull was provided by gently taping the upper beak to this rod. Figure B3 shows the head taped in position. Initially, the beak rod was adjusted to provide a similar orientation of the skull to that used by Karten and Hodos (1967) for their atlas of the pigeon brain. However, later experiments were conducted with the beak rod raised 7.5mm from this position, facilitating the optimal recording of field potentials from vertical electrode tracks. Figure B5 illustrates the two head orientations. The Karten and Hodos orientation is referred to as H1, the angle between the horizontal axis and the ear bar-beak rod axis being 45 degrees; the raised orientation is referred to as H2, the angle between the same axes being 25.5 degrees. The two diagrams were constructed from tracings of photographs taken of the head taped in position in the holder. Five photographs were taken at different stages during a dissection of the head which exposed the retina, optic papilla and brain.

FIGURE B3 HEAD OF CHICKEN IN HOLDER

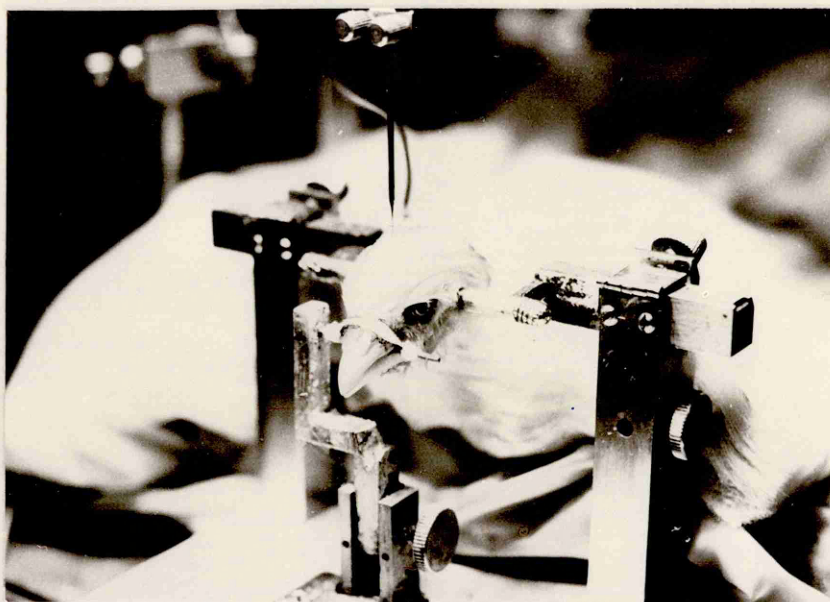
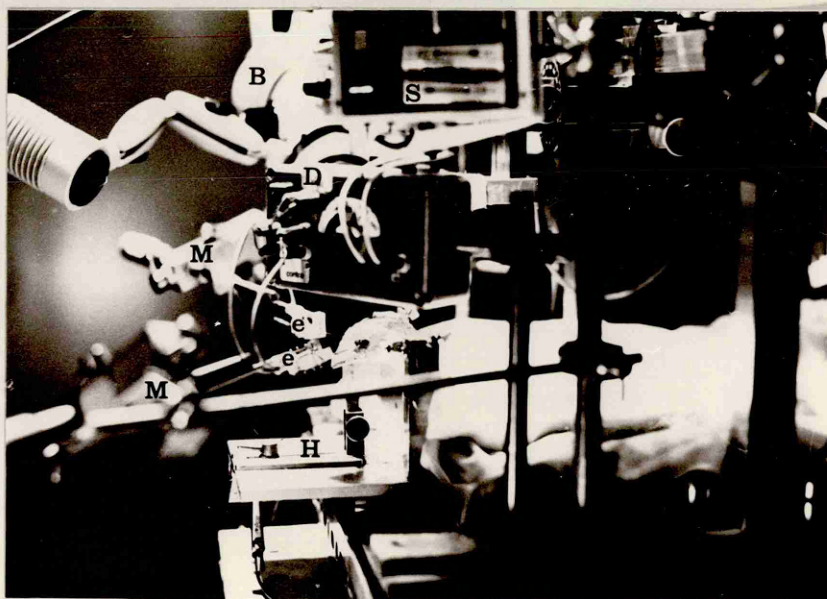


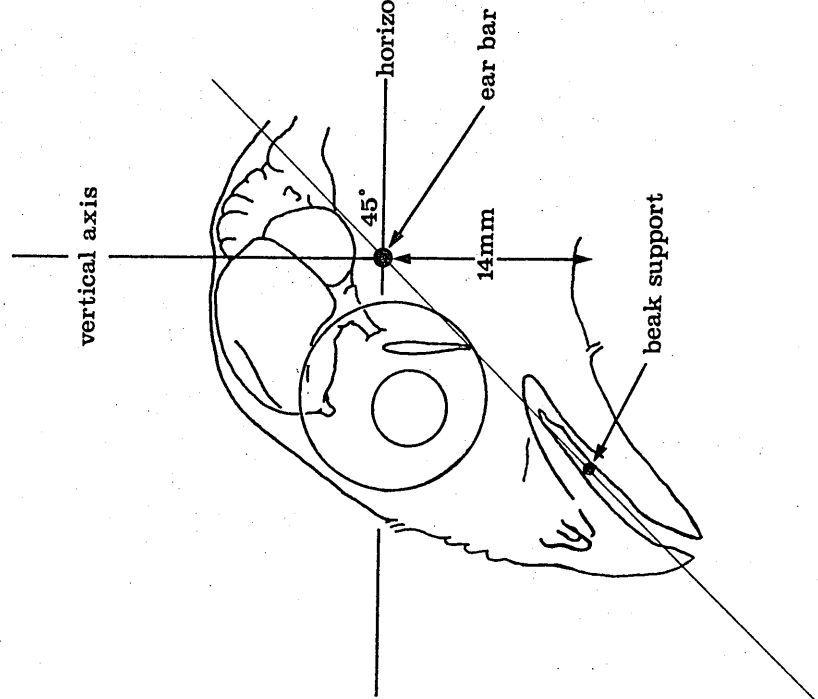
FIGURE B4 EXPERIMENTAL ARRANGEMENT



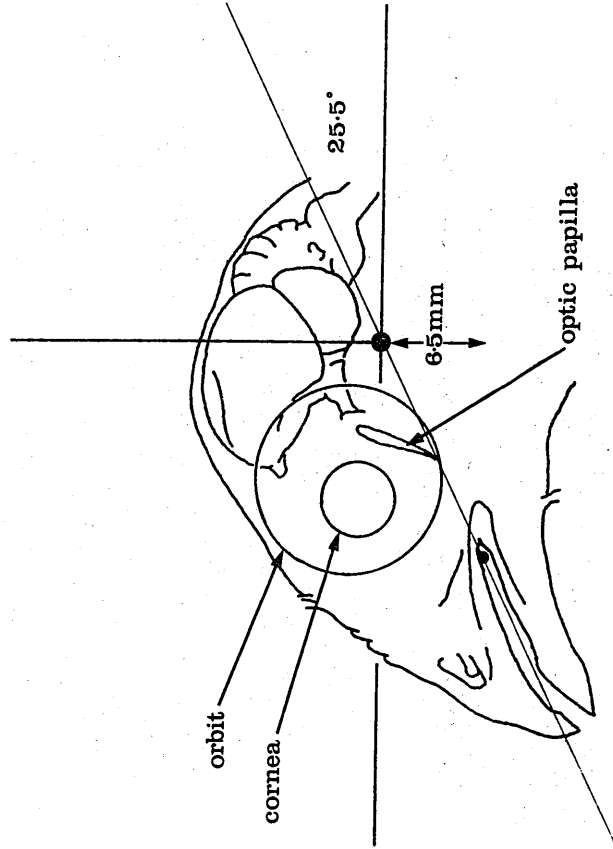
- B : binocular microscope  
S : isolated stimulator  
D : stimulus distribution box  
M : stimulus electrode micromanipulators  
e : stimulus electrode holders  
H : head holder

FIG B5 ORIENTATION OF HEAD IN STEREOTAXIC FRAME

A H1



B H2



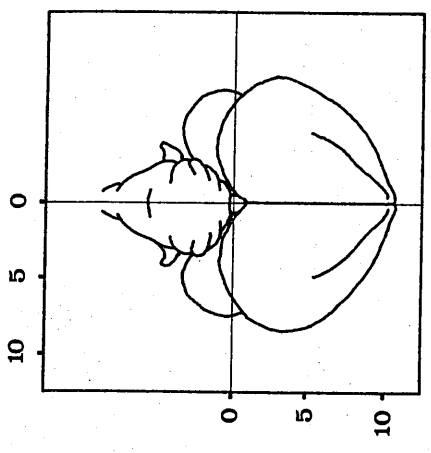
Anterior-posterior coordinates were calculated from a zero position defined by a line scored along the centre of the ear bars. The lateral coordinate zero position was defined by the skull midline suture, or alternatively, by the midpoint between the two ear bars. The reference zero point was marked on the exposed skull using dye from an electrode mounted in the stereotaxic micromanipulator. Figure B6 shows the position of the anterior-posterior and lateral zero axes for the two head orientations. Again, the diagrams were traced from photographs of the head in the stereotaxic holder.

Vertical measurements of electrode placements were taken from the brain surface, or relative to an arbitrary zero in order to obtain regular grids of recording stations for computer analysis of the data.

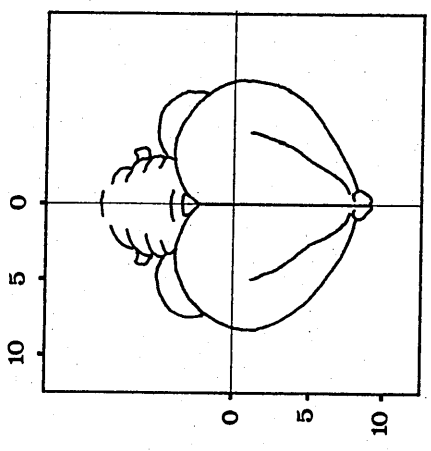
Attempts to construct a standard stereotaxic atlas for the preparation did not result in sufficient accuracy to warrant the development of a final product for the whole brain; large variability was found in the brain size of the chickens at this age, and further problems of reproducibility arose from the flexibility of the skull and the consequent problems of rigid and constant fixing of the head without damage to the ears or beak articulation. However, reproducible placements of electrodes in the diffuse hyperstriatum were possible for the accurate location of evoked field potentials. Crucial comparisons of the spatial distributions of the field potentials were always made using the experimental bird as

FIG B6 STEREOTAXIC CO-ORDINATES (mm)

A H1



B H2



its own control - thus, the effects that different stimulus electrode positions on the retina or optic papilla had upon the localisation of the forebrain potentials were examined by comparing different stimulus placements in the same chicken.

CHAPTER B4 : PREPARATION FOR STIMULATION  
AND RECORDING

B4.1 PREPARATION OF THE EYE

After the bird had been placed in the stereotaxic head holder, the eyes were periodically irrigated with eye drops of 1% w/v amethocaine hydrochloride prior to surgery. Apart from the benefits of local anesthesia, this solution appeared to possess vasoconstrictive properties, greatly reducing bleeding which could occur upon the subsequent removal of the eyelids.

Attempts to guide the placement of stimulating electrodes on the retina ophthalmoscopically, via a small scleral incision, were abandoned due to the difficulties of working in such a small area. Subsequently, in all experiments the cornea and lens were completely removed. The eyelids were removed to expose the cornea and scleral ring. It was not necessary to disturb the nictitating membrane as this remains retracted under the action of the paralyzing agents. The cornea was incised with a cataract knife, and removed using corneal scissors. The lens and aqueous humour were removed by gentle aspiration; stronger aspiration was required to tease the vitreous from the eyeball. Removal of the vitreous body was completed by gently pulling it with forceps. This procedure resulted in no visible damage to the retina.

The pecten and optic papilla could now be clearly seen through the corneal opening. Transillumination of the eyeball facilitated the identification of the optic papilla, appearing under these conditions as a bright line against the dark background of the retina. Placement of the stimulating electrodes on the papilla or retina was made under visual guidance in the transilluminated eye. (A description of the stimulus placements used is given in Section D, Chapter D2.1). The stimulus electrodes were mounted on micromanipulators, as shown in Figure B4. (Details of stimulation and recording techniques are given in Section D Chapter D2.1).

Initially, silicon fluid (60,000 centistokes) was injected into the eye after aspiration to prevent drying of the retina, but this was found later to be unnecessary, adequate moisture being provided by the natural production of lymph.

#### B4.2 EXPOSURE OF THE BRAIN

The skin overlying the hemispheres and cerebellum was removed, and a drop of electrode jelly placed under the loose skin covering the dorsal muscles of the neck for subsequent insertion of an indifferent electrode. The connective tissue adhering to the right cranium was removed, and the thin bone overlying the right Wulst reflected using a No. 23 scalpel blade. With the aid of a binocular microscope, small incisions were made in the dura and arachnoid using a 26 gauge hypodermic needle. The exposed



area of brain was then surrounded by a wall of bone wax and covered with silicon fluid (60,000 centistokes).

SECTION C : HISTOLOGY

CONTENTS OF SECTION C

CHAPTER C1 : METHODS

C1.1 : FIXATION AND BLOCKING

C1.2 : EMBEDDING

C1.3 : STAINING

CHAPTER C2 : THE CHICKEN FOREBRAIN IN NISSL SECTIONS

C2.1 : INTRODUCTION

C2.2 : THE HYPERSTRIATAL LAMINAE

C2.3 : TRANSVERSE SECTIONS OF THE CHICKEN FOREBRAIN

C2.4 : ABBREVIATIONS AND NOMENCLATURE

LIST OF ILLUSTRATIONS FOR SECTION C

- FIGURE C1 : T.S. GENERALISED AVIAN FOREBRAIN
- C2 : THE NOMENCLATURE OF HYPERSTRIATAL LAMINAE
- C3 : T.S. CHICKEN WULST AT ANTERIOR 6.0
- C4 : T.S. CHICKEN WULST AT ANTERIOR 4.0
- C5 : CHICKEN IHA
- C6 : THE CHICKEN FOREBRAIN IN SERIAL T.S.

## CHAPTER C1 : METHODS

### C1.1 FIXATION AND BLOCKING

At the termination of an experiment, the bone overlying the occipital venous sinus above the cerebellum was removed with a scalpel blade. Perfusion with 10% formal saline via the cannulated femoral vein was carried out until the sinus ran almost clear with perfusate; the bird was then decapitated and the whole head immersed in 10% formal saline at 4°C. Omission of the perfusion step did not appear to affect subsequent results. After a minimum fixation time of 12 hours, the head was replaced in the stereotaxic holder and the forebrain blocked in the vertical plane of the stereotaxic.

### C1.2 EMBEDDING

After fixation, the block was placed in a 6% dextran (MW 110,000) - 9.5% saline solution for 12 hours to remove excess water absorbed under the action of formaldehyde (Disbrey and Rack, 1970). Attempts to obtain serial frozen sections from fresh and newly fixed tissue using a carbon dioxide expansion chamber were unsuccessful due to the difficulty of finely controlling the temperature of the chamber. Attempts to increase the rigidity of the tissue by wax embedding resulted in gross shrinkage and distortion, and it was therefore decided to employ a gelatine embedding

technique (see Peacock, 1966). The block was removed from the dextran-saline, washed in distilled water, and immersed in 2.5%, 5.0% and 10.0% gelatine solutions at 34°C for 12 hours in each concentration. Final embedding was carried out in 10% gelatine at 4°C for about 1 hour. After this time the gelatine block was immersed in 10% formaldehyde at 4°C for 12 hours to render the gelatine insoluble in aqueous solutions. The block was then frozen on the CO<sub>2</sub> chamber attached to a Cambridge sledge microtome, and serial sections cut at 30-50µ thickness. The sections were mounted on glass slides with a 1% gelatine solution to which a few drops of glycerol had been added, and allowed to air dry vertically for a minimum of 12 hours. The slides were then immersed in 10% formaldehyde to harden the mountant, and subsequently washed or stored in distilled water.

### C1.3 STAINING

The sections were delipidised by taking them through 25%, 70%, 95% and 100% ethyl alcohol to xylene, and then back to water. Sections were stained for cell bodies with 0.5% cresyl violet and differentiated in Gothard's solution (Gothard, 1898), or in some cases, stained for myelinated fibres with solochrome cyanin (Page, 1965) and counter-stained with either neutral red or cresyl violet. Slides were mounted with DPX synthetic resin.

CHAPTER C2 : THE CHICKEN FOREBRAIN IN  
NISSL SECTIONS

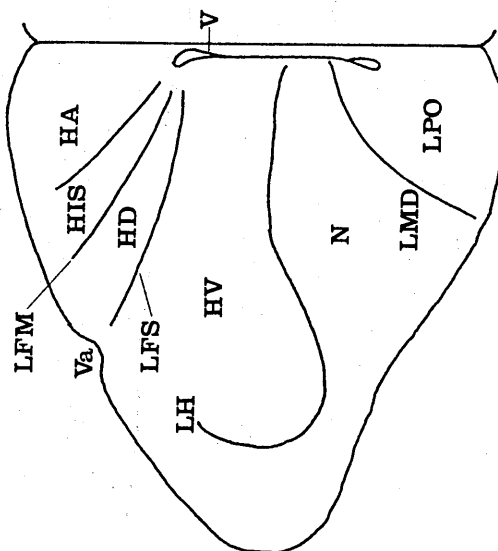
C2.1 INTRODUCTION

In transverse section, the bulk of the avian hemispheres appears as a laminated structure. The anterior, dorsal swelling limited by the midline and the vallecule, and known as the Wulst, is classically described as consisting of three major layers: the hyperstriatum accessorium (HA); an intercalated nucleus, generally referred to as the hyperstriatum intercalatus superior (HIS); and the hyperstriatum dorsale (HD). The whole region is overlain dorsally by a thin, non-laminated corticoid layer which is confluent with the hippocampal areas in the chicken and pigeon (Huber and Crosby, 1929; Kappers et al, 1936; see Karten and Hodos, 1967). Figure C1A shows a diagrammatic representation of the generalised anterior region of the avian Wulst in transverse section. (See C2.4 for a listing of abbreviations and nomenclature).

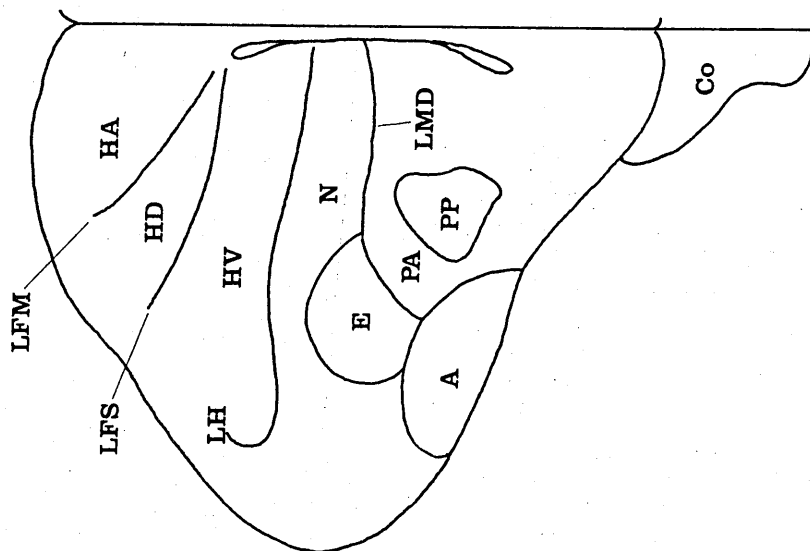
Below the Wulst lie the hyperstriatum ventrale (HV), neostriatum (N) and lobus parolfactorius (LPO). Figure C1B represents a more posterior section of the forebrain, showing the archistriatum (A), ectostriatum (E) and palaeostriatum (PA and PP). The ectostriatum lies above the lamina medullaris dorsale (LMD) and rises into the neostriatum, which itself extends along practically the

**FIG C1** TS. GENERALISED AVIAN FOREBRAIN

**A**



**B**





the whole length of the hemisphere. The palaeostriate region consists of two distinct nuclear masses, the palaeostriatum primitivum (PP) and the surrounding palaeostriatum augmentatum (PA). The archistriatum lies mainly in the ventrolateral area of the posterior hemisphere.

## C2.2 THE HYPERSTRIATAL LAMINAE

The cell density and relative sizes of HA, HIS and HD vary greatly throughout the avian class. The disposition of the hyperstriatal fibrous laminae (the lamina frontalis suprema, LFM; lamina frontalis superior, LFS; lamina hyperstriatica, LH) also varies, but in Galliformes and Columbiformes they generally lie dorsally, their long axis approximating the horizontal plane of the brain. Where clearly differentiated, the intercalated nucleus, generally identified as HIS, necessarily has a similar orientation. The ventral margin of this nucleus is associated with the LFM - there is no intervening fibrous lamina separating the dorsal margin of HIS from the ventral HA. HV is separated from the neostriatum by the LH, and from HD by the LFS. Further lamination of HV into dorsal (HVdv) and ventral (HVvv) fields is apparent in the chicken (personal observation) and pigeon (see Karten and Hodos, 1967).

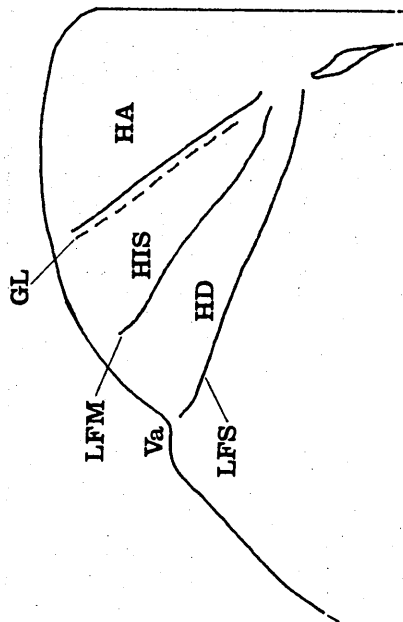
The majority of fibre tracts and cellular nuclei in the chicken forebrain were easily identified by comparison of transverse sections from the chicken with the line drawings and photomicrographs in Karten and Hodos' (1967) stereotaxic

atlas of the pigeon brain. (Other published atlases (adult chicken, van Tienhoven and Juhasz, 1962; adult canary, Stokes et al, 1974; adult quail, Bayle et al, 1974; three-day-old chicken, Youngren and Phillips, 1978) have been less useful in this respect as they contain line drawings only). However, the areas of primary interest in the present research, namely the hyperstriatal laminae, and particularly the intercalated nucleus, have been precisely those which have posed the most difficult problems of identification and nomenclature.

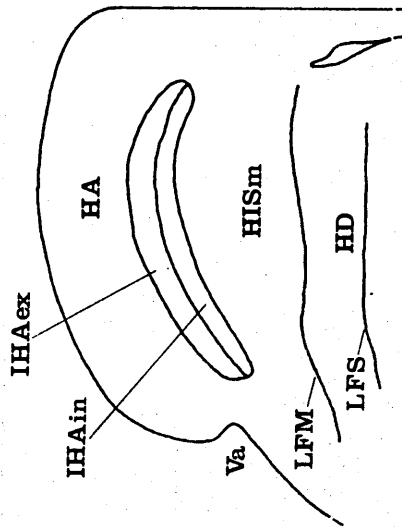
The morphology of the intercalated nucleus varies widely across different avian species. Thus, in the pigeon, HIS is characterised in the atlas of Karten and Hodos (1967) by a dispersed cellular group lying above LFM and HD, and the superficial margin of HIS is delineated by a narrow, darkly staining granular layer (GL). Hunt (1974) provides an identical analysis of these layers. (See Figure C2A). The intercalated nucleus of the burrowing owl, Speotyto cunicularia, however, shows a much more marked internal lamination, with a prominent bilaminar granule layer, the nucleus intercalatus hyperstriatum accessorium interna (IHAIN) and externa (IHAEX). This granule layer overlies a more dispersed cell mass, the hyperstriatum intercalatus suprema (HISM) (Karten et al, 1973; see Figure C2B). However, there appears to be some confusion of nomenclature throughout the literature. Karten et al (1973) present diagrams of the pigeon Wulst which include a layer labelled IHA (on the basis, it seems, of a functional correlation with the owl IHA, being the main projection field for visual

FIGURE C2 : THE NOMENCLATURE OF HYPERSTRIATAL LAMINAE

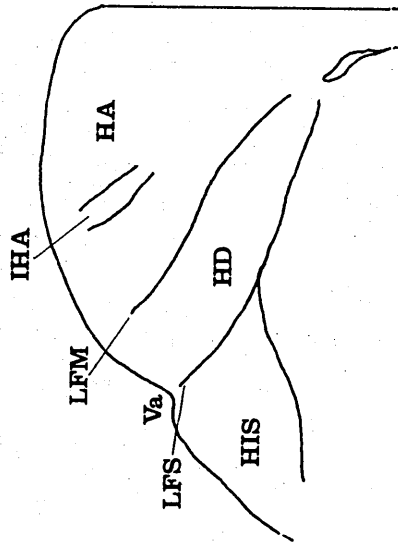
A PIGEON (AFTER KARTEN AND HODOS, 1967; HUNT, 1974)



B OWL (AFTER KARTEN ET AL, 1973)



C PIGEON (AFTER KARTEN ET AL, 1973)

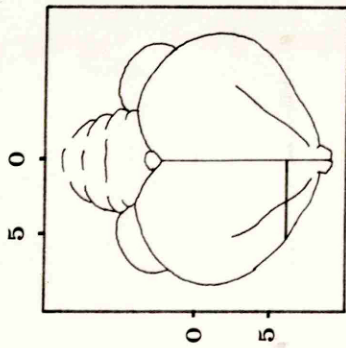


thalamic efferents), and which show HIS to lie ventrally to HD. (See Figure C2C). Indeed, Kappers et al (1936) describe two intercalated nuclei in the anterior avian forebrain, one associated with LFM dorsal to HD, and one associated with LFS ventral to HD. Karten et al (1973) may thus be following this analysis of the hyperstriatal laminar arrangement when they identify the superior intercalated nucleus (HIS) ventral to HD, but they forward no explanation or discussion for this departure from the atlas of Karten and Hodos (1967). It should also be noted that the intercalated nucleus which lies dorsal to HD in the Wulst of the pigeon (and other avian species except the owl) is still generally referred to as HIS by authors other than Karten and his co-workers.

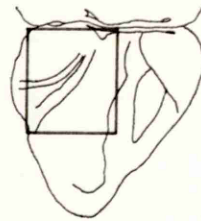
Given the somewhat confused and varied nomenclature in the literature, it was felt to be important that an unambiguous and, hopefully, meaningful system of identification of the chicken hyperstriatal layers should be developed. The morphology of the chicken Wulst, as shown by sections from the experimental animals used for the research reported in this thesis, is different to that of both the pigeon and owl. Photomicrographs of transverse sections through two separate anterior-posterior levels of the chicken Wulst are presented in Figures C3 and C4. It can be seen that in both cases, immediately ventral to the dispersed HA, lies a deeply staining layer of small cells. Figure C5 shows a higher power photomicrograph of the hyperstriatal laminae. The cells in the layer immediately below HA are orientated

**FIG C3 TS CHICKEN WULST AT ANTERIOR 6-0**

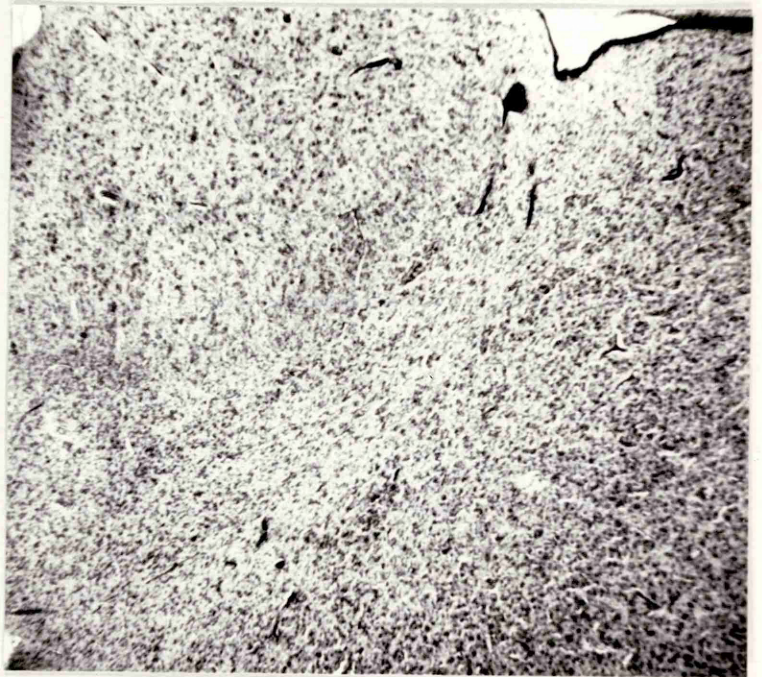
**A LEVEL OF SECTION**



**B PLAN OF SECTION**



**C PHOTOMICROGRAPH**



**D TRACING**

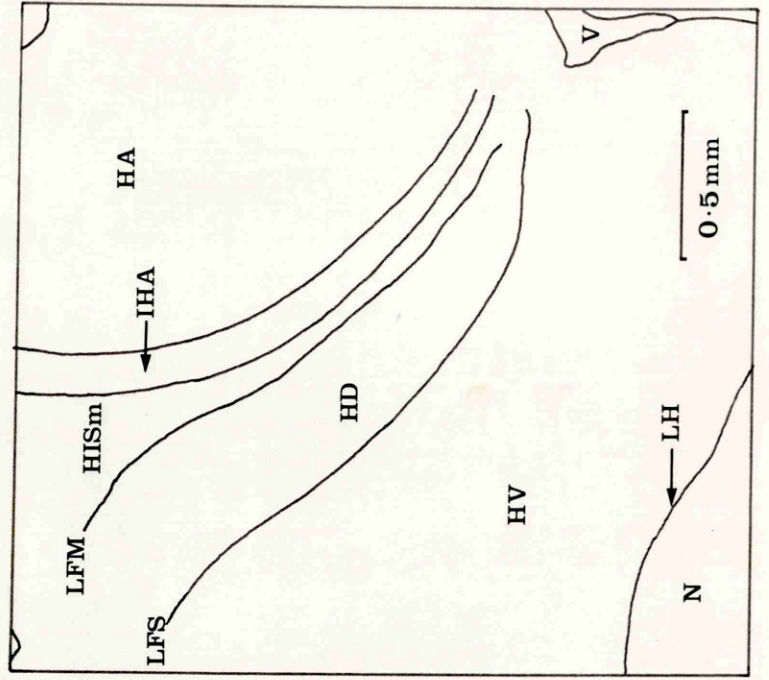


FIG C4 TS CHICKEN WULST AT ANTERIOR 4.0

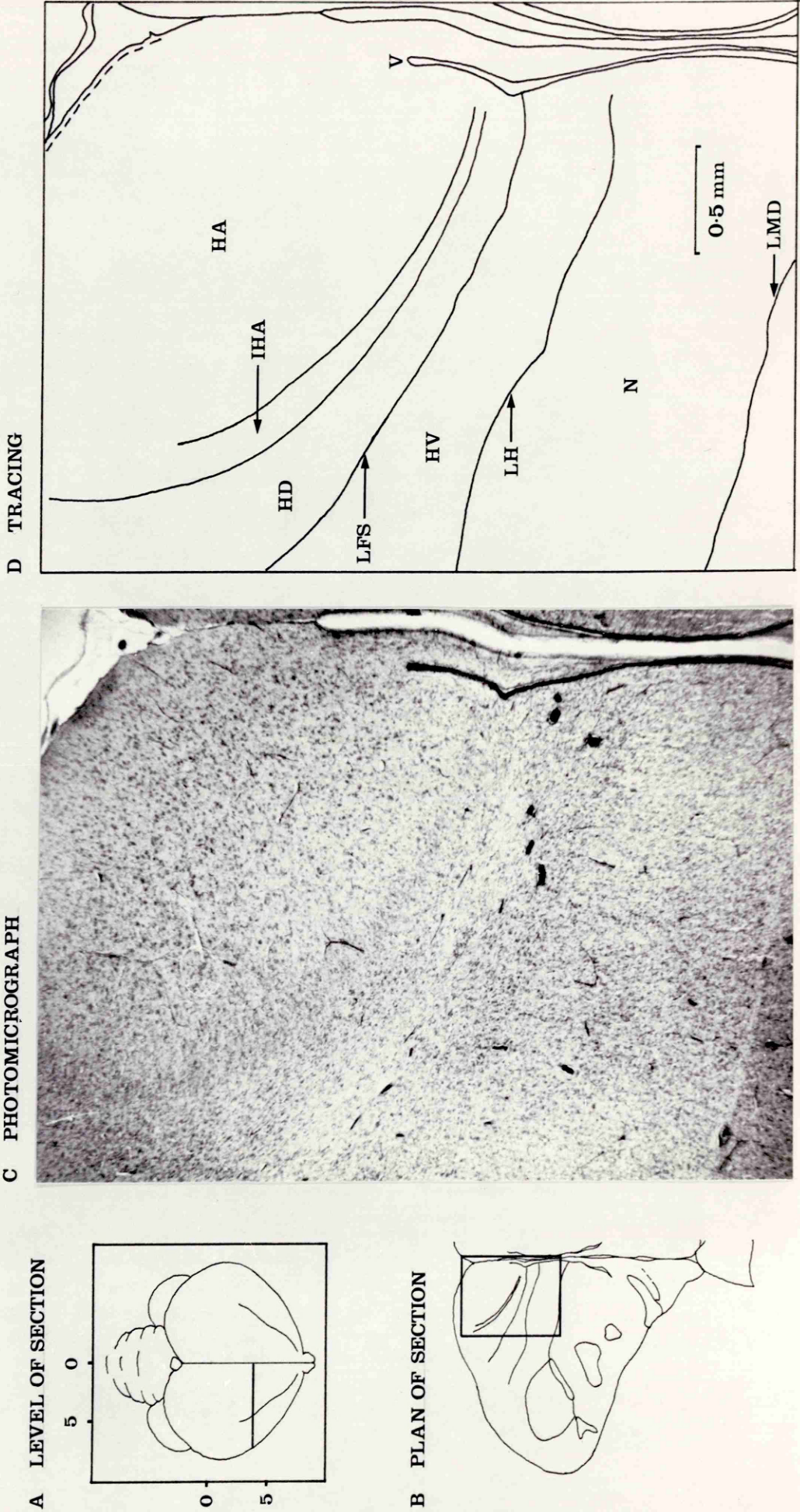
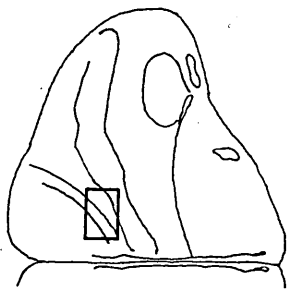
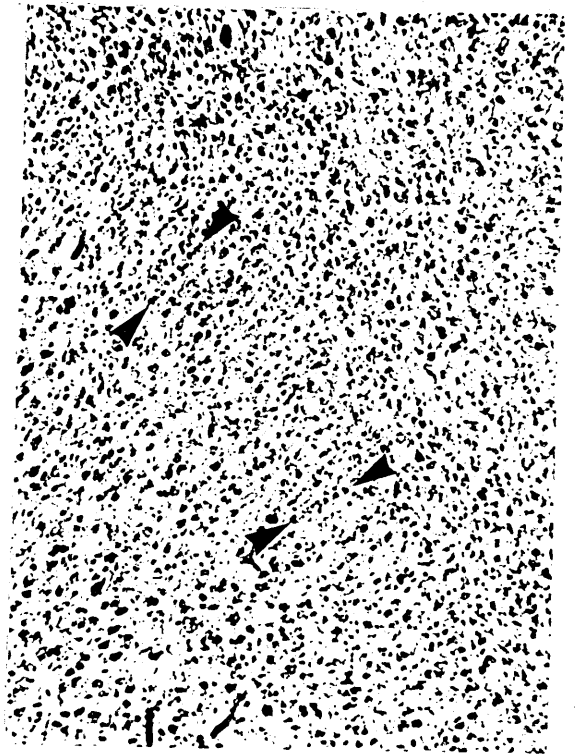


FIG C5 CHICKEN IHA

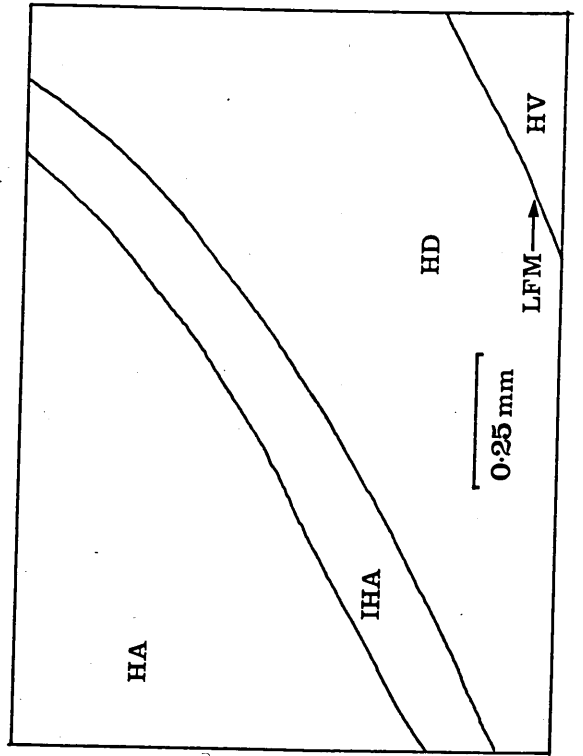
A PLAN OF SECTION



B PHOTOMICROGRAPH



C TRACING



in 'columns' lying perpendicular to the transverse axis of the layer, as indicated by the arrowheads. Beneath this layer, a more dispersed group of larger cells merge into HD, the latter being easily identified by its position, which is dorsal to the prominent LFS. LFM, however, was not easily identifiable in every section. It should be noted in this context that in the adult chicken atlas of van Tienhoven and Juhasz (1962) LFM is delineated only by a broken line, suggesting some difficulty or vagary of identification. Furthermore, these authors label the area between LFS and LFM collectively as 'HI+HD' (nucleus intercalatus hyperstriaticus + hyperstriatum dorsale). Youngren and Phillips (1978) do not label HD and LFM on every relevant section of their atlas of the three-day-old chicken, and do not identify an intercalated nucleus.

The chicken 'granular' layer of cellular columns shown in Figures C3, C4 and C5 was found to be a consistent feature of the hyperstriatum over the area of interest in the present study. Further, by comparison with photomicrographs in Karten et al (1973) and Karten and Hodos (1967), this layer was very reminiscent of the owl granule layer, being deeper and more prominent than the granule layer of the pigeon. It is thus referred to as the nucleus intercalatus hyperstriatum accessorium (IHA) throughout the remainder of this thesis, and is labelled as such on the photomicrograph tracings. (See Section D, Chapter D6 for a discussion of the functional 'appropriateness' of this designation). In transverse sections where LFM could be easily identified, it was clear



that an area of lightly staining, dispersed cells lay between this lamina and IHA. In accordance with Karten et al (1973), this area is designated as the hyperstriatum intercalatus suprema (HISm). This lamina can be identified in Figure C3, but not in Figure C4 - HISm was only apparent as a separate nucleus in sections of the anterior regions of the Wulst. (See Figures C6A-C). The presence or absence of a second intercalated nucleus in the chicken, associated with LFS, was found not to be crucial to the localisation of visually responsive areas in this study, and no attempt has been made to identify such an area.

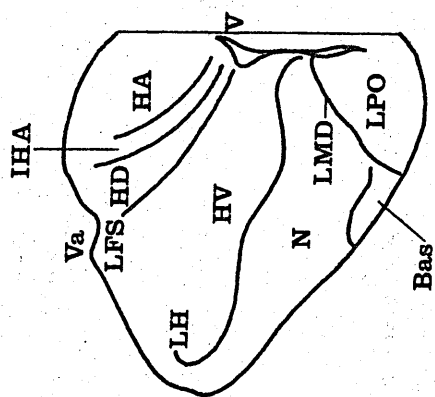
### C2.3 TRANSVERSE SECTIONS OF THE CHICKEN FOREBRAIN

The appearance of the chicken forebrain in Nissl sections is illustrated in Figures C6A-G. The diagrams are tracings made directly from projected images of 50 $\mu$  sections taken from the brain of a 100g chicken blocked at orientation H2 (see Section B, Chapter B3). The anterior-posterior extent of the section sample includes the whole of the visually responsive hyperstriatum delineated by this study (see Section D). The sections have been chosen at 0.2mm intervals between coordinates A3.6 and A6.2. Myelinated fibre tracts, which appear white in the Nissl sections, are indicated by hatching. The lateral and vertical scales have been adjusted to allow for the shrinkage resulting from histological processing. The percentage change (D%) along both axes, as calculated from lesion markings, was as follows:

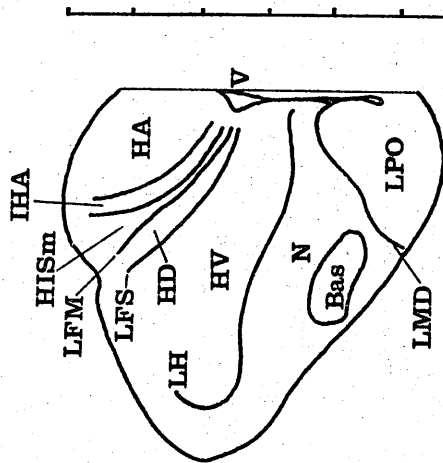
Lateral D% 0; Vertical D% -9.

FIG C6A

A 6·2



A 6·0



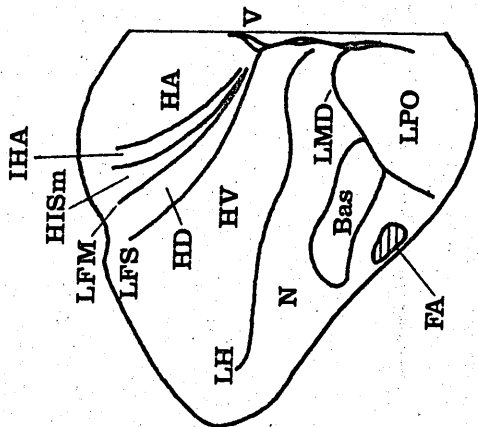
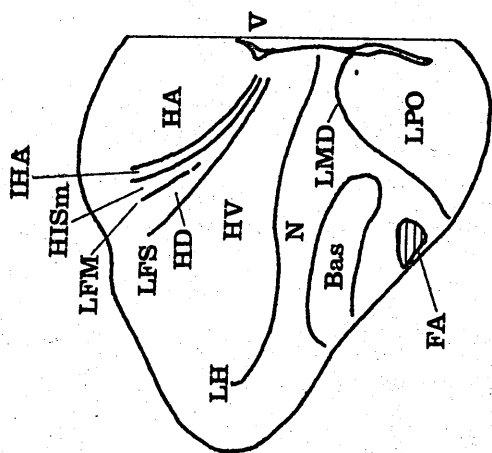
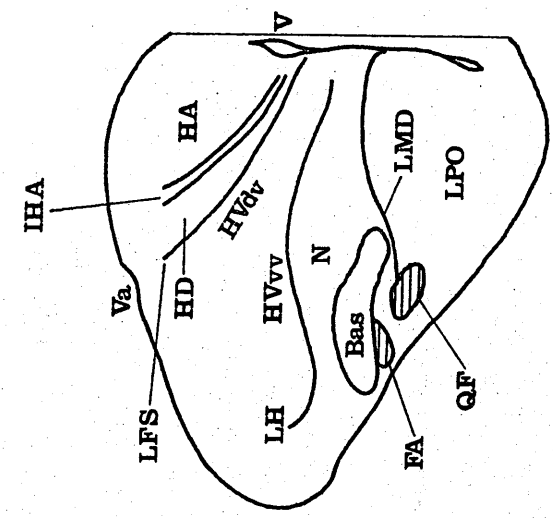
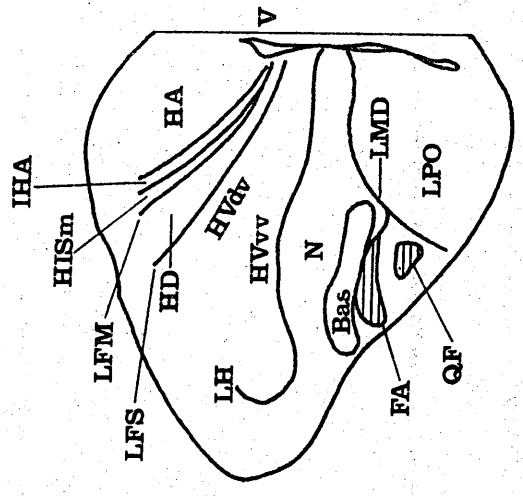


FIG C6B



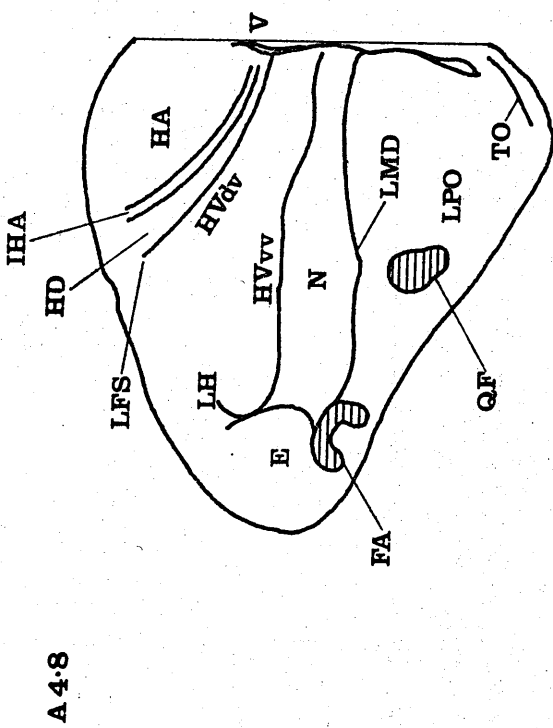
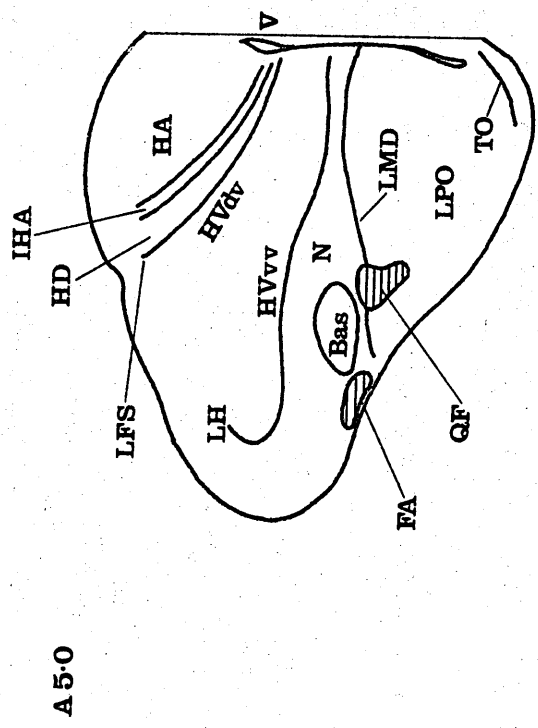
A 5.2



A 5.4

FIG C8C

FIG C6D



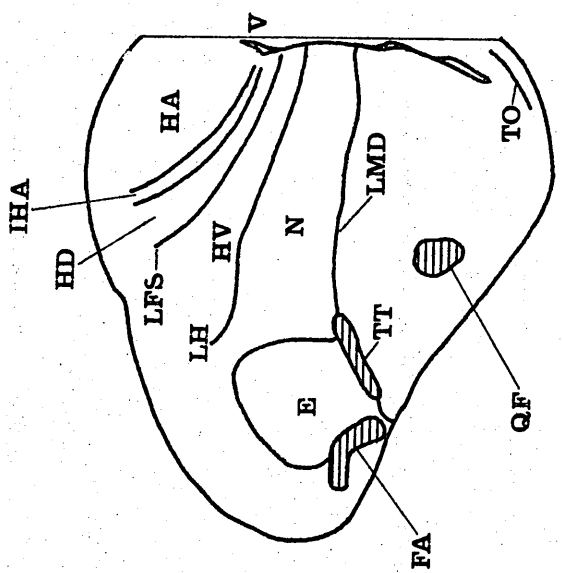
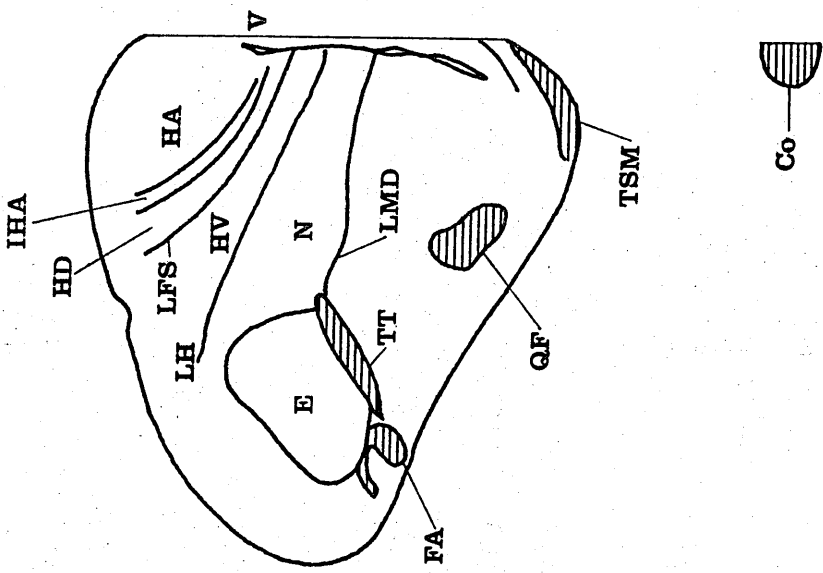


FIG C6E

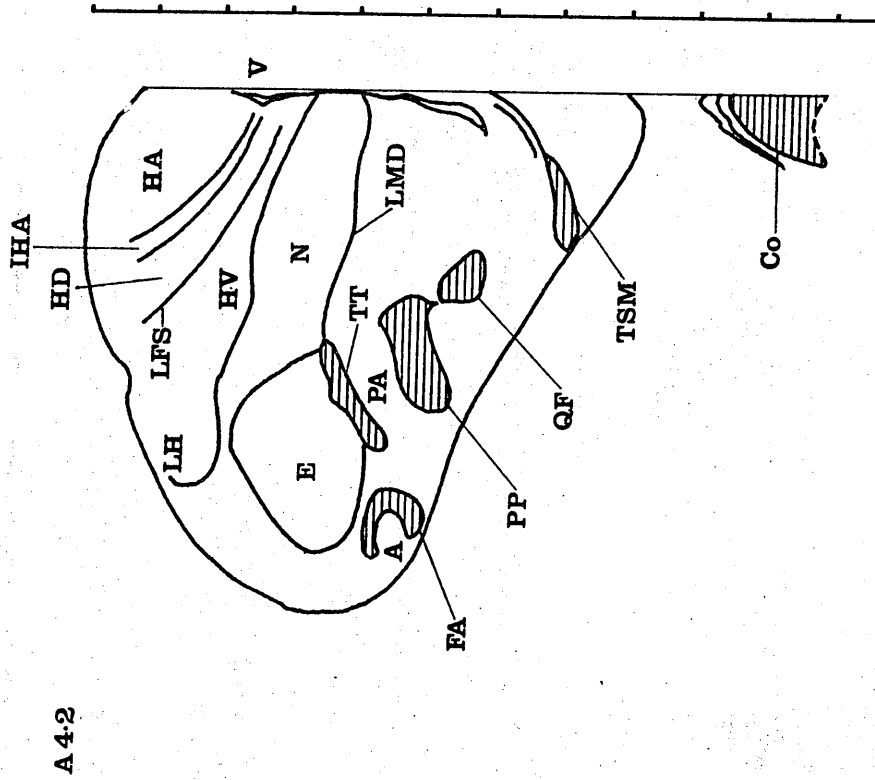
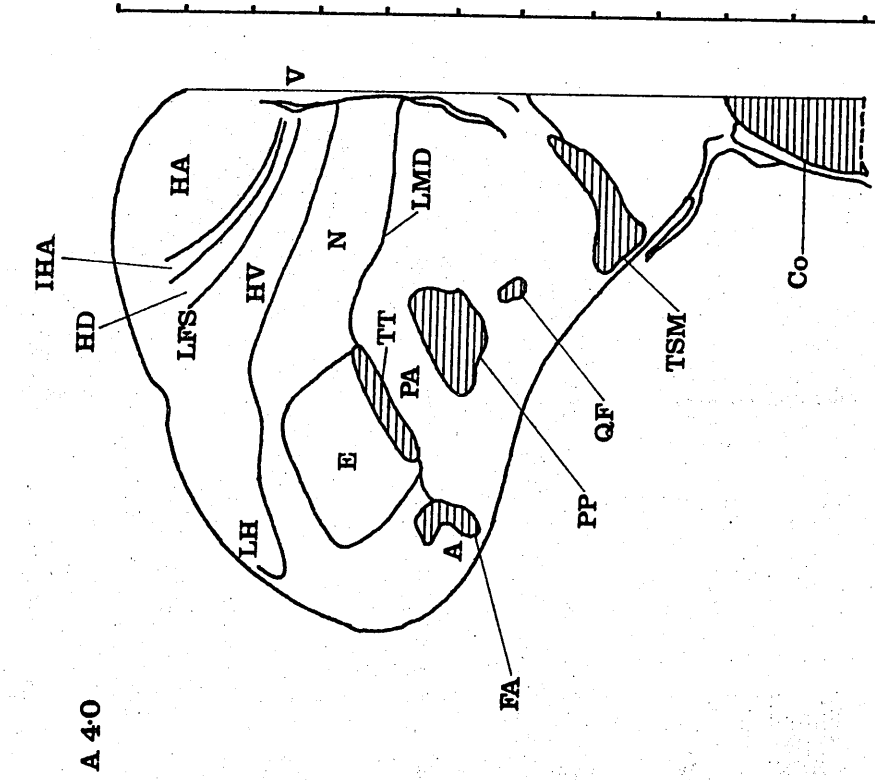


FIG C8F

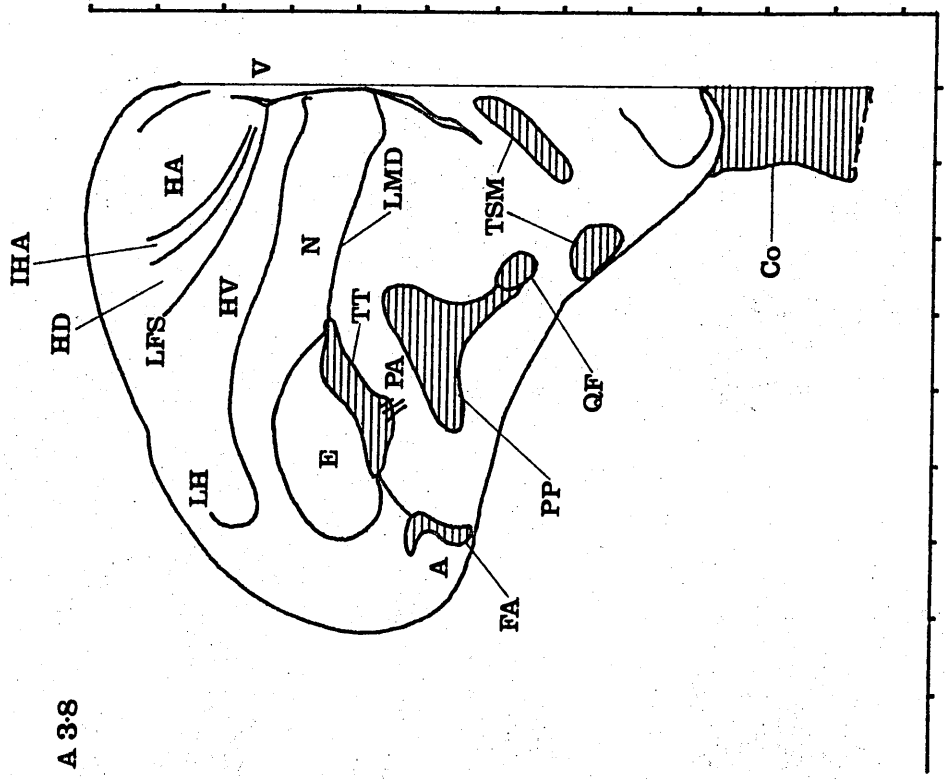
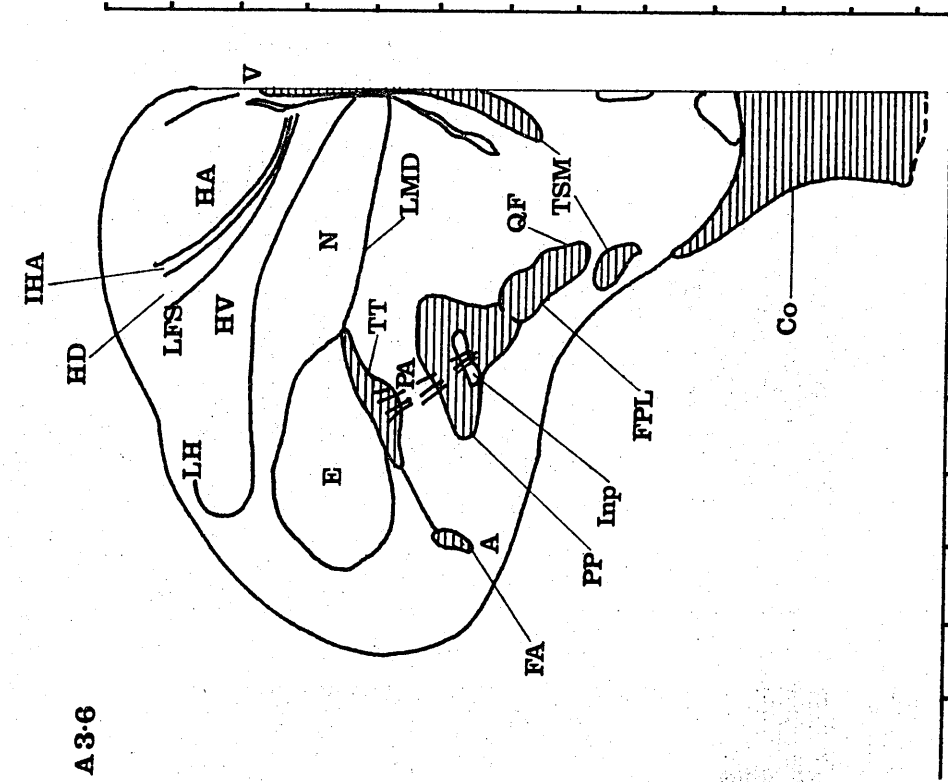


FIG C6G



C2.4 ABBREVIATIONS AND NOMENCLATURE

A	archistriatum
Bas	nucleus basalis
Co	chiasma opticum
E	ectostriatum
FA	tractus fronto-archistriatalis
FPL	fasciculus prosencephali lateralis
GL	granule layer
HA	hyperstriatum accessorium
HD	hyperstriatum dorsale
HIS	hyperstriatum intercalatus superior
HISm	hyperstriatum intercalatus suprema
HV	hyperstriatum ventrale
HVdv	hyperstriatum ventrale dorso-ventrale
HVvv	hyperstriatum ventrale ventro-ventrale
IHA	hyperstriatum intercalatus accessorium
IHAin	hyperstriatum intercalatus accessorium interna
IHAex	hyperstriatum intercalatus accessorium externa
Inp	nucleus intrapeduncularis
LFM	lamina frontalis suprema
LFS	lamina frontalis superior
LH	lamina hyperstriatica
LMD	lamina medullaris dorsale
LPO	lobus parolfactorius
N	neostriatum
PA	palaeostriatum augmentatum
PP	palaeostriatum primitivum

QF      tractus quintofrontalis  
TO      tuberculum olfactorium  
TSM     tractus septomesencephalicus  
TT      tractus tectothalamicus  
V        ventriculus  
Va      vallecula

SECTION D : ELECTRICALLY EVOKED FIELD  
POTENTIALS

CONTENTS OF SECTION DCHAPTER D1 : INTRODUCTIONCHAPTER D2 : METHODS

D2.1 : STIMULATION

D2.2 : RECORDING

CHAPTER D3 : GENERAL PROPERTIES OF FIELD POTENTIALS

D3.1 : DATA ANALYSIS

D3.2 : CONTRALATERAL FIELD POTENTIALS

D3.3 : IPSILATERAL FIELD POTENTIALS

D3.4 : RESPONSIVE AREA OF FOREBRAIN

D3.4.1 : Contralateral responsive area

D3.4.2 : Ipsilateral responsive area

D3.5 : SUMMARY

CHAPTER D4 : DORSOVENTRAL LAMINATION OF FIELD POTENTIALS

D4.1 : DATA ANALYSIS

D4.2 : RESULTS

D4.3 : LATENCY CONSIDERATIONS

D4.4 : SUMMARY

CHAPTER D5 : SPATIOTEMPORAL PATTERN OF FIELD POTENTIALS

D5.1 : INTRODUCTION

D5.2 : DATA ANALYSIS

D5.3 : TRANSVERSE DISTRIBUTION OF POTENTIALS

D5.3.1 : Contralateral transverse potentials

D5.3.2 : Transverse dorsoventral lamination

D5.3.3 : Ipsilateral transverse potentials

D5.4 : SAGITTAL DISTRIBUTION OF POTENTIALS

D5.5 : SUMMARY

CHAPTER D6 : DISCUSSION

LIST OF ILLUSTRATIONS FOR SECTION D

- FIGURE D1 : TECTAL FIELD POTENTIALS
- D2 : LOCALISATION OF TECTAL FIELD POTENTIALS
- D3 : BIPOLAR STIMULATING ELECTRODE
- D4 : STIMULUS PLACEMENTS
- D5 : PONTAMINE SKY BLUE LESIONS
- D6 : BLOCK DIAGRAM OF STIMULATION AND RECORDING  
ARRANGEMENTS
- D7 : EFFECTS OF AVERAGING
- D8 : CONTRALATERAL FIELD POTENTIALS
- D9 : IPSILATERAL FIELD POTENTIALS
- D10: DISTRIBUTION OF CONTRALATERAL RESPONSES
- D11: DISTRIBUTION OF IPSILATERAL RESPONSES
- D12: RESPONSIVE AREA OF FOREBRAIN
- D13: AVERAGED POTENTIALS AND DVT CONTOUR PLOT
- D14: DVT 2309H1 DIRECT STIMULATION OF OPTIC PAPILLA
- D15: DVT 2309H1 RETINAL STIMULATION
- D16: DVT 0706H2 RETINAL STIMULATION
- D17: RANGE AND MEAN PEAK LATENCY (MPL) FOR  
CONTRALATERAL AND IPSILATERAL POTENTIALS (ms)
- D18: DATA OBTAINED FROM TYPICAL TRANSVERSE RECORDING  
GRID
- D19: ISO CONTOUR MAP
- D20: 7JH2 LOCATION OF TRANSVERSE GRID
- D21: 7JH2 ISO CONTOURS GRID2 ANTERIOR RS BIN 48-71
- D22: 7JH2 ISO CONTOURS GRID2 ANTERIOR RS BIN 48-92
- D23: 7JH2 ISO CONTOURS GRID2 POSTERIOR RS BIN 48-92
- D24: 1605H2 LOCATION OF TRANSVERSE GRID

D25: 1605H2 ISO CONTOURS IPSILATERAL STIMULATION

D26: 2111H2 LOCATION OF SAGITTAL GRID

D27: 2111H2 ISO CONTOURS GRID2 ANTERIOR RS

## CHAPTER D1 : INTRODUCTION

Initial efforts to characterise the visual projection area in the chicken hyperstriatum were directed towards the analysis of receptive field properties of extracellularly recorded single units. The vast majority of units were found to be movement sensitive, and showed a range of selectivity for the direction of movement of bar and spot stimuli, together with some preferences for the velocity of stimulus movement. However, the wide area and range of depths over which these units could be isolated reflected the impression gained from the literature of a generally diffuse projection with unknown boundaries and spatial organisation (see Section A, Chapter A3). For reasons discussed in Section A, together with the need to predict more precisely the probable locations of visual units, it was decided that the area should be mapped as completely as possible using evoked field potential techniques.

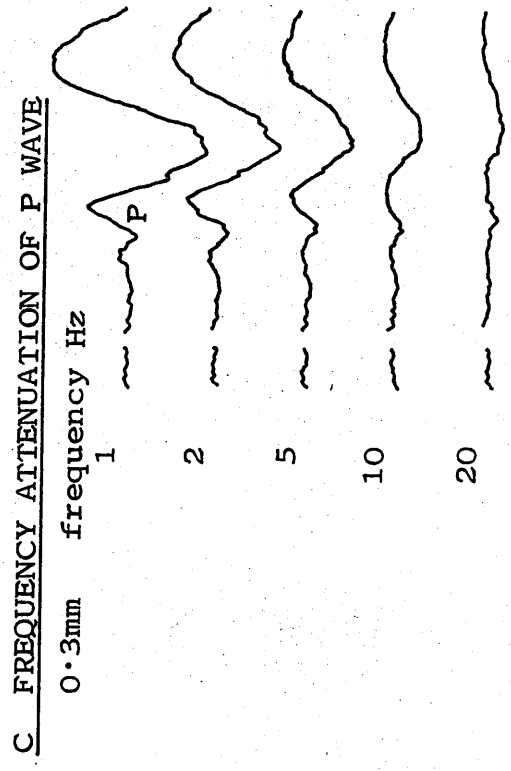
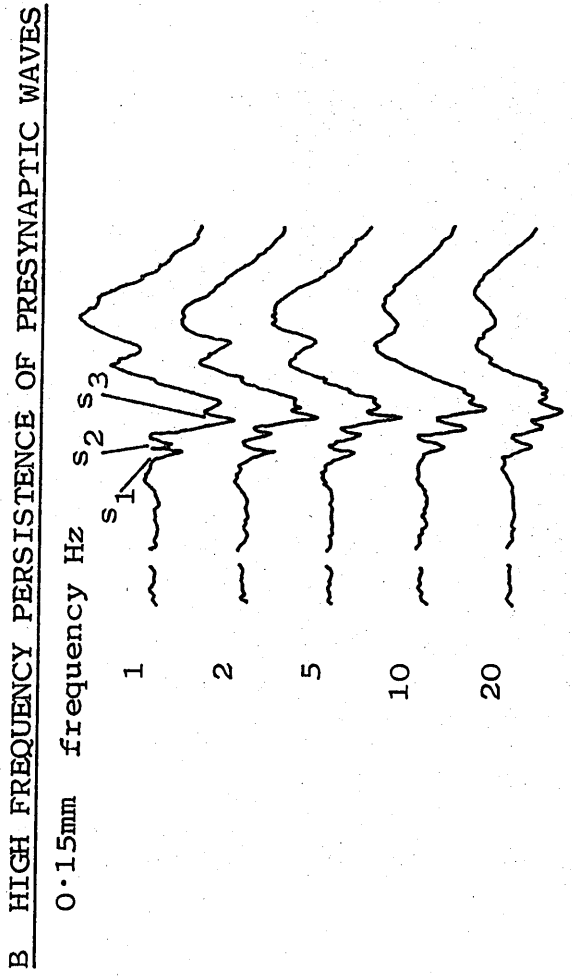
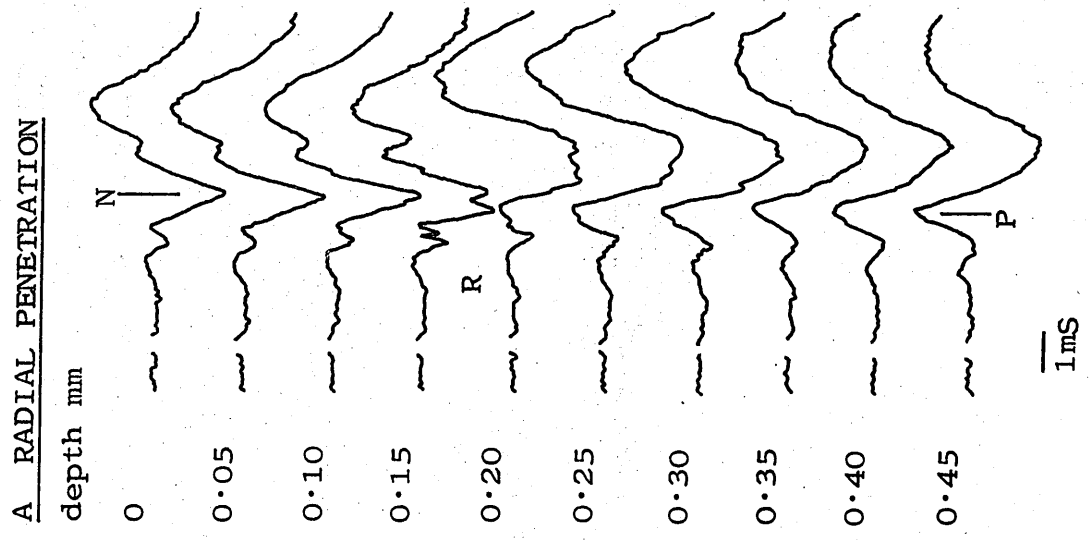
Pilot recordings were made from the optic tectum in order to establish the stimulation and recording techniques to be used. Tectal field potentials evoked by photic or electrical stimulation of the retina and optic papilla have been described in the adult pigeon (Holden, 1968a,b; Robert and Cuenod, 1969; Stone and Freeman, 1971; Mori, 1973; Mori and Mitarai, 1974) and for the adult duck and goose (O'Leary and Bishop, 1943). Results obtained from the chicken were essentially identical to those reported by these authors.

The highly laminated avian optic tectum receives a massive primary retinal projection. Incoming retinotectal fibres run along the surface of the tectum, forming the stratum opticum (SO). Within this layer, they turn sharply inwards to penetrate the tectum radially, terminating in the superficial half of the stratum griseum et fibrosum superficiale (SGFS). Contralateral enucleation in the pigeon has revealed afferent terminals in sublayers a-f of the SGFS (Cowan et al, 1961), although a more recent Golgi study by Stone and Freeman (1971) has shown retinotectal terminal plexuses only in sublayers c-f of the SGFS. The latter authors found the majority of afferent terminals to be in contact with tectal cells with radial processes, and that these radial cells constitute most of the SGFS. The distinctive waveforms of the evoked tectal field potentials have been related to the known anatomy of the primary afferent termination in the pigeon optic tectum. The following results obtained from young chickens illustrate the similarity of these tectal field potentials to those reported for the adult pigeon.

Figure D1A shows a series of potentials recorded from a radial electrode penetration in the tectum of a 95g chicken anaesthetised with urethane, and reveals the negative-reversal-positive pattern first reported in the pigeon by Holden (1968a,b). The contralateral optic papilla was stimulated directly with a bipolar electrode positioned at the superior margin of the pecten, and the potentials recorded via a 2M NaCl filled pipette with a tip resistance



FIGURE D1 TECTAL FIELD POTENTIALS

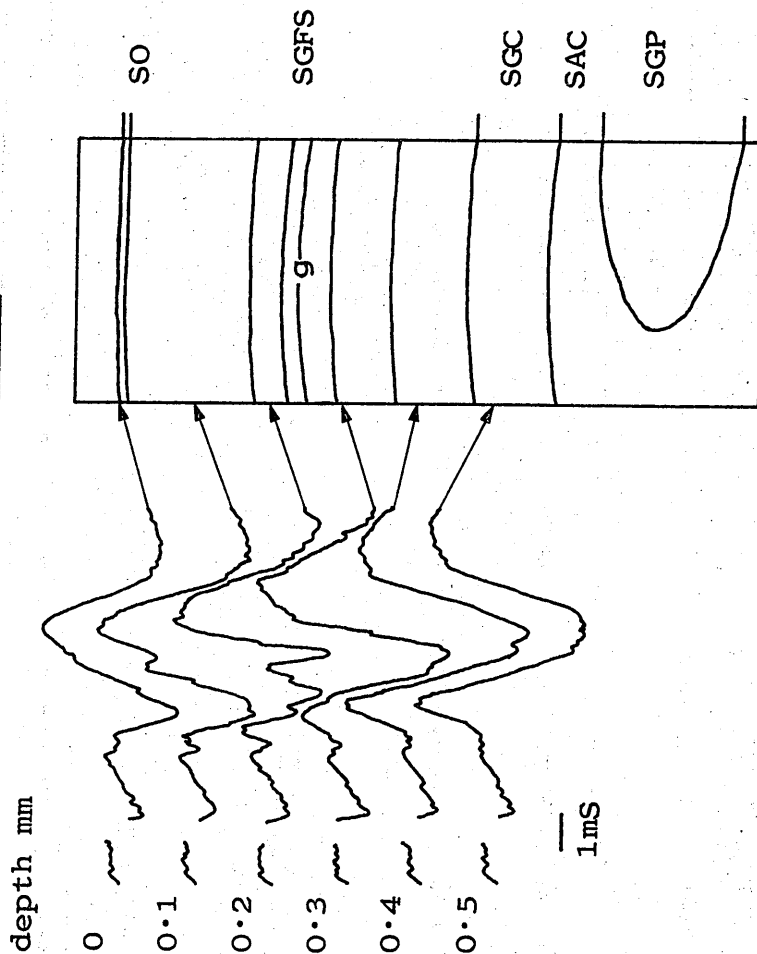


of 0.5Mohm. The break in the baselines indicates the stimulus artifact. A total of three presynaptic waves are evident at a depth of 0.15mm (see Stone and Freeman, 1971), followed by the postsynaptic N wave, which is evident from the surface to a depth of 0.15mm (see Holden, 1968a). The reversal zone (R) lies between 0.15 and 0.20mm from the surface. Below 0.2mm, the P wave persists throughout the depth of the tectum. Figure D1B shows the persistence of the presynaptic waves ( $s_1$ ,  $s_2$ ,  $s_3$ ) recorded at 0.15mm with increasing stimulus frequency, and the accompanying loss of N components. Figure D1C illustrates the attenuation of the postsynaptic P wave recorded at 0.3mm with increasing stimulus frequency (see Holden, 1968a; Stone and Freeman, 1971).

Figure D2A shows a series of tectal potentials from a 90g chicken, and the origin of these potentials within the tectal layers. Figure D2B shows the area of tectum represented in Figure D2A. Figure D2C shows the potential profile of the variation of N wave amplitude with depth. The reversal of the N wave occurs at a depth of 0.24mm from the tectal surface, corresponding to sublayer g (the lower limit of optic nerve afferent terminals) of the SGFS, as shown in Figure D2A; this reversal level coincides exactly with that reported by the above authors. It was felt confidently that these results showed that the system of stimulation and recording employed could provide data on the localisation of hyperstriatal field potentials that was consistent and free from artifact.

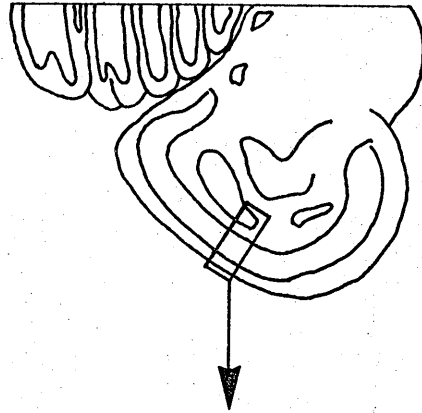
FIGURE D2 LOCALISATION OF TECTAL FIELD POTENTIALS

A ORIGIN OF POTENTIALS

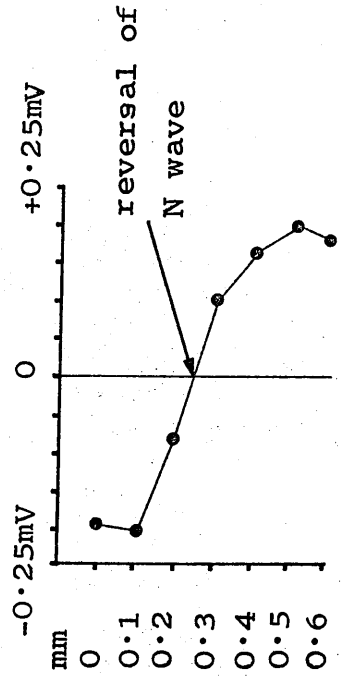


- SO : Stratum opticum
- SGFS: Stratum griseum et fibrosum superficiale
- SGC : Stratum griseum centrale
- SAC : Stratum album centrale
- SGP : Stratum griseum periventriculare

B T.S. CHICKEN MIDBRAIN X5



C FIELD POTENTIAL PROFILE



## CHAPTER D2 : METHODS

### D2.1 STIMULATION

The retina and optic papilla were stimulated with single square wave pulses derived from an isolated stimulator (Neurolog NL800, Digitimer Limited) and delivered via semi-micro bipolar electrodes (Clark Electromedical; see Figure D3 for the dimensions of one of the electrode pairs). The pulses had a duration of 0.1ms, and were delivered at a frequency of 0.33Hz. The isolated stimulator was set for a current limit of 10mA, the stimulus required for a maximal response always being between 2.5 and 3.5mA. (Holden, 1968a, used current strengths of 1-10mA to stimulate the optic papilla; Robert and Cuenod, 1969, used strengths of 1-5mA). The positions of the stimulus electrode placements are drawn to scale in Figure D4. Stimuli were applied to both the contralateral (C) and ipsilateral (I) eye, and either directly upon the optic papilla (shown by column D in Figure D4), or to the retina anterior to the optic papilla (column A) or posterior to the optic papilla (column P). A total of four levels of the electrode position relative to the attachment of the pecten were investigated (shown by the rows labelled 1 to 4 in Figure D4).

The stimulating electrode was positioned on the optic papilla or retina with the aid of a microdrive. For experiments designed to investigate the differential

FIGURE D3 BIPOLAR STIMULATING ELECTRODE

(measurements in mm)

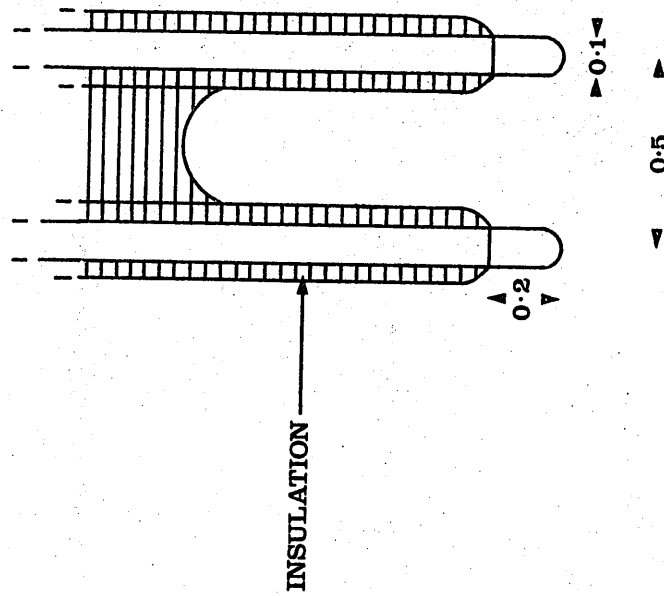
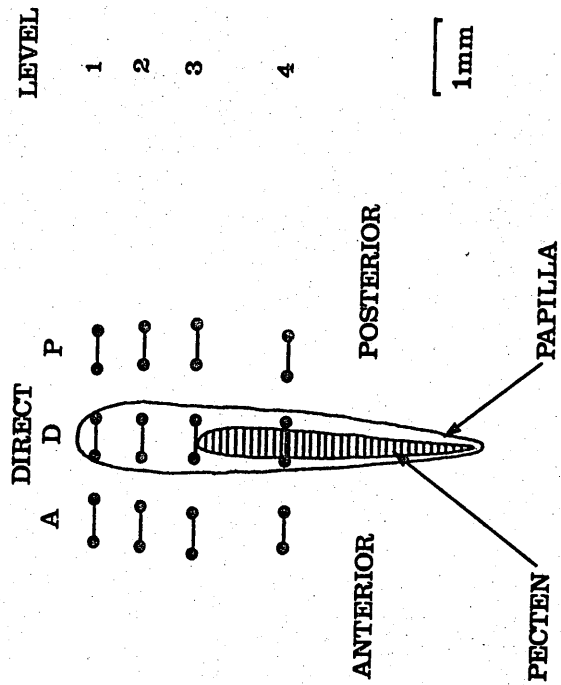


FIGURE D4 STIMULUS PLACEMENTS



distribution of potentials derived from stimulation at placements anterior and posterior to the optic papilla, two bipolar electrodes were mounted upon a single microdrive. The separation of the two bipolar pairs was adjusted to result in the two proximal tips to lie 0.5mm either side of the optic papilla when the electrodes made contact with the retina.

## D2.2 RECORDING

Field potential recordings were made using glass microelectrodes broken to a tip diameter of 10-20 $\mu$ , and with a tip resistance of 0.5-3.0Mohm at 60Hz (measured according to the method of Stone, 1973). A small piece of silver wire was inserted into the dorsal muscles of the neck to serve as an indifferent electrode. Glass recording electrodes were pulled with a few glass fibres inserted into the bore (Scientific Research Instruments Microelectrode Puller), and filled with electrolyte under vacuum. Electrodes filled with 2M NaCl, 4M NaCl, K Citrate and 0.5M Na Acetate all furnished identical results. A number of combinations of electrolyte and ionic dyes were investigated for the iontophoretic marking of electrode positions. A saturated solution of fast green FCF (Sigma Chemical Company) in either 2M or 4M NaCl (see Thomas and Wilson, 1965) was found to result in negligible and inconsistent marking. The best combination was found to be a 2% solution of pontamine sky blue (Sigma Chemical Company) in 0.5M Na Acetate (see Hellon, 1971). A current injection of 12-15 $\mu$ V for 3-5 minutes

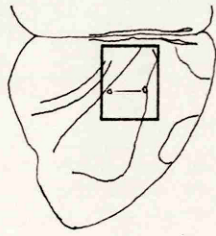
resulted in bright blue lesions of 50-100 $\mu$  in diameter. Figure D5 shows a photomicrograph of two typical lesions, made 1mm apart along a vertical electrode track. The lesions were easy to indentify in both stained and fresh tissue. The section illustrated in Figure D5 was stained in the routine manner with cresyl fast violet.

The recorded potentials were amplified and filtered by standard equipment (Neurolog Headstage, NL100; AC Preamp, NL103; AC Amp, NL105; Filters, NL115). All potentials were recorded without the use of a 50Hz notch, and within the bandwidth of 10Hz-1KHz (or very occasionally 10Hz-100Hz) in order to reduce large scale deflections due to unitary activity.

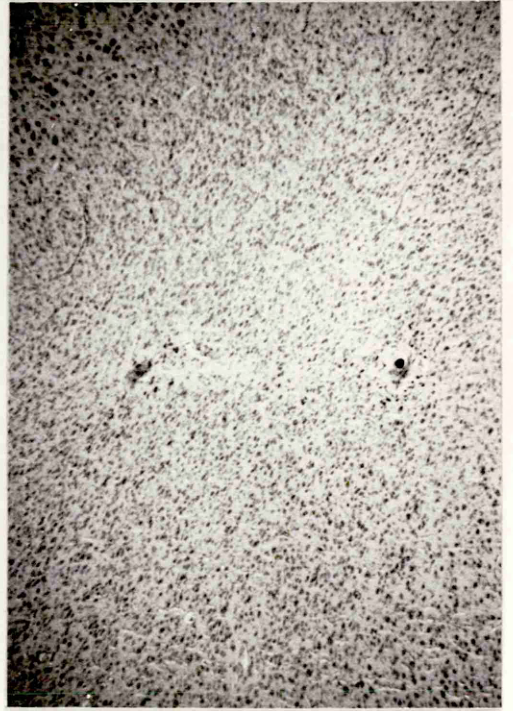
Pilot recordings of hyperstriatal field potentials were made in order to determine the optimal interval between vertical recording positions. Initially, an interval of 0.5mm was used, as this was the interval between recordings from the pigeon Wulst presented by Perisic et al (1971). However, this interval was found to be too large, and resulted in the omission of potential changes which occurred along vertical electrode tracks. Consequently, vertical intervals of 0.1, 0.2 and 0.4mm were investigated along an electrode penetration which sampled activity at every 0.1mm. Intervals of 0.1mm were found to result in the aquisition of much redundant information - the field potentials often showed very little or no changes in amplitude over three adjacent vertical positions when recorded at this interval.

**FIG D5** PONTAMINE SKY BLUE LESIONS

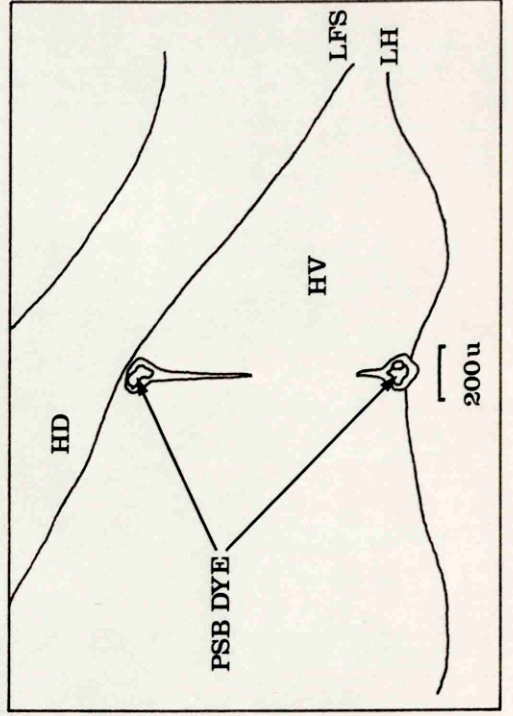
**A** PLAN OF SECTION



**B** PHOTOMICROGRAPH



**C** TRACING



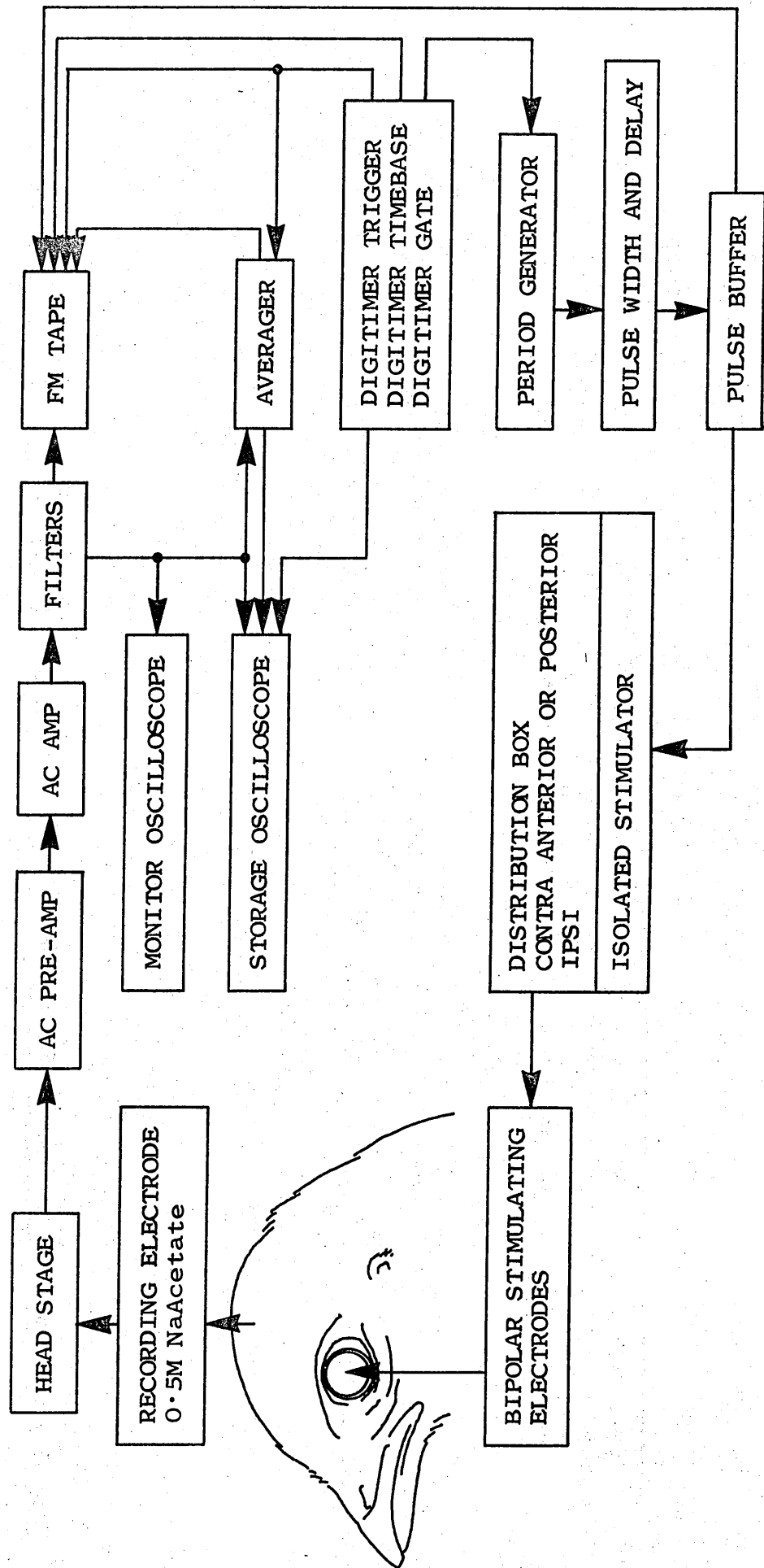


Conversely, analysis of the potentials obtained at 0.4mm intervals showed omissions of amplitude variation when compared with the whole series of 0.1mm recordings. An interval of 0.2mm, however, was found to produce results falling between the two extremes. Although the potentials occasionally showed little variation between adjacent 0.2mm recording points, no gross omissions of amplitude or latency changes were noticed at this recording interval. Therefore, a recording interval of 0.2mm was used for all of the potential records presented in Section D. Although the data that would have been obtained from 0.1mm intervals would also have been meaningful (and indeed, less prone to any unnoticed omissions of information), it would have been impossible to either record or handle the enormous amount of data that the experiments reported in Chapter D5 would have required at this interval. For example, 1,924 averaged data point records at 0.1mm intervals would have been required from one experiment to generate the isopotential maps presented in Chapter D5.3.

At every recording position, and for each stimulus condition tested, an average of four evoked potentials was taken using a Neurolog Averager NL750. A sample period of 100mS was used, which included a 10mS pre-stimulus baseline. The average contained 256 sample bins of 0.4mS width. This average was then stored on magnetic tape (Phillips 7 channel Instrumentation Recorder, EL1020), together with a sample of the raw waveform, a time scale, stimulus marker and trigger pulse. Figure D6 shows a block diagram of the stimulation and

recording arrangements. The different methods used to analyse the data will be described at the beginning of each relevant chapter.

FIGURE D6 : BLOCK DIAGRAM OF STIMULATION AND RECORDING ARRANGEMENTS



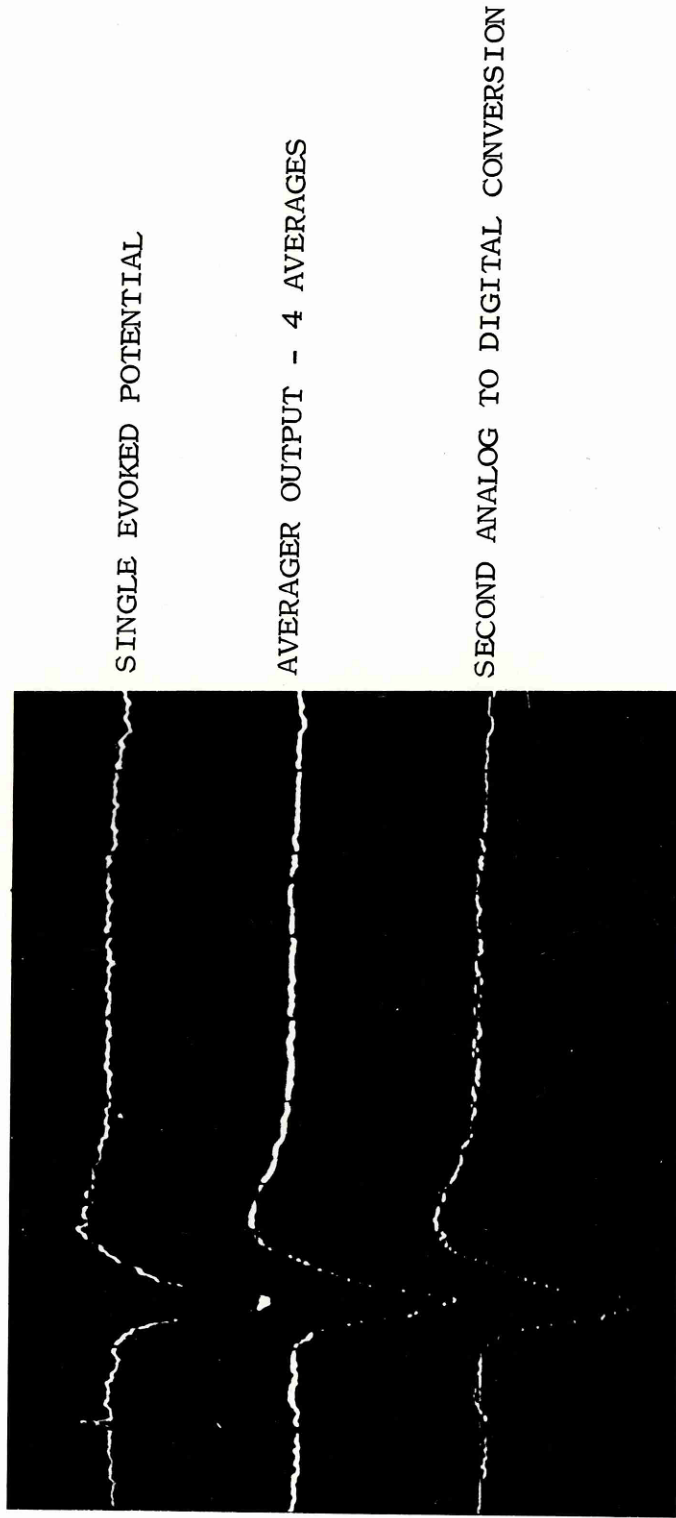
CHAPTER D3 : GENERAL PROPERTIES OF  
FIELD POTENTIALS

D3.1. DATA ANALYSIS

The data discussed in this chapter are presented as averaged waveforms of evoked field potentials. To obtain hard copies of the averages, which were stored on magnetic tape, they were first reconverted into binary form, using the averager in a 'single average' mode. This procedure resulted in only a small increase in the noise level of the averages, as shown in Figure D7. This figure was photographed from the screen of a storage oscilloscope. The upper trace shows a single raw evoked potential which was previously stored on magnetic tape, and then replayed through the oscilloscope. The stimulus artifact can be seen approximately 1cm (=10mS) from the start of the trace. The centre trace shows the average of the potentials evoked by four stimulations, again previously stored on tape, and replayed directly through the oscilloscope. The lower trace shows the result of replaying this average through the averager, to re-convert the data to binary form. The use of this procedure eliminated the necessity for on-line analyses.

The resulting binary representation of the averaged evoked potential was then transferred to the memory of a microprocessor unit (Motorola M6800, constructed at the

FIGURE D7 EFFECTS OF AVERAGING



Open University). The contents of the microprocessor memory were then output to a lineprinter to provide a decimal printout, and also ASCII coded paper tape, of the contents of the time bins of the average. Each time bin (256 bins, 100mS total) was represented as 256 voltage units, consisting of 0-128 negative voltage increments, and 128-256 positive voltage increments, on the printout.

The printouts were used to locate precisely the time of the stimulus artifact, together with the latency and magnitude of the voltage changes.

The paper tape was used to load the averaged potential data onto computer disc for further analysis (see Chapters D4.1 and D5.2), and for output to a Hewlett Packard Graphic Plotter (7203A). The microprocessor also controlled an X-Y plotter (Rikadenki Kogyo Company Limited) to give hard copies of the averaged waveforms for routine inspection and comparisons.

### D3.2 CONTRALATERAL FIELD POTENTIALS

Field potentials recorded from the hyperstriatum subsequent to stimulation of the contralateral eye characteristically showed a negative waveform lasting for 10-20mS, followed by a slower and smaller positive wave. Occasionally, a very small and variable positive deflection was seen to precede the negative wave. Peak amplitudes of the negative waves were between 0.2 and 0.5mV. No reversals or inversions of polarity were found, and any variations from the simple

negative-positive waveform were interpreted as being produced by superimposed unitary activity. In any single penetration through a responsive area, the main variations of the waveform with depth were found to be those of amplitude and latency. At recording stations giving maximal or very large field potential responses, evoked unitary activity often was found to be present and synchronous with the slow potential - however, units whose latency was longer than that of the field potentials, but which were also reliably driven by the stimulation, were isolated throughout the area of the hyperstriatum which yielded field potential responses. (This is discussed in Section E, Chapter E4). Careful control of electrode tip diameter and recording bandwidth were necessary in order to obtain averaged field potentials which were not unduly affected by superimposed unit responses. Replacement of recording electrodes in previously sampled areas of the Wulst revealed the recorded potentials to be consistent and reproducible over the recording periods in any one experiment. (The longest survival time of a 100g chicken was 19 hours, giving a maximum recording time of approximately 15 hours.)

Figure D8 illustrates a typical series of contralateral field potentials, together with the location of the electrode penetration. This penetration was made with the head at orientation H1 (see Section B, Chapter B3). The stimulus was applied directly to the contralateral optic papilla at level 2 (see Figure D4). The transverse section plan shown in Figure D8C was traced from the projected histological

section. The position of the electrode penetration, shown in Figure D8C, was reconstructed relative to the lesion. The penetration has been marked at the 0.2mm intervals used to record the potentials shown in Figure D8A. The responses were localised throughout the depth of HA, and in IHA. A number of maxima are apparent, and the peak latencies decrease with the depth of recording. The largest and earliest potential occurs at a depth of 1.8mm, and is located within IHA, just ventral to the HA/IHA border. It can be seen that this field potential is very 'spiky', reflecting a large amount of evoked unitary activity at this depth. The evoked field potentials disappear at a depth of 2.2mm, at the IHA/HISM border.

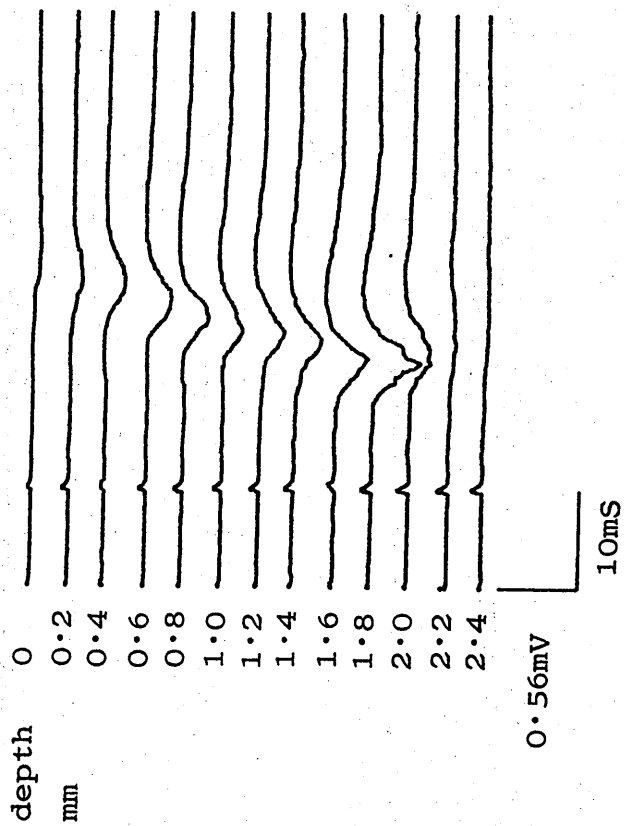
Initially, electrode penetrations were made to depths of 3-4mm, sampling the whole of the vertical extent of HV, and sometimes the neostriatum. However, as none of these penetrations revealed any activity below IHA, subsequent penetrations, such as the example shown in Figure D8, were all made to depths of between 2.2 and 3.0mm only.

No attempt was made to interpret the negative field potentials in terms of their relation to the synaptic organisation of the retino-Wulst pathway, due to the lack of information regarding the connectivity of the thalamic relay (see Section A, Chapter A3). It is therefore only assumed that the field potentials recorded from the Wulst represent the activity evoked in the hyperstriatal terminal fields of a polysynaptic visual projection to this area. The consistent

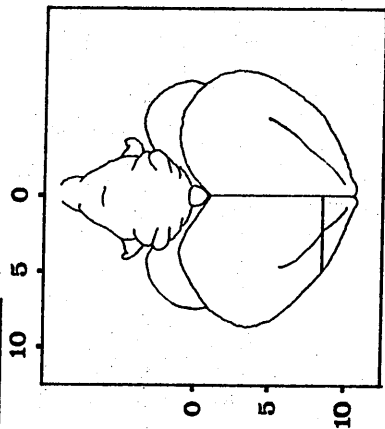


FIGURE D8 CONTRALATERAL FIELD POTENTIALS

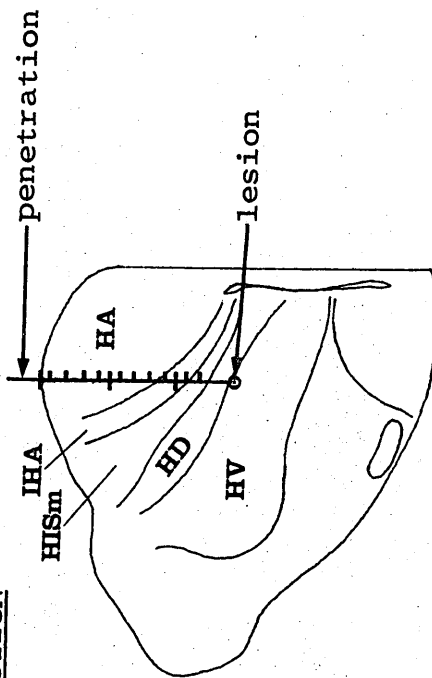
A AVERAGED WAVEFORMS



B LEVEL OF SECTION



C PLAN OF SECTION



negative-positive field potentials are interpreted as being the reflection of the sum of transmembrane currents in the immediate area of the electrode tip. The analysis of field potentials recorded at 0.1mm intervals (see Chapter D2.2), suggests the area of tissue sampled by the electrode tip is of the order of 100-200 $\mu$  in diameter. The early, large negative potentials are further interpreted as indicating a fairly synchronous burst of activity in the deep Wulst following electrical stimulation of the contralateral optic papilla. (Further discussion of this point is given in Section E, Chapter E4).

All evoked potentials exhibited marked frequency attenuation, shown by a 50% decrease of amplitude at a stimulus frequency of 2Hz.

### D3.3 IPSILATERAL FIELD POTENTIALS

Figure D9 illustrates a typical series of ipsilateral field potentials, together with the location of the electrode penetration. These potentials were recorded from the same penetration as the contralateral potentials illustrated in Figure D8. The stimulus was again applied directly to the optic papilla at level 2 (see Figure D4). Ipsilateral responses were always very much smaller than contralateral responses, typical ipsilateral peak amplitudes being between 0.03 and 0.06mV. As shown in Figure D9A, ipsilateral responses only exhibited a single maximum in any one vertical series. The duration of ipsilateral responses was very

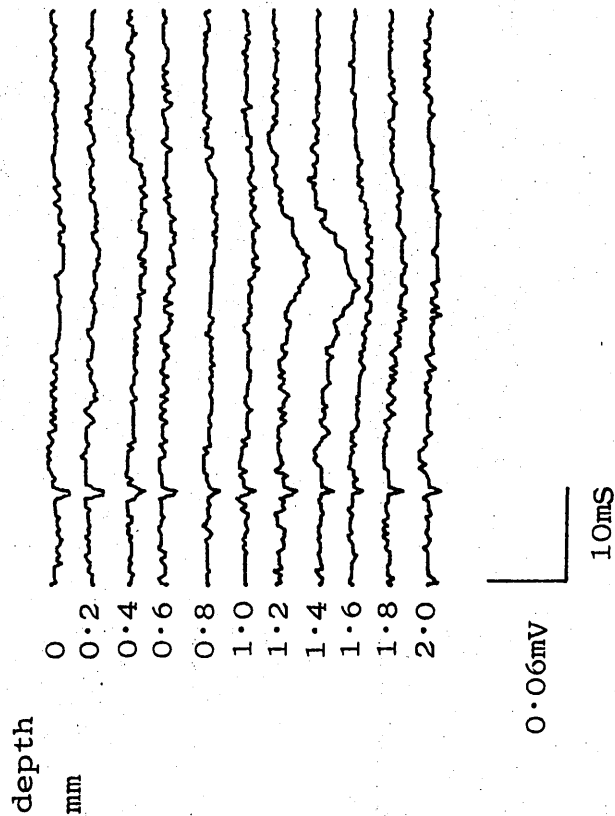
variable, ranging between 15 and 30ms. The ipsilateral response could only be obtained from very small areas of the Wulst. The largest and earliest response in the example shown in Figure D9 is located at a depth of 1.4mm, in the ventral region of HA. Ipsilateral responses were always recorded in this area, no responses being obtained from the IHA or dorsal HA, HISm, HD or HV.

Comparison of the localisation of the contralateral responses shown in Figure D8, and that of the ipsilateral responses shown in Figure D9 reveals the ipsilateral response to be located within the contralaterally responsive area of the ventral HA. Electrode penetrations which sampled ipsilateral activity were always found to pass through contralaterally responsive areas both dorsal and ventral to the location of the ipsilateral response.

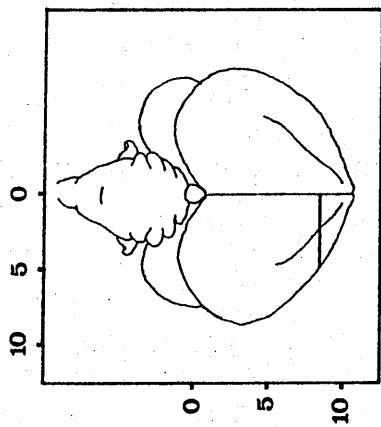
The assumptions and interpretations made for the contralateral responses (Chapter D3.2) were also made for the ipsilateral field potentials. However, the small size and long duration of the ipsilateral responses were further interpreted as indicating the ipsilateral terminal field to be smaller than the contralateral field, and the ipsilateral response to be less synchronous than the contralateral responses recorded from the same area.

FIGURE D9 IPSILATERAL FIELD POTENTIALS

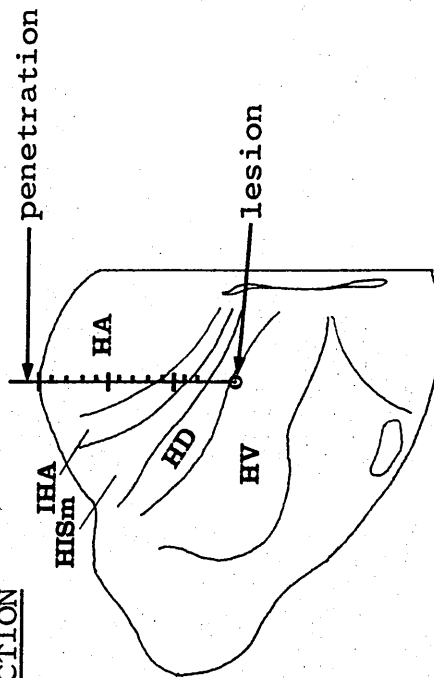
A AVERAGED WAVEFORMS



B LEVEL OF SECTION



C PLAN OF SECTION



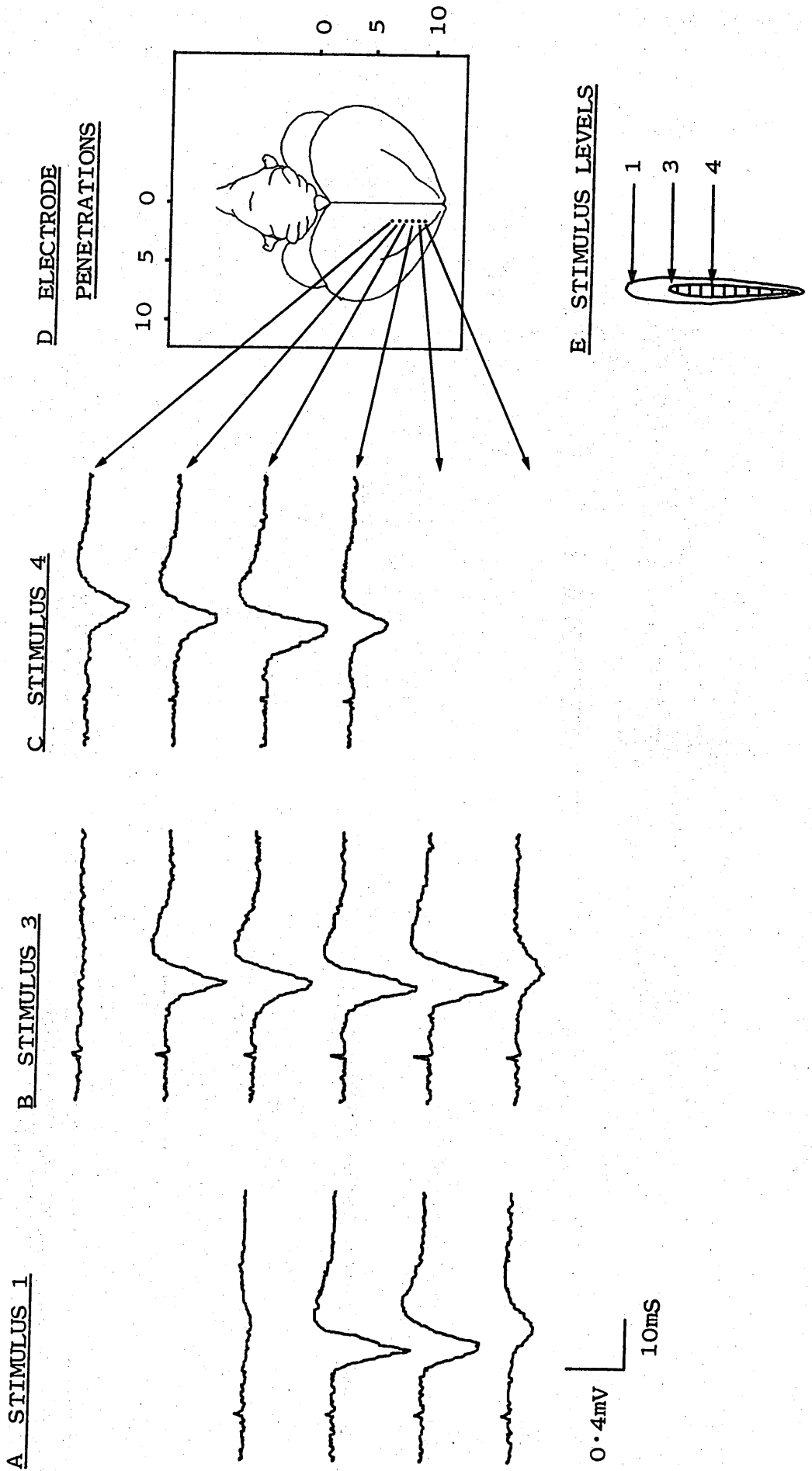
### D3.4 RESPONSIVE AREA OF FOREBRAIN

#### D3.4.1 Contralateral responsive area

In the early stages of this study, it became apparent that a definite relationship existed between the position of the stimulus electrode along the superior-inferior axis of the contralateral optic papilla and the position of the maximum response along the anterior-posterior axis of the forebrain. The results from a typical experiment designed to examine this relationship are presented in Figure D10. Column A shows the early, deep maximum potential recorded from each of four electrode penetrations in response to direct stimulation of the contralateral optic papilla at level 1 (see inset E). Similarly, column B shows the maximum responses to stimulation at level 3, and column C shows the maximum responses to stimulation at level 4. A definite retino-Wulst topography was established; the consistent finding throughout the study, as shown in the example in Figure D10, was that the more inferior the stimulus placement on the contralateral optic papilla, the more posterior the location of the maximum response in the Wulst. Furthermore, stimulation of the portion of the optic papilla between stimulus levels 2 and 3 (see Figure D4) activated the largest area of the Wulst.

Maximum deep responses were obtained typically from electrode penetrations placed between 1.3 and 1.7mm laterally from the midline. Figure D12A shows the total area of the Wulst found

FIGURE D10 DISTRIBUTION OF CONTRALATERAL RESPONSES



to be responsive to stimulation of the contralateral optic papilla. (Figures D12A and D12B summarise data obtained from 100 vertical penetrations made throughout the Wulst in 14 chickens; investigation of the different contralateral and ipsilateral stimulus placements yielded 202 potential series from the 100 penetrations). The contralaterally responsive area is shown mapped upon a dorsal view of the brain at orientation H1. The responsive area extends 3.5-4.0mm along the anterior-posterior axis of the Wulst. No responses were found in the most anterior 0.5-1.0mm of the Wulst. Responses showed a graded reduction in amplitude at locations either side of the maximal 1.3-1.7mm central strip, disappearing completely within 0.5-1.0mm of the midline, and 0.5-1.0mm of the vallecule.

Although stimulation of the superior regions of the contralateral optic papilla resulted in activation of the largest area of the Wulst, it is not possible to determine from these results whether this phenomenon constitutes a true magnification or over-representation of a particular area of the retina. If the chicken retina is organised in an identical manner to that of the pigeon (see Polyak, 1941; Bingelli and Paule, 1969), then the superior optic papilla may indeed receive axons from the laterally situated fovea. However, the superior region of the optic papilla in the chicken is noticeably wider than inferior regions (see Figure D4), and so direct stimulation, using the present methods, may simply result in the stimulation of larger numbers of axons in the superior regions.

### D3.4.2 Ipsilateral responsive area

Responses to stimulation of the ipsilateral optic papilla were obtained from a very restricted area, located deep within the contralaterally responsive HA. Figure D11 shows a typical distribution of maximum responses recorded following the direct stimulation of the ipsilateral optic papilla at level 2. All of these responses were located in the ventral HA, and could be recorded only over a vertical distance of 0.2-0.6mm. Stimulation of the ipsilateral optic papilla at levels inferior to level 2 did not result in any response.

Figure D12B illustrates the ipsilaterally responsive region of the Wulst. Although the responsive region is represented on a dorsal view of the brain, it should be remembered that the region lies deep within the Wulst. The region covered an area of only  $0.5-1\text{mm}^2$ , and was located within the medial, anterior region of the contralaterally responsive Wulst. Due to the smallness of this region, and the fact that only stimulation of levels 1 and 2 of the ipsilateral optic papilla gave rise to field potential responses, it was not possible to determine whether a topographical relationship similar to that found between the contralateral optic papilla and the Wulst existed between the ipsilateral optic papilla and the Wulst.



FIGURE D1.1 DISTRIBUTION OF IPSILATERAL RESPONSES

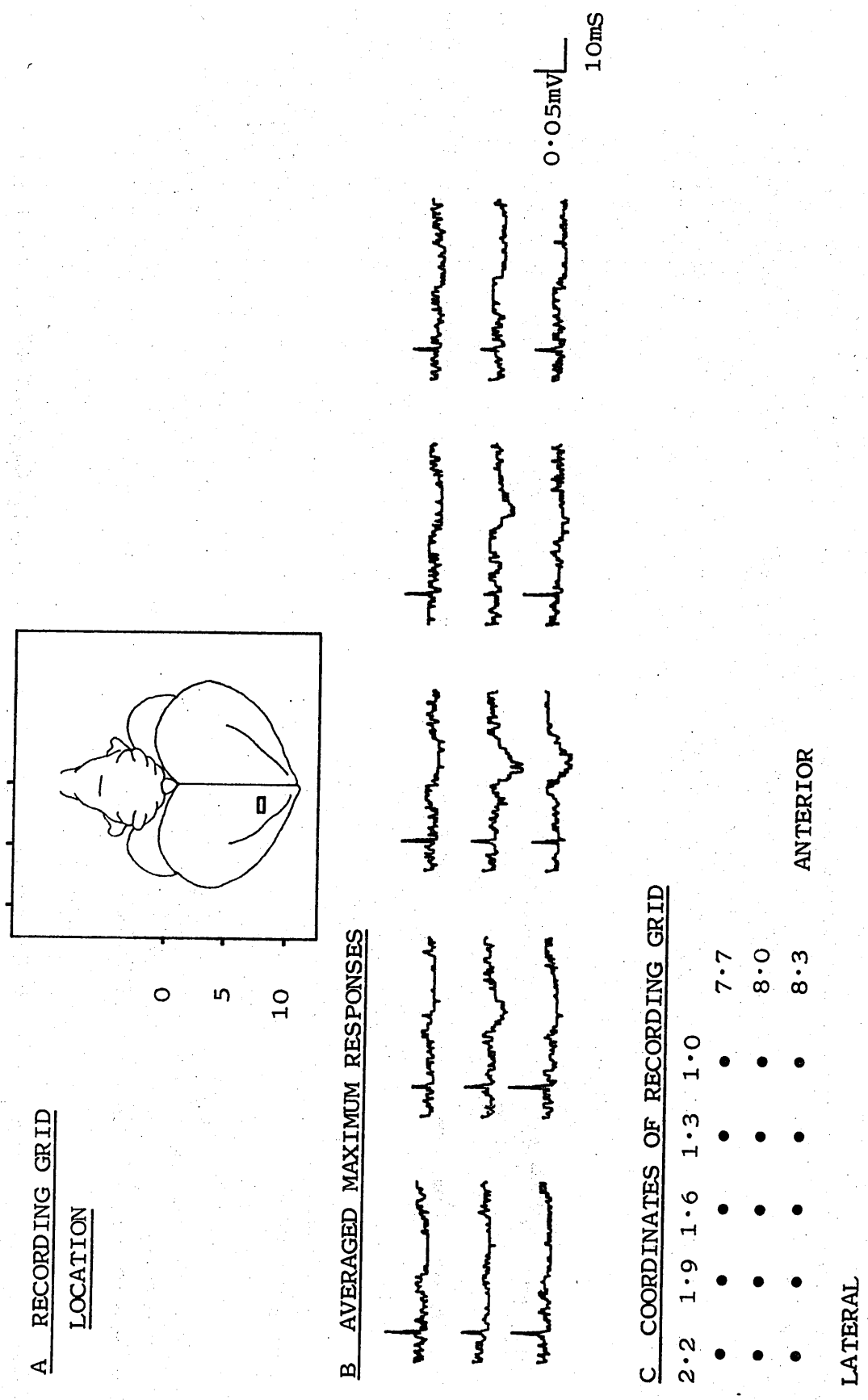
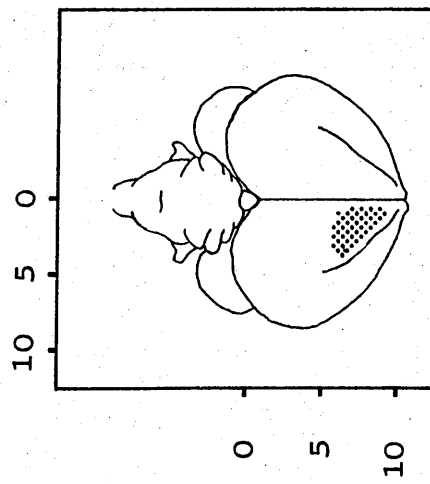


FIGURE D12 RESPONSIVE AREA OF FOREBRAIN (ORIENTATION H1)

A CONTRALATERAL

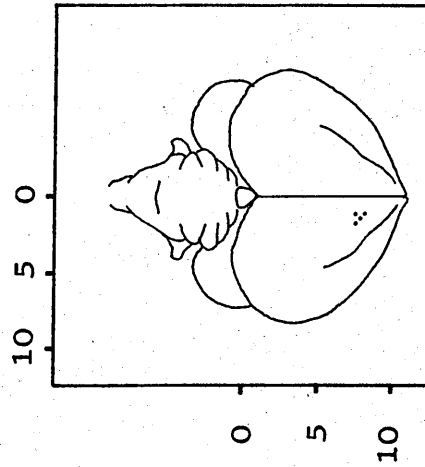


APPROXIMATE COORDINATES:

ANTERIOR 6.0-9.5

LATERAL 0.5-3.5


B IPSILATERAL



APPROXIMATE COORDINATES:

ANTERIOR 7.5-8.5

LATERAL 1.0-2.0

RESPONSIVE AREAS - 

D3.5 SUMMARY OF THE GENERAL PROPERTIES OF THE FIELD  
POTENTIALS

1. Contralateral field potentials showed a characteristically smooth negative-positive waveform. The major negative component had a duration of 10-20mS, and showed typical peak amplitudes of between 0.2 and 0.5mV.
2. Contralateral responses were located throughout the depth of HA, and in IHA.
3. Ipsilateral field potentials showed a characteristically small negative waveform, with a variable duration of 15-30mS. Ipsilateral peak amplitudes typically were between 0.03 and 0.06mV.
4. Ipsilateral responses were located in ventral HA, just dorsal to the HA/IHA border.
5. The contralaterally responsive area of the forebrain was limited to the Wulst. Maximum responses were obtained from medial regions of the Wulst.
6. The ipsilaterally responsive area of the forebrain was very small, and was located deep within the anterior region of the contralaterally responsive Wulst.
7. Contralateral responses evoked by stimulation of the inferior regions of the optic papilla were localised in the posterior Wulst, whilst responses evoked by stimulation of the superior regions of the optic papilla were localised in the anterior Wulst.

CHAPTER D4 : DORSOVENTRAL LAMINATION OF FIELD  
POTENTIALS

D4.1 DATA ANALYSIS

The results discussed in this chapter were obtained from comparisons of averaged evoked potentials, recorded from single vertical electrode penetrations. The potentials which were recorded following stimulation of the contralateral and ipsilateral optic papillae and/or retinae were compared to determine the vertical spatial organisation of the inputs from both eyes, and the latency relationships between the evoked potential peaks. Direct stimulation of the contralateral optic papilla was found to result in up to four negative potential peaks at different latencies, each peak occurring at a different vertical location along the electrode penetration. (See Chapter D3.2). Comparisons of many such vertical series' of waveforms became very difficult and time consuming, involving repeated calculations of amplitudes, and constant referral to the decimal printouts (see Chapter D3.1) in order to calculate latencies. Therefore, a system of representing the data was developed to enable easier visual comparison of the latency, magnitude and depth of field potentials obtained either from different penetrations, or from the same penetration in response to different stimulus placements. An example of the procedure will now be described in some detail.

The paper tape codes of the field potential data (see Chapter D3.1) were loaded onto computer disc. With the aid of programming assistance, Basic and Fortran software were developed to sort the data from single penetrations by computer (Nova 820, Data General), and to convert the voltage data into isopotential contours for VDU display and hard copying by the Hewlett Packard graphic plotter. An example of one of the resulting 'depth versus time' (DVT) contour plots, together with the vertical series of waveforms from which it was derived, is given in Figure D13. A relatively simple series of waveforms, recorded after stimulation of the contralateral retina, has been chosen for this example.

The first point to be stressed is that the derivation of the DVT plot from the field potentials involves no alteration of the data - it is simply a different representation of the information contained in the vertical series of potentials. Figure D13A shows the first 60ms (150 bins) of the averaged evoked potentials, including a pre-stimulus baseline of approximately 10ms. These potentials were recorded at 0.2mm intervals along a single vertical electrode penetration through the Wulst. Two negative maxima are evident, separated both spatially and temporally: an early peak is located at 1.4mm below the surface, and a later peak appears at 0.4mm below the surface. A simple exercise will enable the relationship between the potential series shown in Figure D13A and the DVT plot shown in Figure D13B to be appreciated.

If one were to imagine each of the averaged potentials to be rotated through 90 degrees towards the top of the figure, about the axis described by their baselines, they would project vertically from the surface of the paper. A

'mountain-valley' range would project from the plane of the paper, following a negative-up convention. The DVT plot is simply a contour representation of the voltage peaks and valleys. The valleys (ie. positive voltages) are indicated by hatching on the DVT plot.

As with any contour representation of a physical variable, one assumption has been made - that the variable changes in a linear fashion (in this case, with respect to time and depth). This assumption was felt to be valid in the case of voltage recordings made along a vertical penetration in the Wulst, as no myelinated fibre tracts are present in this area - therefore, the resistivity and conductance of the tissue may be assumed to be constant along a vertical penetration. Thus, the contours of isopotential in the DVT plot are drawn as straight lines joining points of equal voltage along the depth and time axes of the vertical potential series. The linear interpolation used is the simplest way to obtain contours, and does not alter the data in any way - each data point is used, and interpolations are only made at points where the contour values fall between recorded data point values.

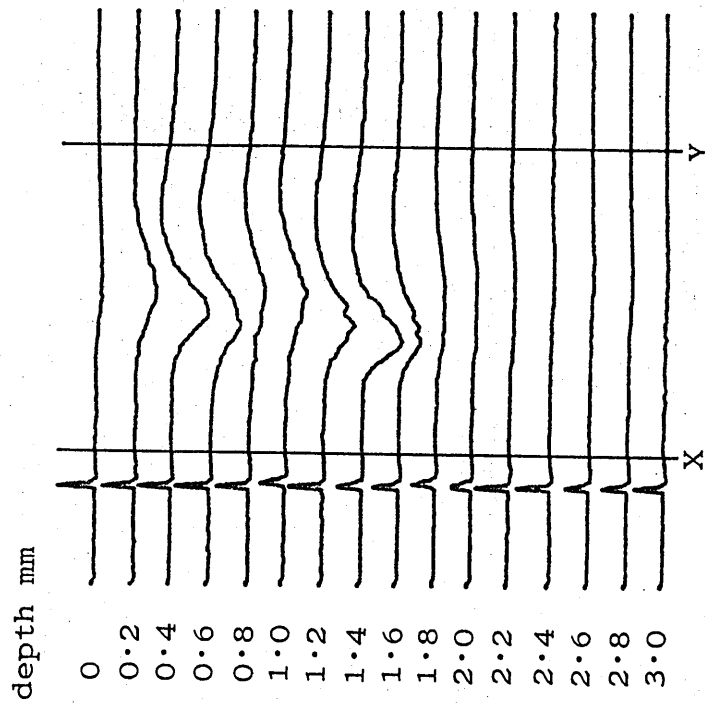
The vertical axis of the DVT plot in Figure D13B represents the depth of recording of the averaged potentials. The

horizontal axis of the DVT plot represents the time period between points X and Y on the field potential series in Figure D13A. This is equivalent to a sample time of 5.6-45.6mS after the stimulus artifact. The software operated in terms of time bins, and the sample interval of the DVT plot was variable in terms of the number of bins between each contour point on the horizontal time axis. The ticks on the horizontal axis of the DVT plot represent a sample interval of 2 bins (ie. 0.8mS) - the latency scale (in mS from the stimulus) was added subsequently. The contour step was also continuously variable, and was adjusted in each case to provide a suitable number and separation of contours from the field potentials being investigated. In this example, each isopotential contour represents a voltage increment of 20 $\mu$ V.

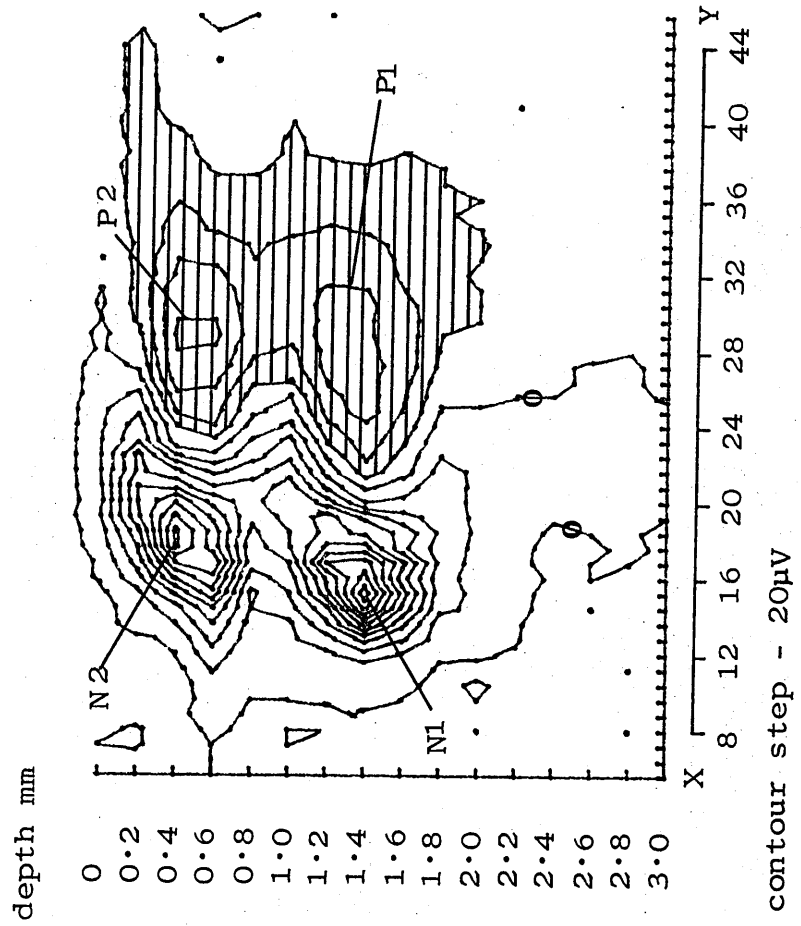
The DVT plot in this example (Figure D13B) describes the two negative peaks shown in the waveform series (Figure D13A), and would be interpreted as follows. The first negative peak (N1) occurs at a depth of 1.4mm below the surface of the brain, with a latency of 15.2mS, and an amplitude of 200 $\mu$ V; the second negative peak (N2) occurs at 0.4mm below the surface, with a latency of 17.6-18.4mS, and an amplitude of 180 $\mu$ V. The potentials shown in Figure D13A indicate that small positive deflections occur after the negative waves - the peaks of these deflections are shown at P1 and P2 on the DVT plot.

FIGURE D13 AVERAGED POTENTIALS AND DVT CONTOUR PLOT

A AVERAGED POTENTIALS



B DVT CONTOUR PLOT



contour step - 20µV  
 sample interval - 0.8ms  
 sample time - 5.6-45.6ms

0.42mV

10ms

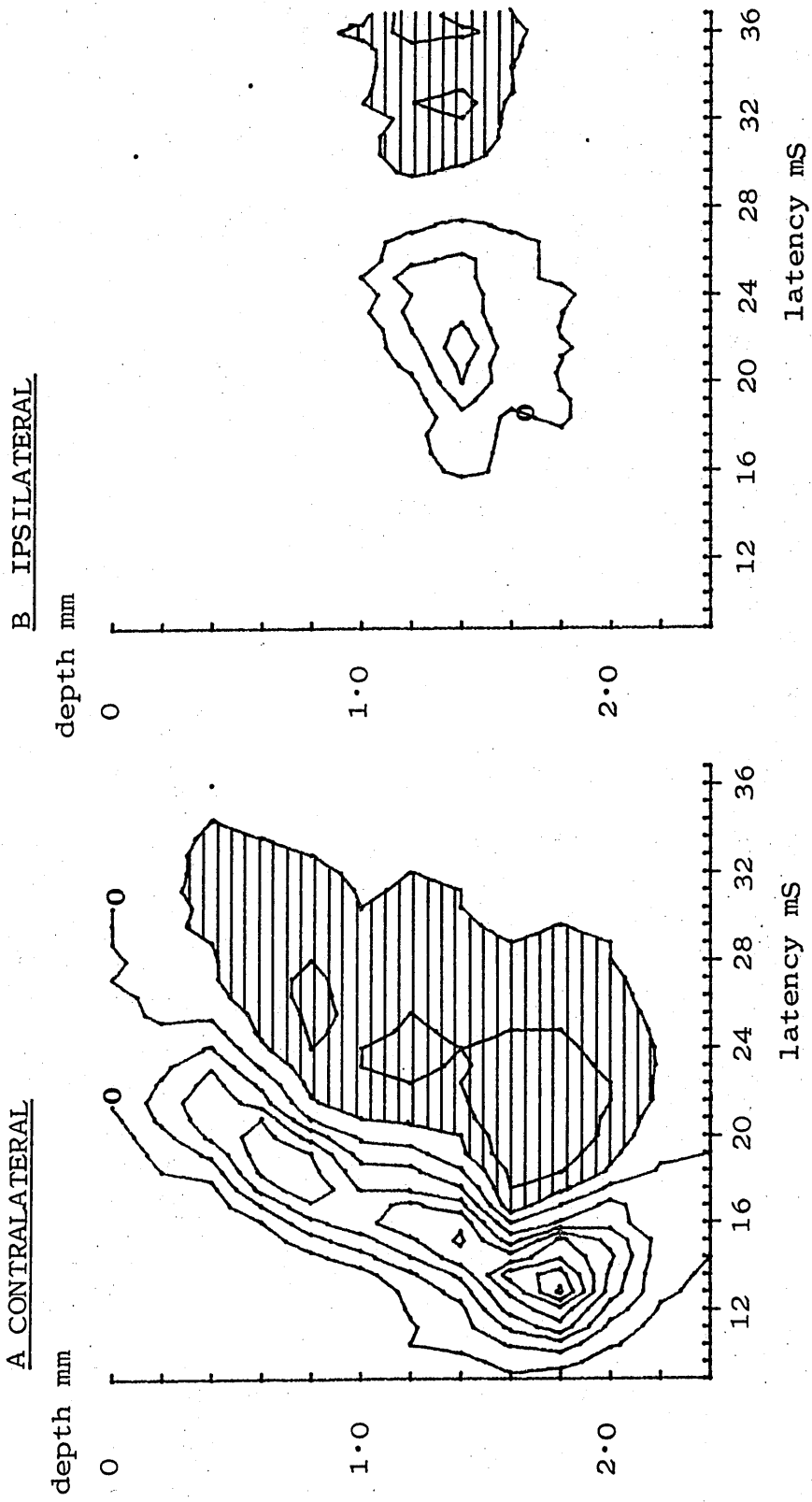


#### D4.2 RESULTS

Figure D14A illustrates the DVT analysis of the field potentials recorded in response to direct stimulation of the contralateral optic papilla. These potentials were recorded from a vertical penetration made at orientation H1 (see Section B, Chapter B3) through the medial Wulst. The waveform series exhibits three spatially separate maxima, having peak latencies of 12.8, 15.2 and approximately 17.6mS. Figure D14B illustrates the ipsilateral DVT plot derived from the field potentials recorded along the same electrode penetration to direct stimulation of the ipsilateral optic papilla. The ipsilateral response shows a single maximum, with a latency of 20.8mS. Comparison of Figure D14A and B shows the ipsilateral response to be located within the area of the contralateral response - the contralateral response extends between 0.2 and about 2.0mm below the brain surface, and the ipsilateral response extends between 1.2 and 1.6mm below the surface. This spatial relationship of the two responses is identical to that reported in Chapter D3.3.

Further analysis of the sequence of contralateral maxima along vertical penetrations, however, revealed additional aspects of the dorsoventral lamination of the visual input to the medial Wulst. Stimulation of the contralateral retina resulted in a different spatiotemporal pattern of potentials from that occurring after direct stimulation of the optic papilla. Thus, Figure D15 shows the DVT plots

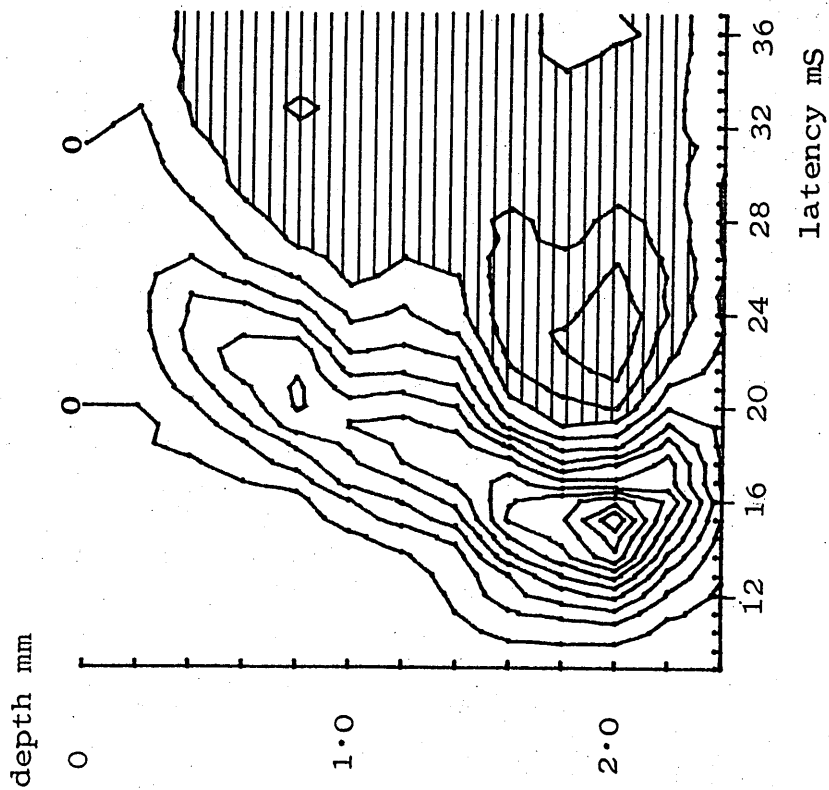
FIGURE D14 DVT 2309H1 DIRECT STIMULATION OF OPTIC PAPILLA



derived from contralateral waveforms recorded from the same position as those in Figure D14A, but with the stimulus electrode moved to retinal placements 0.5mm anterior (D15A) or posterior (D15B) to the optic papilla. Comparison of Figures D15A and B shows two maxima resulting from both stimulus conditions, one superficial and one deep. The early, deep maximum has a latency of 15.2ms in both cases; the late, superficial maximum has a latency of approximately 19-20ms in both cases. Although showing similar latencies, however, the two superficial responses are spatially separate. The anterior superficial maximum is located 0.8mm below the surface, whilst the posterior superficial maximum is located 1.2mm below the surface. Similarly, the two deep maxima occur at different depths, although some overlap of the deep responses is evident. Thus, the anterior deep response occurs mainly between 1.8 and 2.0mm, whilst the posterior deep response occurs mainly between 1.6 and 1.8mm. It was found typically that the two deep responses showed a maximum either at the same depth, or, as shown in the example in Figure D15, at depths separated by only 0.2mm. The two superficial maxima, however, were never recorded from the same location - the anterior superficial response always occurred dorsally to the posterior superficial response area. The interpretation of these results is that the complex sequence of waveforms obtained to direct stimulation of the contralateral optic papilla (Figure D14A) results from the addition of responses due to simultaneous stimulation of at least two separate retinal fibre groups: one arising from the anterior or nasal retina, and one from the posterior

FIGURE D15 DVT 2309H1 RETINAL STIMULATION

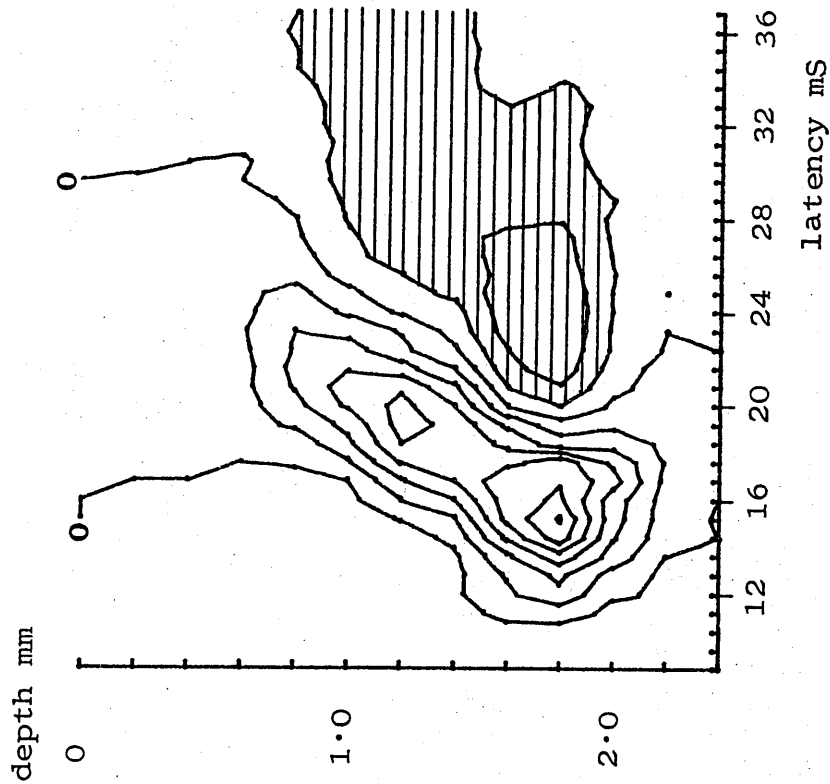
A ANTERIOR RETINA



contour step - 20 $\mu$ V

sample interval - 0.8mS

B POSTERIOR RETINA

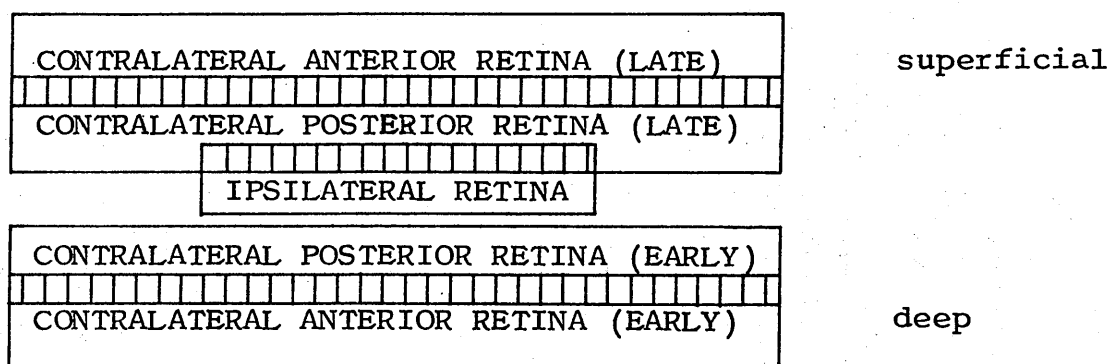


contour step - 20 $\mu$ V

sample interval - 0.8mS

or temporal retina. Furthermore, both of these fibre groups give rise to two spatially and temporally separate responses in the medial Wulst when stimulated electrically.

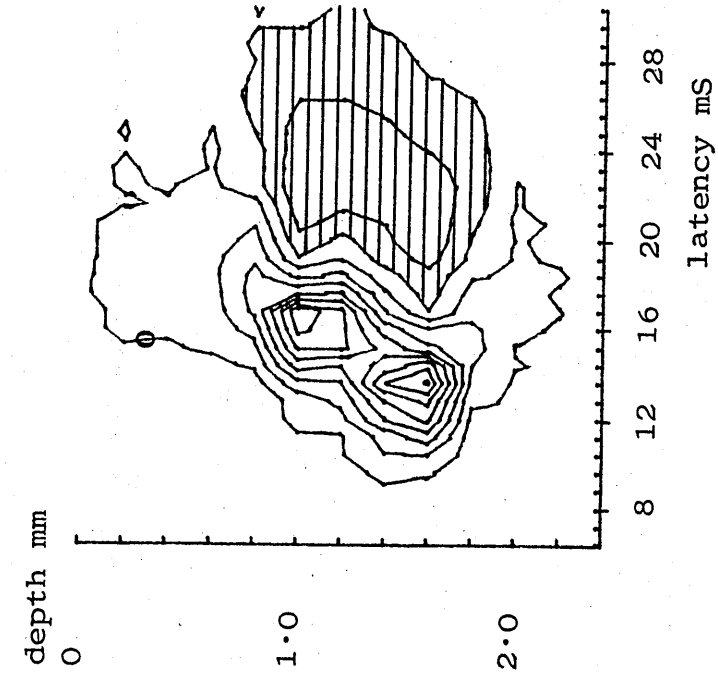
Comparison of Figure D14B with Figures D15A and B shows the single ipsilateral response to lie between the deep and superficial contralateral responses. Furthermore, the ipsilateral response overlaps the posterior contralateral response at 1.2mm below the surface, the ipsilateral maximum occurring at 1.4mm, and the posterior superficial maximum occurring at 1.2mm. The interpretation of these results may be summarised as follows. Along vertical penetrations in the medial Wulst, the lamination of visual inputs shows the following pattern:



Overlapping areas of input are indicated by hatching - these are areas where responses could be recorded in the same location, or where responses were separated only by one recording interval step (0.2mm).

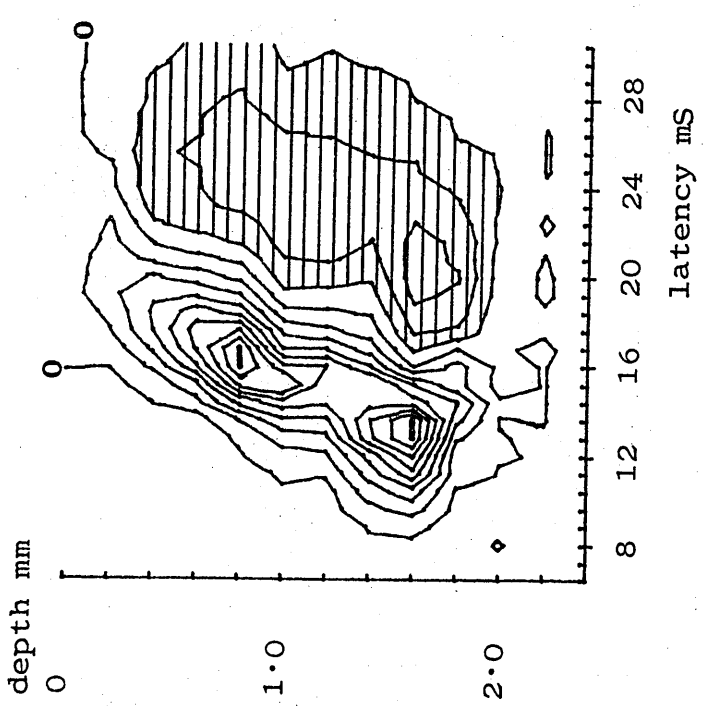
The superficial contralateral maxima shown in Figures D15A and B are smaller than the corresponding deep maxima. This was a typical finding of all the DVT analyses of potentials

recorded at orientation H1. Comparison of such potentials recorded from penetrations arranged along the anterior-posterior axis of the Wulst (in response to a constant stimulus placement) showed that the H1 orientation placed the superficial maximum in front of the vertical plane which passed through the deep maximum. Thus, H2 was adopted later to obtain maximal superficial and deep responses from single vertical penetrations. Furthermore, to ensure that the dorsoventral lamination of responses to stimulation of the contralateral anterior and posterior retina was not an artifact resulting from repeated penetrations at the same point, and/or re-placements of the stimulus electrode on the retina, two bipolar electrodes were attached to a single microdrive and positioned simultaneously on the retina. Thus, recordings of responses to either stimulus placement could be obtained from a single penetration. The results from these experiments, recorded at orientation H2, were consistent with the pattern of lamination derived from the experiments using orientation H1. Figure D16 illustrates the DVT plots derived from potentials recorded at orientation H2 in response to stimulation of the contralateral anterior retina (D16A) and the contralateral posterior retina (D16B) using two linked sets of stimulus electrodes. These figures show the contralateral superficial responses to be of a similar magnitude to the contralateral deep responses. This example shows the two deep maxima to occur at the same depth, whilst the anterior superficial response is located dorsally to the posterior superficial response.



contour step - 30 $\mu$ V  
sample interval - 0.8mS

A ANTERIOR RETINA



contour step - 30 $\mu$ V  
sample interval - 0.8mS

B POSTERIOR RETINA

FIGURE D16 DVT 0706H2 RETINAL STIMULATION

### D4.3 LATENCY CONSIDERATIONS

Comparison of the peak latencies for contralateral potentials recorded from different penetrations, but to the same stimulus, indicated that there was a complex movement of negativity in both the transverse and sagittal planes. Latencies of the potentials recorded from penetrations along these planes were all different, suggesting a spread of activity emanating from a particular locus. (This will be described in detail in Chapter D5). Thus, comparison of deep and superficial peak latencies, both within and between penetrations, was difficult except for those experiments where a spatial distribution of penetrations showed that the earliest events had been sampled. The earliest potentials isolated were obtained from the medial Wulst area shown to be the location of maximum responses (see Chapter D3.4.1). Furthermore, only comparison of those contralateral maxima obtained by discrete stimulation of the retina were meaningful, due to the addition of potentials resulting from direct stimulation of the optic papilla (see Chapter D4.2) and the consequent appearance of spurious peaks.

Therefore, an analysis was made only of the peak latencies of responses recorded from penetrations in the medial Wulst giving both superficial and deep maxima (ie. at orientation H2 - see Chapter D4.2) to retinal stimulation at level 2 (see Figure D4), and showing the earliest events from a spatial distribution of penetrations in each experiment. The contralateral latencies were also compared to the ipsilateral latencies recorded under the same conditions.



Figure D17 tabulates the mean peak latency (MPL), standard deviation (sd) and range for the responses fitting the above criteria. The data presented in this figure were obtained from 32 penetrations made in 8 chickens.

FIGURE D17 : MEAN PEAK LATENCY (MPL) AND RANGE FOR  
CONTRALATERAL AND IPSILATERAL POTENTIALS (mS)

STIMULUS	EVOKED POTENTIAL					
	DEEP			SUPERFICIAL		
	MPL	sd	RANGE	MPL	sd	RANGE
CONTRA ANTERIOR	14.3	<u>+0.7</u>	13.2-15.2	18.5	<u>+1.6</u>	16.4-21.2
CONTRA POSTERIOR	14.9	<u>+1.0</u>	13.6-16.0	17.2	<u>+0.9</u>	16.4-18.8
IPSI	21.8	<u>+3.0</u>	16.0-25.6			

As the standard deviations of the sample means vary considerably, the Mann Whitney U test (two-tailed) was used to test for differences between the means, rather than Student's t-test.

No significant differences were found between the deep contralateral anterior latency and the deep contralateral posterior latency; similarly, there was no significant difference between the two contralateral superficial latencies. As can be seen from Figure D17, the two deep response means and ranges are almost identical, as are the two superficial means and ranges.

The two superficial latencies, however, are both significantly different from the two deep latencies ( $p < 0.01$ ). It is concluded that the deep and superficial field potential responses reflect activity in two separate latency populations of units.

The ipsilateral response latency was significantly different from the deep anterior response latencies ( $p < 0.01$ ), but there was no significant difference between the ipsilateral latency and the superficial anterior latencies. The initial, deep contralateral response, therefore, occurs earlier than the ipsilateral response - whether the ipsilateral delay is due solely to the longer pathway recrossing the midline at DSOD, or to thalamic circuitry, is not known (see Section A, Chapter A3). Interestingly, however, the similar response latencies of the ipsilateral input and the late, superficial contralateral input, suggest the capacity for the integration of information from both eyes in the Wulst. As shown in Chapter D4.2, the location of the ipsilateral response overlaps that of the superficial contralateral response to stimulation of the posterior contralateral retina. It is concluded, therefore, that the Wulst contains an area which may subserve the binocular integration of visual information. (The presence of single units in the Wulst which respond to stimulation of both eyes was investigated by the experiments reported in Section E).

#### D4.4 SUMMARY OF THE DORSOVENTRAL LAMINATION OF THE FIELD POTENTIALS

1. Stimulation of the contralateral anterior retina resulted in two spatially separate field potentials: an early response (mean peak latency, MPL,  $14.3 \pm 0.7\text{ms}$ ) which was located deep within the Wulst; and a later response (MPL  $18.5 \pm 1.6\text{ms}$ ) located in the superficial Wulst.
2. Stimulation of the contralateral posterior retina resulted in two spatially separate field potentials: an early response which was located deep in the Wulst (MPL  $14.9 \pm 1.0\text{ms}$ ); and a later response (MPL  $17.2 \pm 0.9\text{ms}$ ) located more superficially in the Wulst.
3. The contralateral anterior deep maximum was recorded typically from either the same depth as the contralateral posterior deep maximum, or  $0.2\text{mm}$  ventral to the posterior deep maximum. The contralateral anterior superficial maximum was always located dorsally to the posterior superficial maximum.
4. Stimulation of the ipsilateral optic papilla gave rise to a single response (MPL  $21.8 \pm 3.0\text{ms}$ ), located above the deep contralateral responses, and overlapping the superficial posterior contralateral response.
5. Analysis of the mean peak latencies of the field potentials recorded from the medial Wulst indicated that the deep and superficial contralateral responses reflected activity in two separate latency populations of units. The ipsilateral response latency was longer than the deep

contralateral latencies. There was no significant difference between the ipsilateral response latency and the superficial contralateral latencies.

6. The results indicate the capacity for the integration of binocular information within the Wulst.

CHAPTER D5 ; SPATIOTEMPORAL PATTERN OF FIELD  
POTENTIALS

D5.1 INTRODUCTION

As mentioned in Chapter D4.3, the analysis of the latencies of field potentials recorded from spatially separate penetrations indicated that the negative potentials showed a specific sequence of events, and travelled in particular directions. This was investigated further by recording field potentials from regular grids of penetrations made in the transverse and sagittal planes. The results of these experiments are presented in this chapter. The data obtained from the recording grids were used to generate isopotential contour maps (ISO). The ISO maps were superimposed upon tracings of histological sections taken at the levels of the recording grids, and show the precise depth and extent of the field potential activity across two dimensional slices of the Wulst.

Consistent and reproducible results were obtained from the analysis of 120 penetrations made in 6 chickens. The experimental design restrictions discussed fully in Section B, Chapter B3, preclude the presentation of combined data from different animals. Therefore, the following results are presented as an example of the general findings, and consist of data obtained from individual chickens recorded after stimulation of the contralateral and ipsilateral retina or

optic papilla.

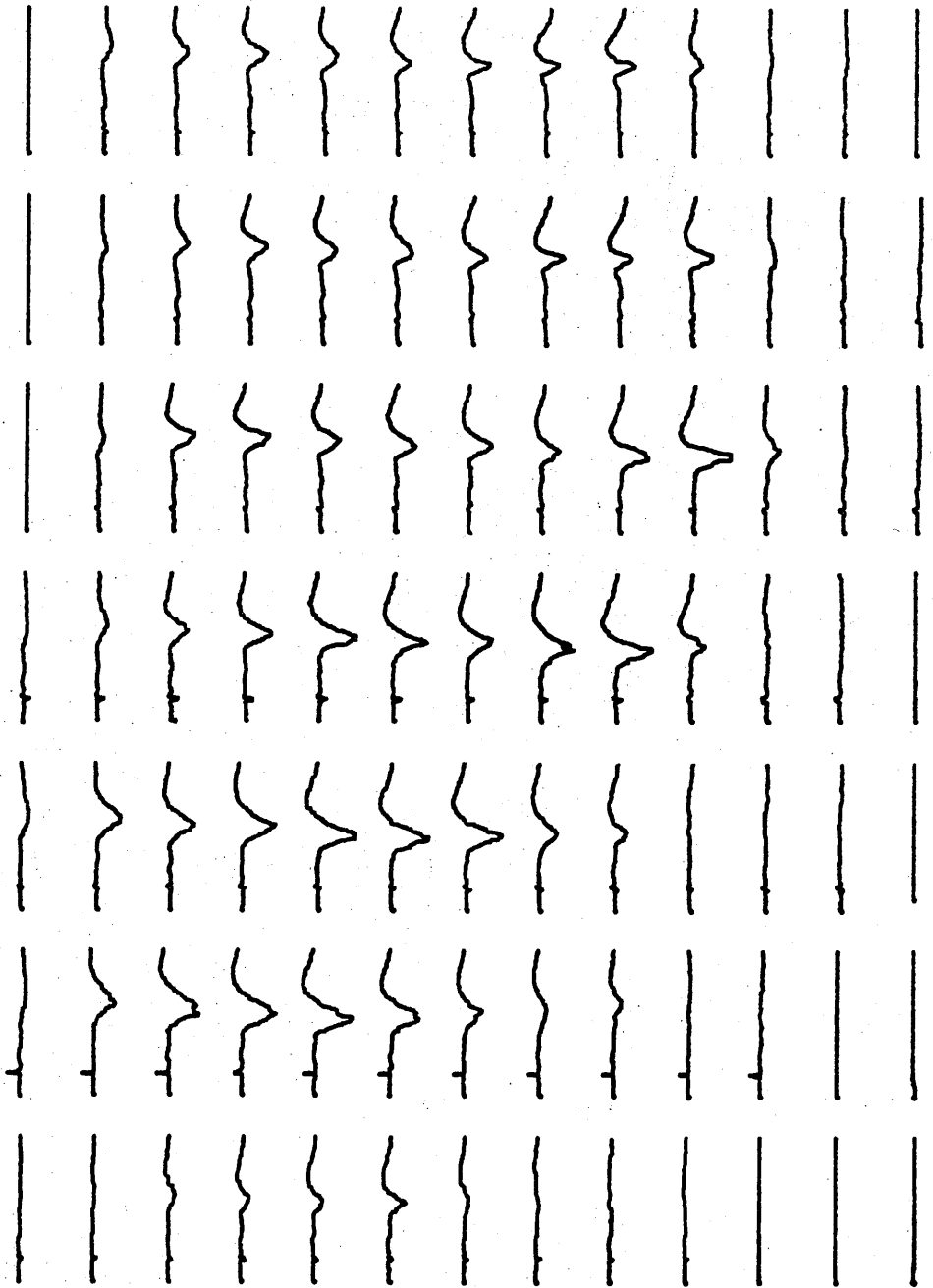
## D5.2 DATA ANALYSIS

The ISO contour maps presented in this chapter differ from the DVT contour plots discussed in Chapter D4 - DVT plots analysed the data obtained from individual electrode penetrations, whereas ISO maps analyse the information obtained from a two dimensional spatial grid of recording stations. This grid is formed by the regular separation of a number of electrode penetrations. The ISO computer programme makes the same assumptions of linearity discussed in Chapter D4.1, but the isopotential contours are plotted within two spatial axes, rather than within the spatial versus temporal axes of the DVT plots.

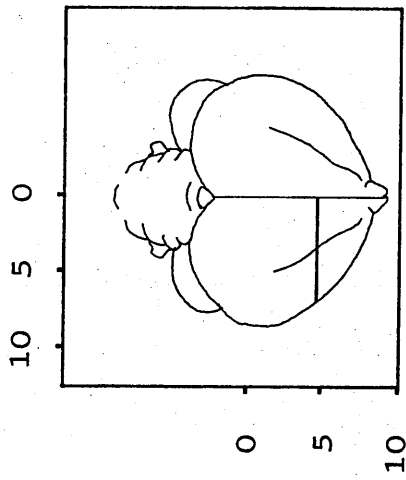
A typical example of the raw data used to generate a series of ISO maps is shown in Figure D18A. The location of the recording grid is shown in Figure D18C. All of the recordings discussed in this Section were obtained from experiments using orientation H2 (see Chapter D4.2, and Section B, Chapter B3). This example shows 7 electrode penetrations made at 0.2mm lateral intervals across the transverse plane of the Wulst. Recordings of field potentials were made at 13 0.2mm vertical intervals along each penetration. The stimulus in this example was delivered to the contralateral anterior retina. The ISO contour maps were designed to indicate the magnitude of the voltage changes across the recording grid at any particular time after the stimulus.

FIGURE D18 DATA OBTAINED FROM TYPICAL TRANSVERSE RECORDING GRID

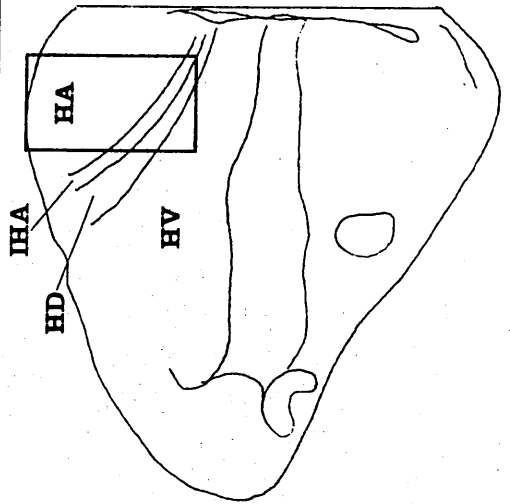
A AVERAGED POTENTIALS



B LEVEL OF SECTION



C LOCATION OF RECORDING GRID



They are spatial maps in the true sense, representing the voltage distribution across the tissue slice as isopotential contours. To illustrate the temporal sequence of voltage change across the slice, a sequence of 'frames' is presented for each case under study, the sequence covering the time period of field potential activity after the stimulus. The particular time instant represented by each frame will be indicated by both the latency (T) from the stimulus artifact in mS, and the bin number (B).

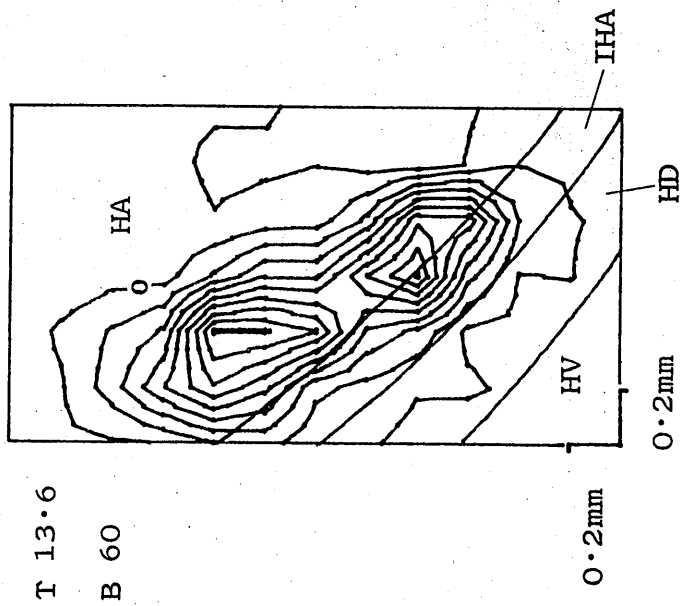
An example of one such ISO frame, derived from the data in Figure D18A, is given in Figure D19A. This frame illustrates the location of isopotential contours across the transverse slice at 13.6mS (bin 60) after the stimulus. The contours have been plotted upon a projected tracing of the section shown in Figure D18C. The ISO software was designed so that the proportions of the contour map could be varied precisely to allow for the distortion of the tissue sections due to fixing, cutting and staining. Percentage distortions were calculated from lesion markings - typical values were lateral distortion 0%, vertical distortion 9-10% shrinkage. The ISO frame illustrated in Figure D19A shows two regions of negativity across the slice at 13.6mS latency: a deep region of activity on the HA/IHA border; and a more superficial region of activity within HA. As with the DVT plots, the ISO maps require no modification of the raw data - the maps simply represent the data in a different way.

Finally, as an aid to the visualisation of the information presented in the ISO frame shown in Figure D19A, Figure D19B



FIGURE D19 ISO CONTOUR MAP

A ISO



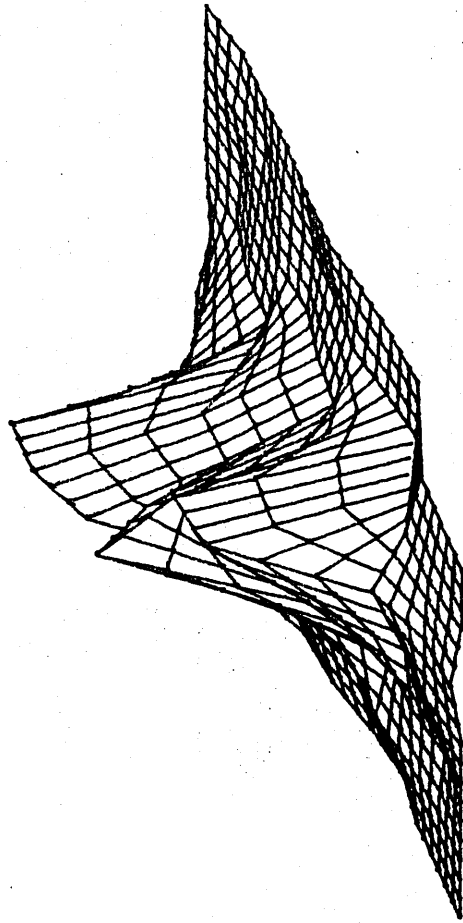
T 13.6

B 60

0.2mm

0.2mm

B TOPRE



shows a three-dimensional, negative-up representation of the contour map. The software needed to generate such 3-D maps (TOPRB) was developed initially to provide simple visual comparisons of the voltage activity across different tissue slices, or across the same slice to different stimulus positions. However, the angled view of the TOPRB plots, necessary to obtain a visually recognisable 3-D picture, meant that the histological sections had to be rendered with an identical angular distortion. This was found to be difficult to accomplish by hand, and was thought to result in a less accurate picture of the location of the voltage changes relative to the hyperstriatal laminae than that provided by the ISO maps. Thus ISO maps were used exclusively for the analysis of the spatiotemporal variation of voltage across the tissue slices.

The ISO frames to be presented in this chapter have the zero (baseline) contour marked with a nought. All positive voltages are indicated by horizontal hatching, or by stippling, added by hand.

### D5.3 TRANSVERSE DISTRIBUTION OF POTENTIALS

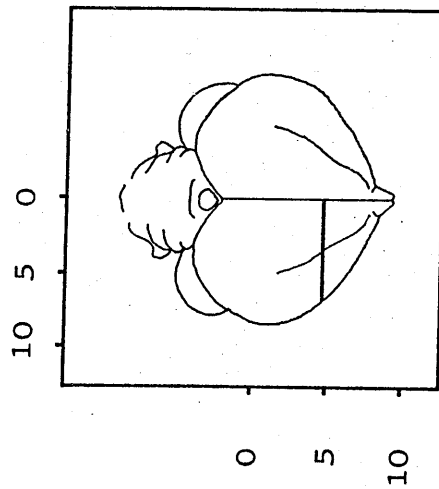
#### D5.3.1 Contralateral transverse potentials

The first series of ISO maps which will be discussed in this chapter were derived from potentials recorded after stimulation of the contralateral anterior retina. The sequence, but not location, of potentials resulting from posterior retinal stimulation was found to be identical to that resulting from anterior retinal stimulation. Therefore, the anterior series of ISO frames only is presented in detail for clarity, and illustrates the sequence of events across a transverse slice of the Wulst following discrete stimulation of the contralateral retina. The differences between the locations of the anterior and posterior responses will be discussed later in this chapter (D5.3.2).

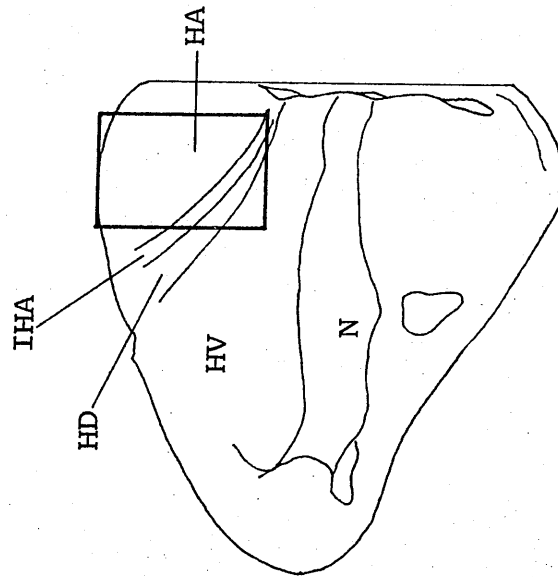
The location of the recording grid from which the recordings of the anterior potentials were made is shown in Figure D20. This was number 2 of 3 transverse grids made in this experiment, and passes through the anterior level of the maximum responses. Eight vertical penetrations were made at lateral intervals of 0.2mm. Recordings were taken at thirteen 0.2mm intervals along each electrode track. A total of 104 data points were used to generate the ISO maps. The maps are presented in Figure D21A and B. Every bin between bins 48 and 71 are shown in these figures to illustrate the sequence of events following anterior retinal stimulation in as much detail as possible. The ISO frames therefore illustrate the activity at 0.4mS intervals, and are identified

FIGURE D20 7JH2 LOCATION OF TRANSVERSE GRID 2

A LEVEL OF SECTION



B RECORDING GRID



by the bin number. The sequence covers the latency period of 8.8 to 18.0mS. The contour step is 30 $\mu$ V.

Considering the frames in Figure D21A in sequence, an initial development of both a deep region of activity in IHA, and a more superficial region of activity in HA, is evident. The IHA response first reaches 50% of its maximum amplitude at bin 55, and its maximum (240 $\mu$ V) at bin 58; the HA response first reaches 50% of its maximum amplitude at bin 57, and its maximum (also 240 $\mu$ V) at bin 59. Continuing the sequence in Figure D21B, the IHA response remains localised within IHA and around the HA/IHA border, falling to 50% of its maximum at bin 65. The HA response, however, becomes dispersed throughout HA, different areas showing maximal responses until bin 68, and does not fall to 50% of its maximum until bin 71. The IHA negative response has completely disappeared by bin 67, the responsive region becoming positive thereafter. This interpretation of these results suggests the following sequence of events:

1. initial activity arises in IHA;
2. activity then arises in HA, dorsal and lateral to the IHA response;
3. the HA activity persists after the disappearance of the IHA activity, and becomes dispersed throughout HA.

The timing of these events may be summarised as follows:

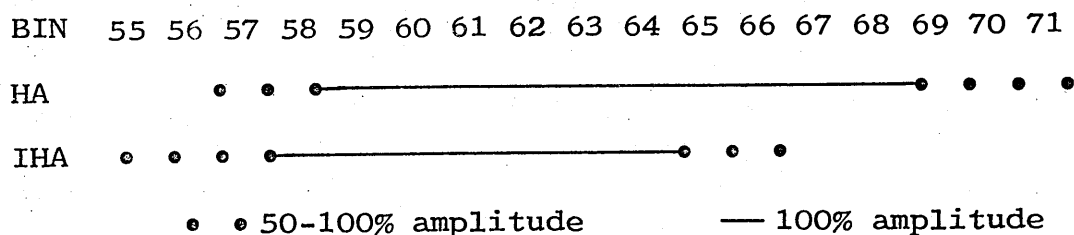
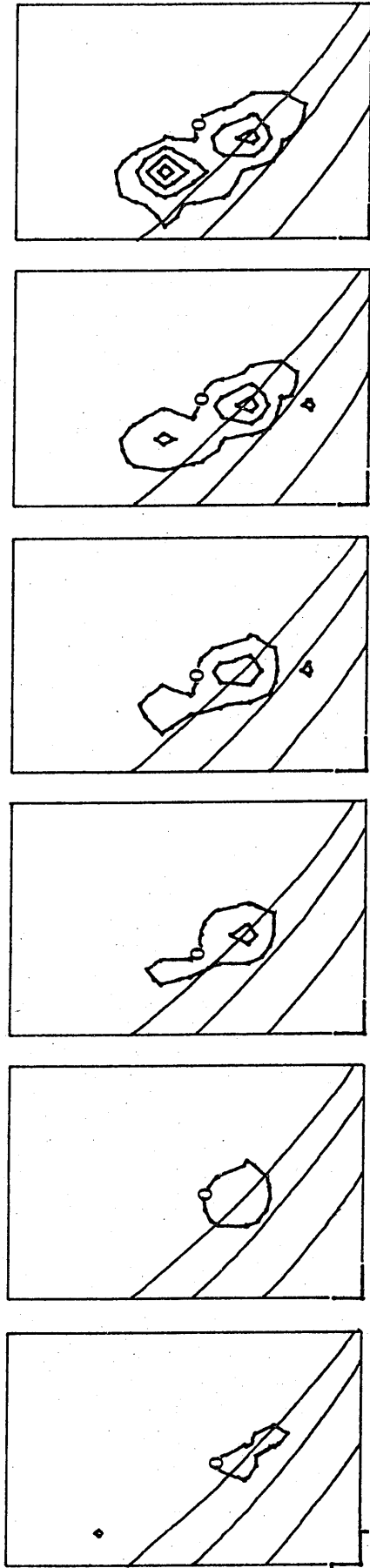
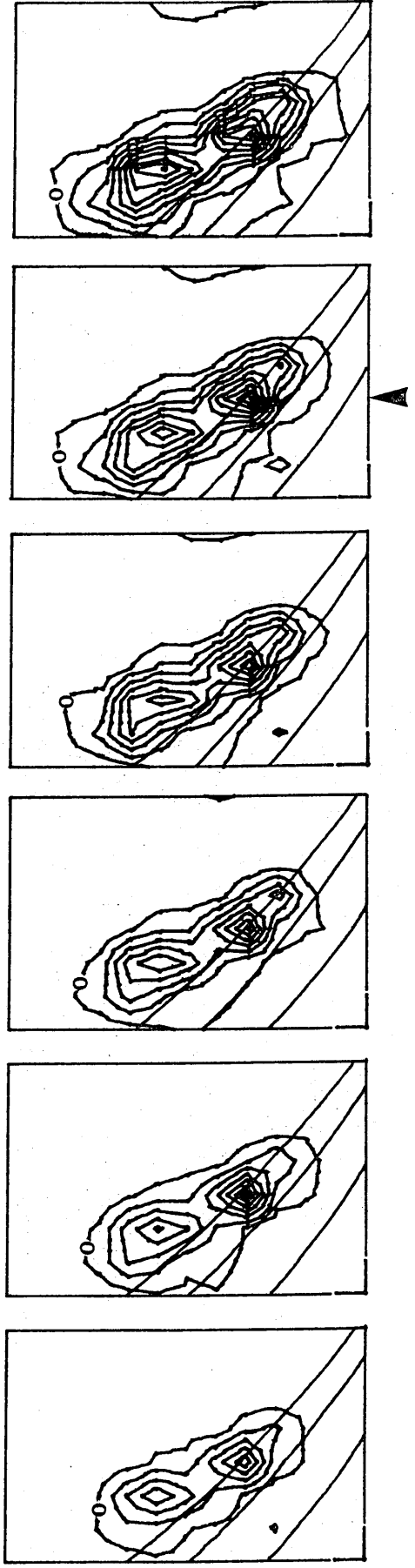


FIG D21A 7JH2 ISO CONTOURS GRID 2 ANTERIOR RS BIN 48-59

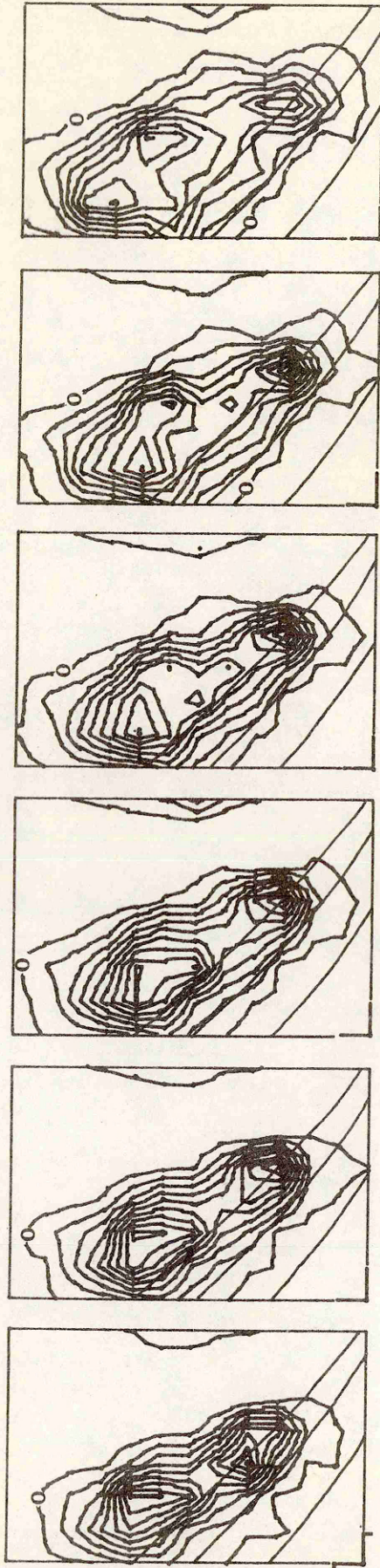


B48-53

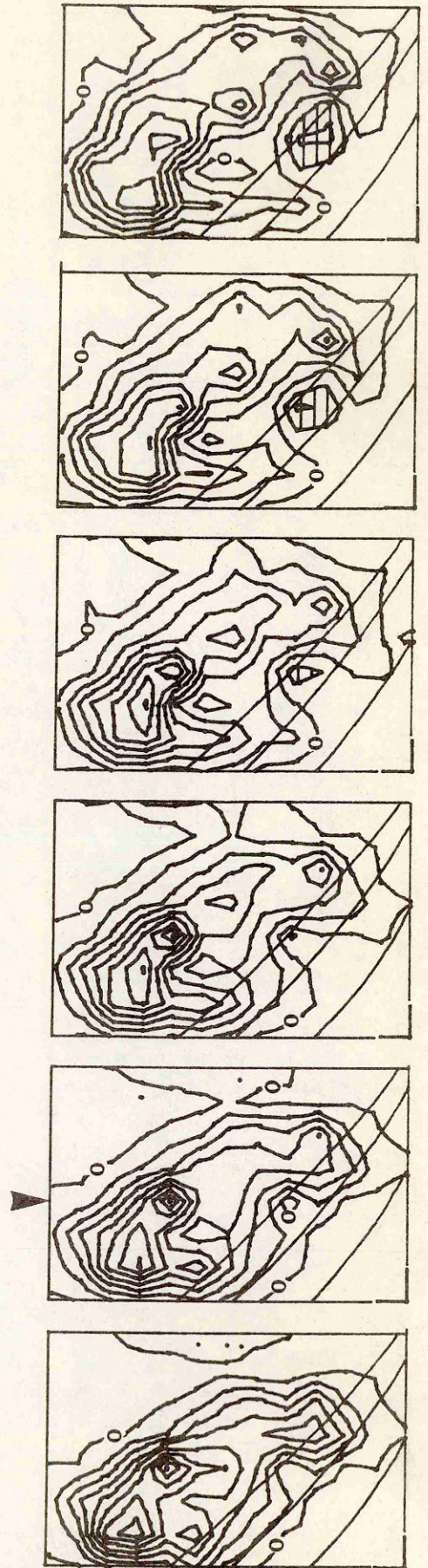


B54-59

FIG D21B 7JH2 ISO CONTOURS GRID 2 ANTERIOR RS BIN 60-71



B60-65



B66-71

Thus, the temporal difference between the development of the IHA and HA responses is only of the order of 1-2bins, ie. 0.4-0.8mS. This is considerably less than the latency difference found between deep (ie. IHA) and superficial (ie. HA) responses suggested by the analysis of the recordings made from single penetrations in the medial Wulst: these results were summarised in Chapter D4.3, Figure D17. The mean peak latency for deep anterior responses was  $14.3 \pm 0.7$ mS, and for superficial anterior responses was  $18.5 \pm 1.6$ mS. These figures indicate a temporal separation of approximately 2-5mS between the responses, and it was concluded in Chapter D4.3 that two separate latency populations of activity were being sampled.

The apparent discrepancy between the two sets of figures (0.4-0.8mS and 2.0-5.0mS) can be reconciled by studying the detail of the ISO map sequence presented in Figures D21A and B. The ISO frame of bin 58 in Figure D21A has an arrowhead placed at the lateral level of the penetration which sampled the maximal IHA response. The same penetration is also indicated by an arrowhead on the ISO frame of bin 68 in Figure D21B, the latest bin at which an area of HA shows a maximal response. This penetration, medially placed within the grid and the Wulst, thus sampled both the deep IHA maximum and a superficial maximum occurring 10 bins (4mS) later. Therefore, the medial penetrations discussed in Chapter D4 were sampling the deep IHA response, and the later (2.0-5.0mS), superficial dispersed HA response.



### D5.3.2 : Transverse dorsoventral lamination

The analysis of ISO maps across transverse grids, therefore, has revealed the responsive area of HA to be very complex in its organisation: early HA activity (0.4-0.8mS later than IHA activity) is located laterally and dorsally to the IHA activity, and becomes dispersed within HA, across regions of HA located above the responsive area of IHA. Furthermore, the dispersed HA activity persists after the disappearance of the IHA activity.

Due to the complexities of the thalamo-hyperstriate relationships revealed in the pigeon (see Section A), and the lack of knowledge concerning the chicken thalamus, it was thought that it would be premature to attempt to analyse the preceding data in terms of synaptic delays and the synaptic organisation of the chicken retino-Wulst pathway. However, the complex nature of the sequence of events within HA following retinal stimulation does at least suggest the possible involvement of intra-HA collaterals or interneurons in this pathway. It is interesting to note in this context that Mark (personal communication) has found that some HA cells injected with HRP show a stellate appearance.

As mentioned previously, the responses recorded across transverse grids after stimulation of the posterior contralateral retina showed the same deep and superficial sequence of events as the responses recorded after stimulation of the anterior retina. However, the location of the two sets of responses differed, and reflected the dorsoventral lamination of potentials discussed in Chapter D4.

The next two figures will illustrate the dorsoventral lamination of potentials across the transverse grid shown in Figure D20. ISO frames will be presented at 4bin (1.6mS) intervals for clarity, showing the activity between bins 48 and 92. Figure D22 shows the ISO maps of the activity following anterior retinal stimulation (RS) (the same series shown at 1 bin intervals in Figure D21); Figure D23 illustrates ISO maps across the same grid following posterior retinal stimulation. Comparison of Figure D22A bins 56 and 60 with Figure D23A bins 56 and 60 shows the same sequence of activity following anterior and posterior retinal stimulation - however, the anterior HA response is located dorsally to the posterior HA response. The anterior and posterior IHA responses occur at the same depth, although the larger anterior response is dispersed somewhat deeper throughout IHA. The dorsoventral lamination is also exhibited by the later, dispersed HA activity - comparison of Figure D22A bin 68 and Figure D23A bin 68 shows the anterior dispersed HA activity to be located dorsally to the equivalent posterior activity. In both cases, the IHA response has disappeared by bin 68, and looping of the zero contour around the area of initial activity shows that the area is beginning to become positive. This is shown in both cases from bin 72 onwards. Figures D22B and D23B illustrate how all of the areas involved in the negative activity gradually become positive.

Thus, a comparison of the ISO maps generated by the recordings following anterior and posterior contralateral stimulation reveals the dorsoventral lamination discussed in Chapter D4

FIG D22A 7JH2 ISO CONTOURS GRID 2 ANTERIOR RS

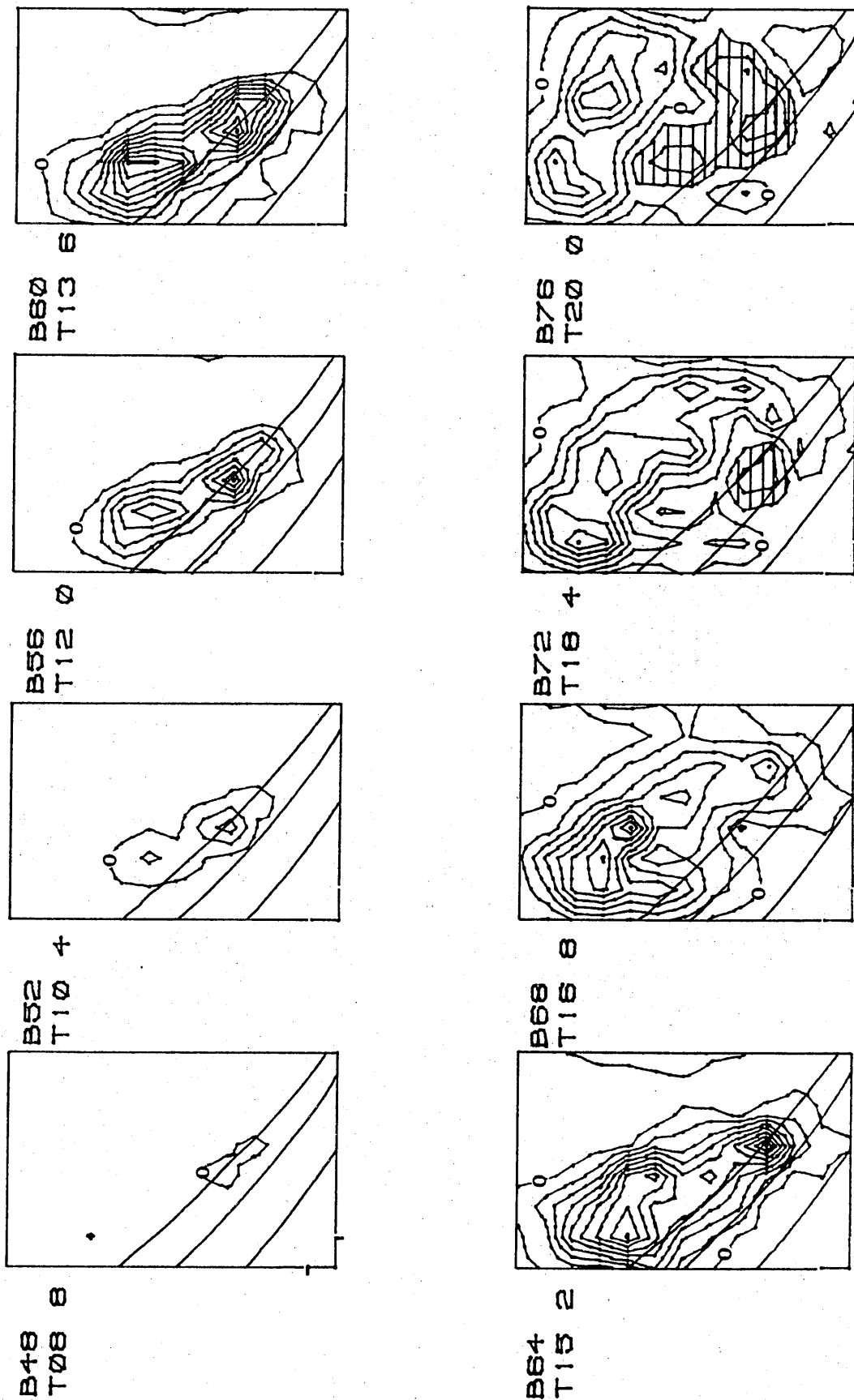
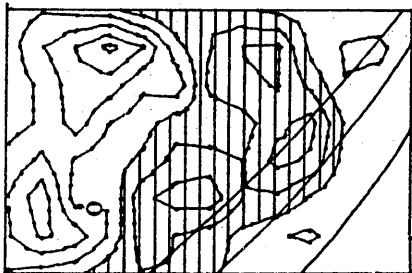
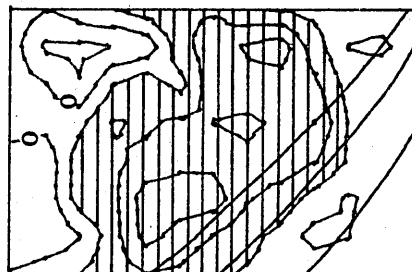


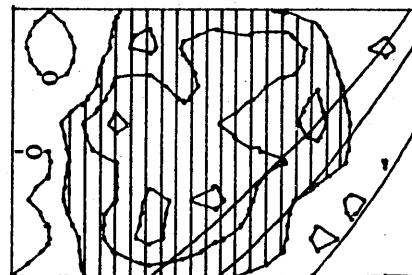
FIG D-22B 7JH2 ISO CONTOURS GRID 2 ANTERIOR RS



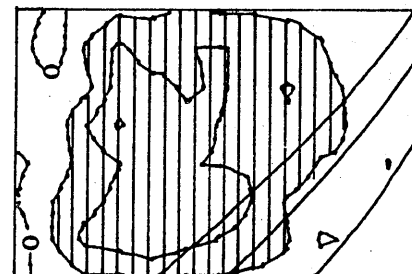
B80  
T21 6



B84  
T23 2



B88  
T24 8



B92  
T26 4

FIG D23A 7JH2 ISO CONTOURS GRID 2 POSTERIOR RS

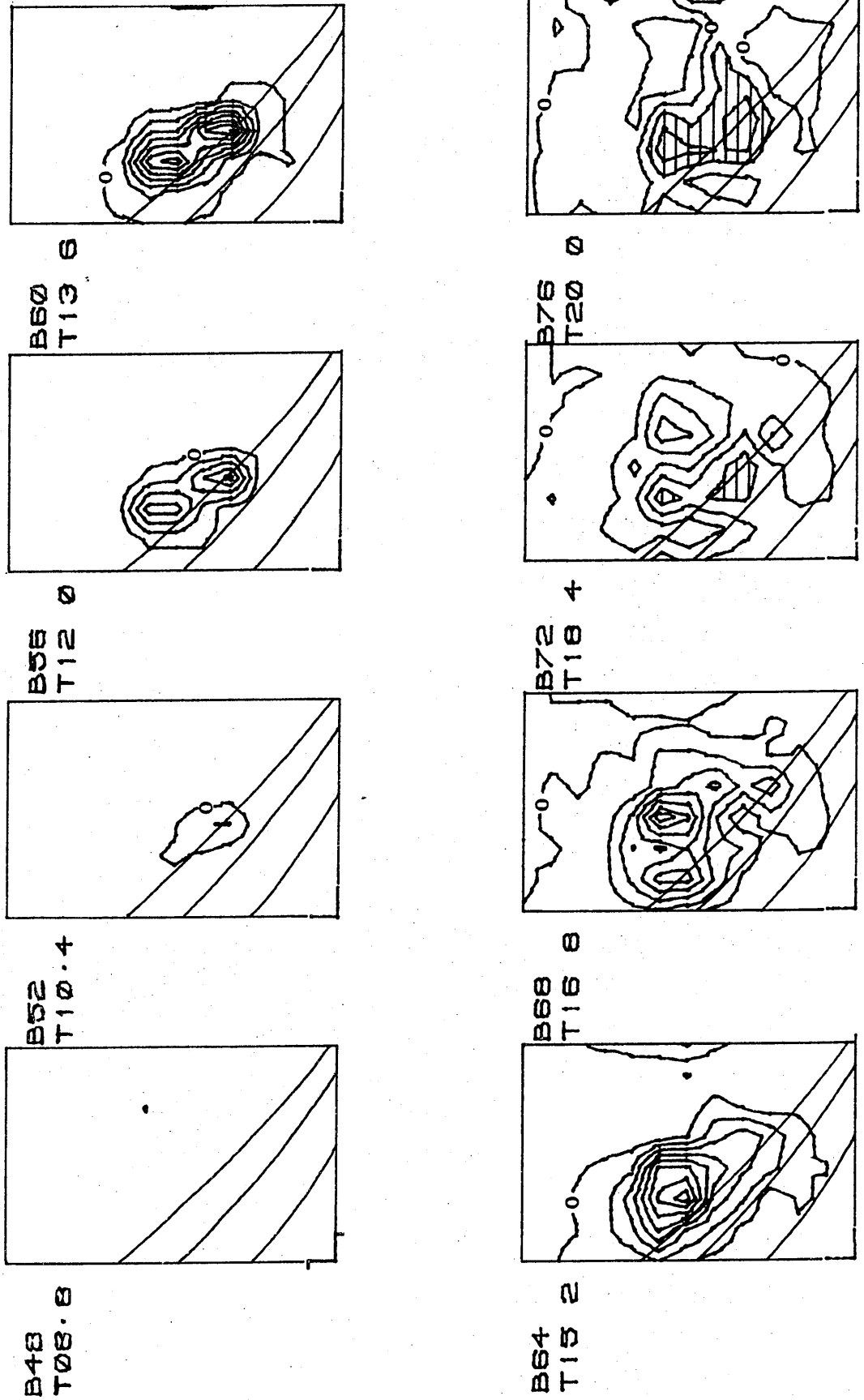
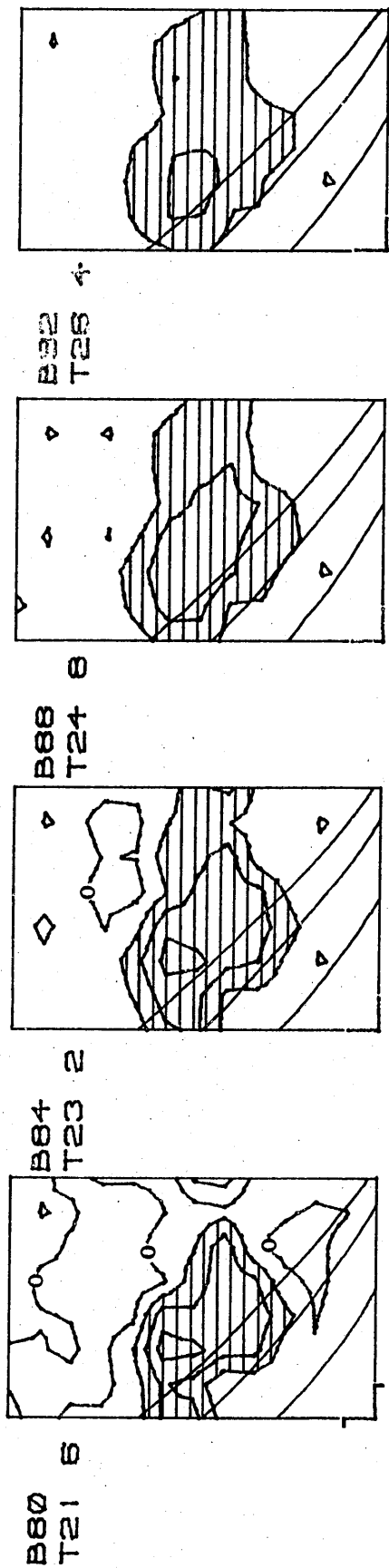


FIG D23B 7JH2 ISO CONTOURS GRID 2 POSTERIOR RS



to be maintained across transverse slices through the Wulst.

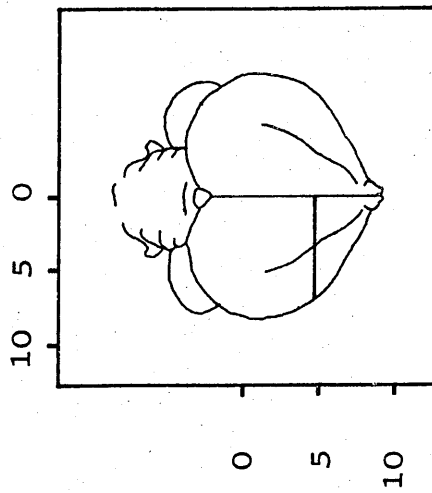
### D5.3.3 Ipsilateral transverse potentials

Maps of ipsilateral isopotential contours across transverse grids reflected the very localised activity revealed by the analysis of single penetrations (see Chapter D3.4.2). Figure D25 illustrates an isopotential series, across the transverse grid shown in Figure D24, following direct stimulation of the ipsilateral optic papilla at level 2. The low signal to noise ratio of the small ipsilateral responses made the generation of such maps difficult, but that shown in Figure D25 is typical. The response is small (contour step =  $20\mu\text{V}$ ), maximising at bin 68 (latency 16.0mS). The area of maximum response is located in the ventral HA, very close to the HA/IHA border. Very little spatial or temporal variation is evident, although the maps at bins 80 and 84 do suggest a limited dorsal spread of activity.

The isopotential maps obtained from ipsilateral responses are therefore in agreement with the dorsoventral lamination of potentials discussed in Chapter D4. The area of ipsilateral activity across a transverse slice of the Wulst lies in a very restricted region of ventral HA, near the HA/IHA border. This area lies between the location of the contralateral, IHA early response, and the contralateral, HA late responses.

FIGURE D24 1605H2 LOCATION OF TRANSVERSE GRID

A LEVEL OF SECTION



B RECORDING GRID

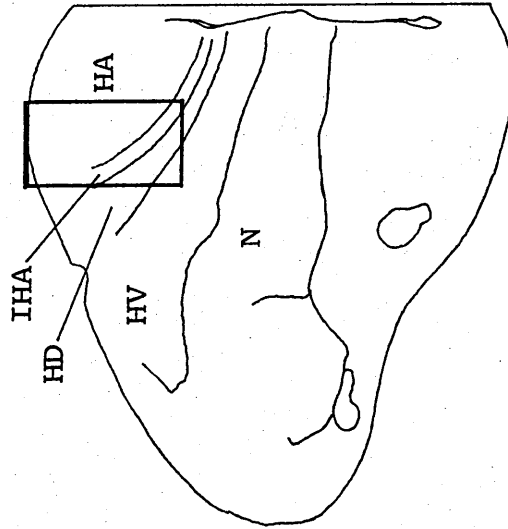
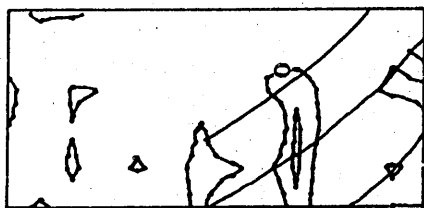




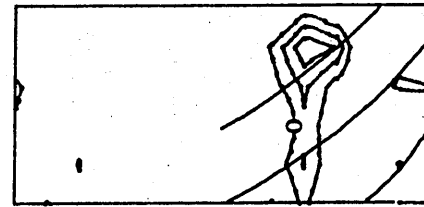
FIG D25 1605H2 ISO CONTOURS IPSILATERAL STIMULATION



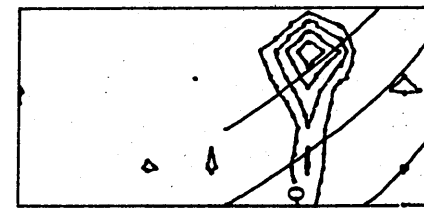
B56  
T12 0



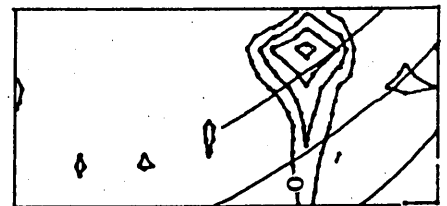
B60  
T13 6



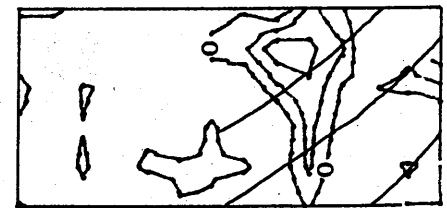
B64  
T15 2



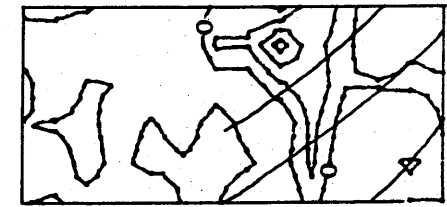
B68  
T16 8



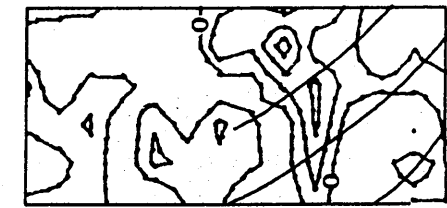
B72  
T18 4



B76  
T20 0



B80  
T21 6



B84  
T23 2

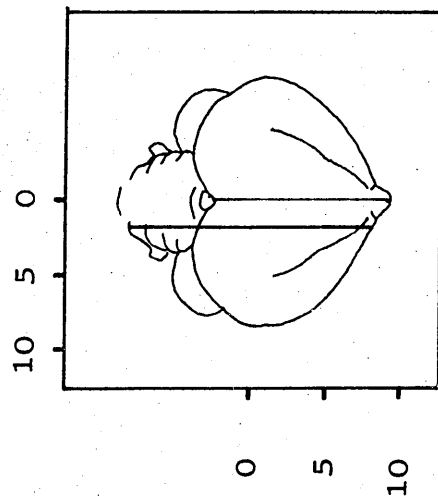
#### D5.4 SAGITTAL DISTRIBUTION OF POTENTIALS

Analysis of the data from up to three transverse grids arranged along the anterior-posterior axis in the same chicken suggested that the late, superficial activity recorded from HA following stimulation of the contralateral retina became dispersed not only laterally, but also posteriorly within the Wulst. The following data were obtained from an experiment designed to show the sagittal distribution of potentials resulting from stimulation of the anterior contralateral retina. (Again, the sequence of events following posterior retinal stimulation was identical). Figure D2 shows the position of the recording grid. This grid was the second of two that were investigated in this chicken, and sampled both the IHA response and the late, dispersed HA response. Six penetrations were made at 0.7mm sagittal intervals. Potentials were recorded at 0.2mm vertical intervals.

Figure D27 illustrates the ISO maps across the sagittal grid. The maximum IHA response occurs at bin 66 (Figure D27A). After this time, the response in HA increases, reaching maximum amplitude at bin 74 - this is 8 bins later than the IHA response, ie. 3.2mS. The HA response persists until bin 82-84, the IHA response having virtually disappeared by bin 74. From bin 66 onwards, it can be seen that the HA response becomes dispersed throughout the posterior extent of the grid. This HA activity is equivalent to the dispersed HA activity seen to arise laterally across transverse grids

FIGURE D26 LOCATION OF SAGITTAL GRID 2111H2

A LEVEL OF SECTION



B RECORDING GRID

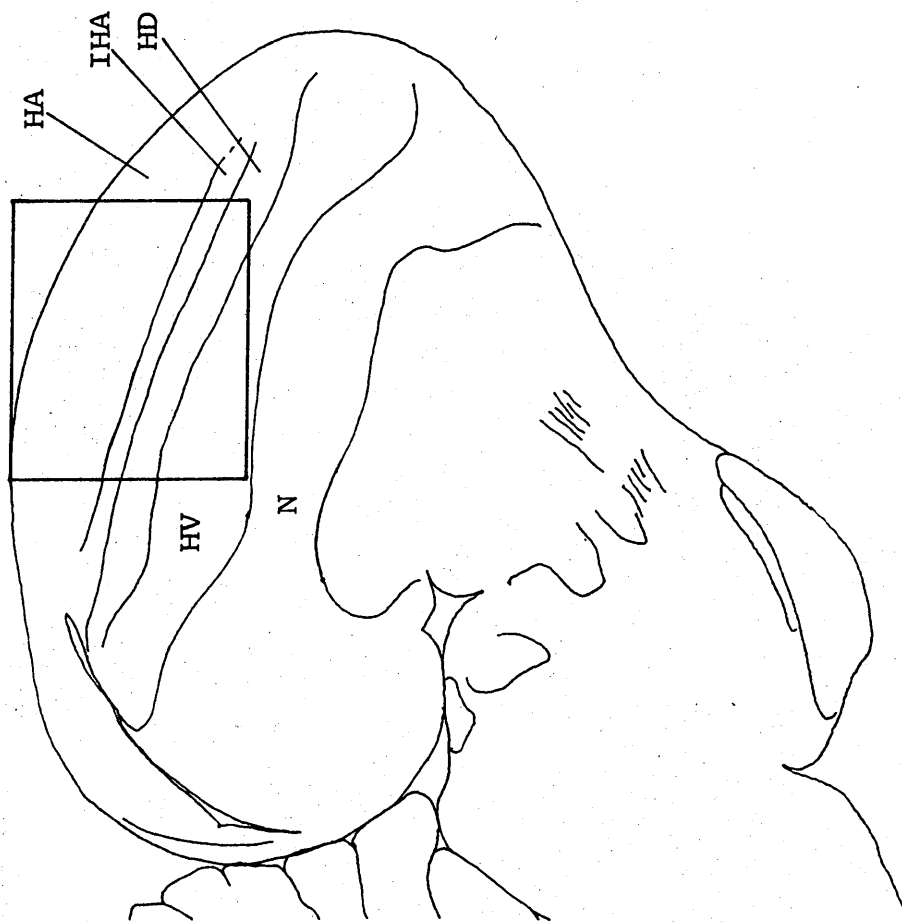
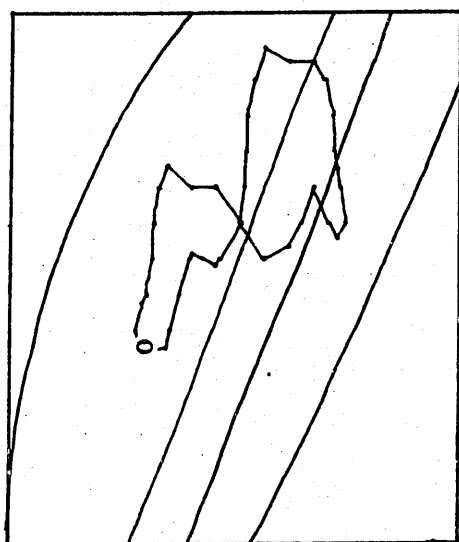
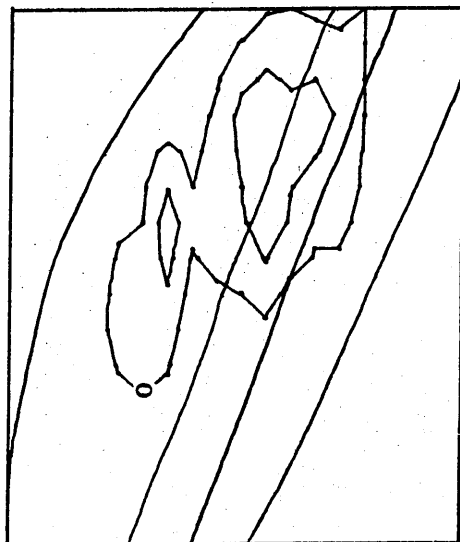


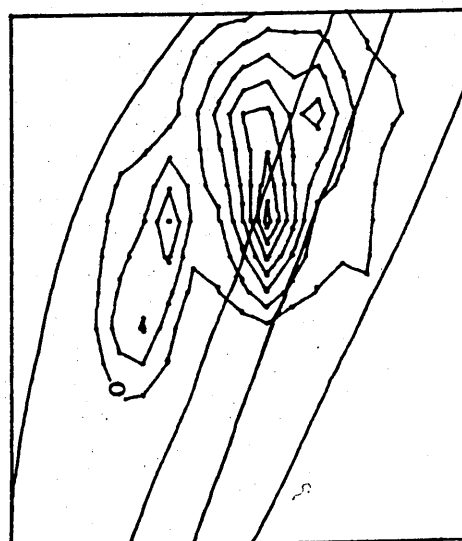
FIG D27A 2111H2 ISO CONTOURS GRID 2 ANTERIOR RS BIN 54-66



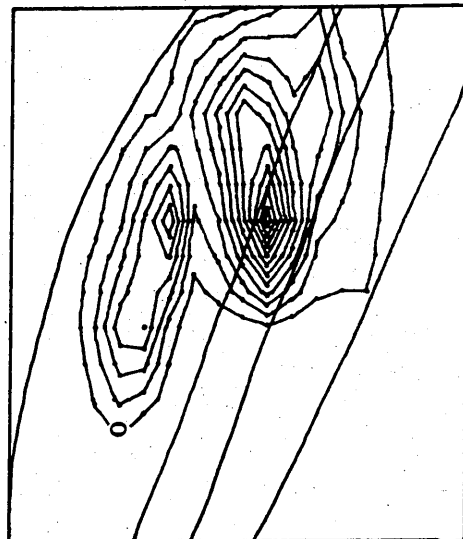
B54  
T10.4



B58  
T12.0

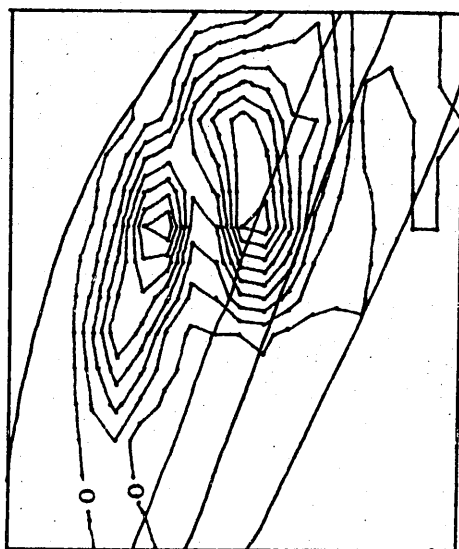


B62  
T13.6

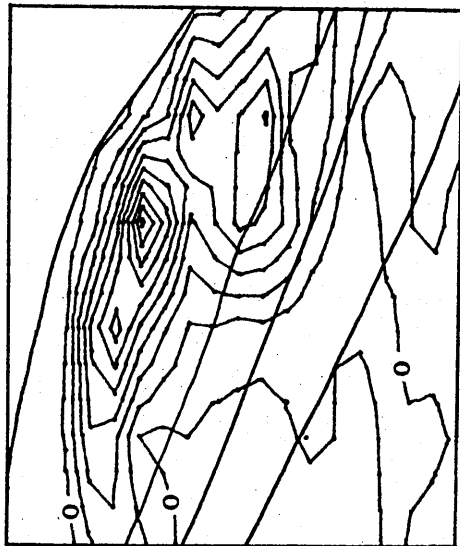


B66  
T15.2

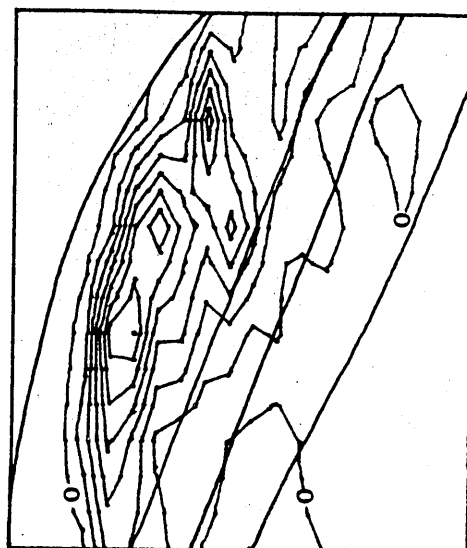
FIG D27B 2111H2 ISO CONTOURS GRID 2 ANTERIOR RS BIN 70-82



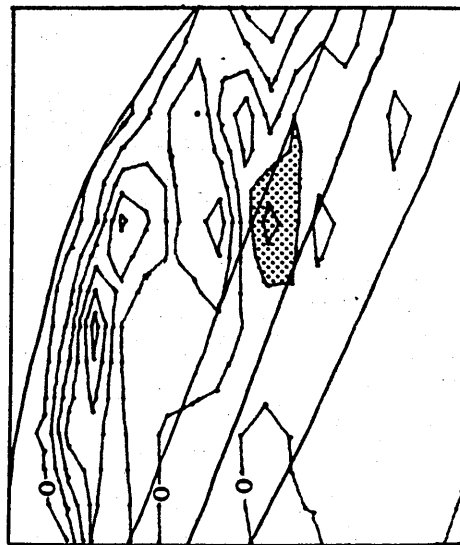
B70  
T16.8



B74  
T18.4

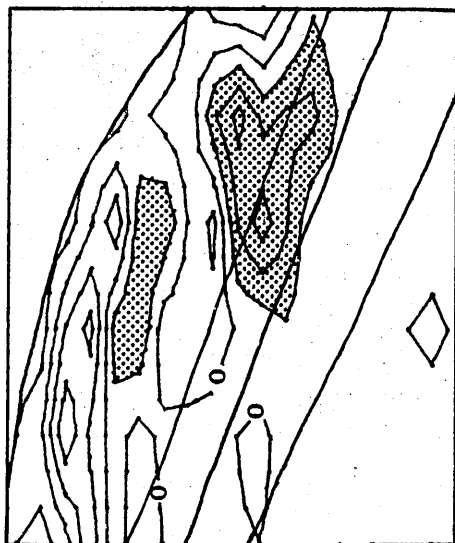


B78  
T20.0

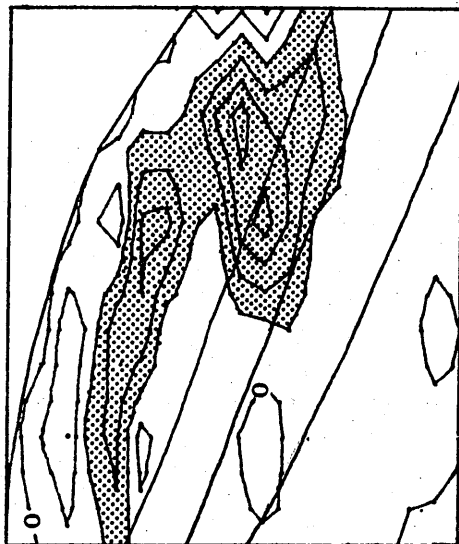


B82  
T21.6

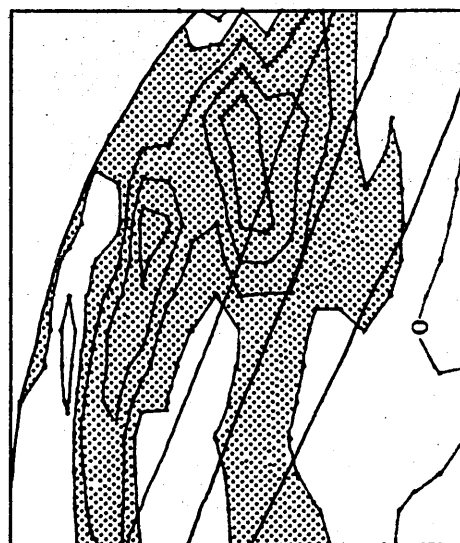
FIG D270 2111H2 ISO CONTOURS GRID 2 ANTERIOR RS BIN 86-98



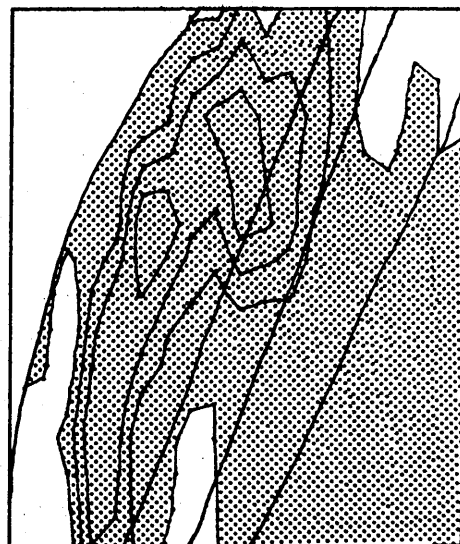
B86  
T23.2



B90  
T24.8



B94  
T26.4



B98  
T26.0

(see Chapter D5.3), as it occurs at a similar time after the IHA response, and is located in a similar lateral plane to the maximum IHA response.

#### D5.5 SUMMARY OF THE SPATIOTEMPORAL PATTERN OF FIELD POTENTIALS

1. The early, deep field potential response to stimulation of the contralateral retina is located in IHA and on the HA/IHA border.
2. The late, superficial response to stimulation of the contralateral retina occurs in HA, and shows a complex sequence of events which suggests the involvement of collateral branches or interneurons within the HA terminal field.
3. The response to stimulation of the ipsilateral optic papilla is located in ventral HA, near the HA/IHA border.
4. Following stimulation of the contralateral retina, the HA response becomes dispersed across both the transverse and sagittal planes, spreading posteriorly throughout HA. This activity persists after the disappearance of the IHA response.
5. The dorsoventral lamination of visual inputs to the Wulst (described in Chapter D4) was maintained across two-dimensional recording grids.

CHAPTER D6 : DISCUSSION

The results presented in Section D describe the total area of the chicken Wulst which is responsive to electrical stimulation of the optic papillae (see Figure D12). The area of the anterior forebrain exhibiting responses to stimulation of the contralateral optic papilla extends some 3 to 4mm along the anterior-posterior axis of the Wulst. The most anterior point of the responsive area lies about 1mm posterior to the anterior pole of the hemisphere. The lateral margin of the responsive area was found to lie approximately 0.5-1.0mm medial to the valleculla, whilst the medial margin lay a similar distance from the midline. Maximum responses were always obtained from a central strip running along the anterior-posterior axis of the Wulst. The longitudinal boundaries of this strip were located approximately 1.3 and 1.7mm lateral to the midline. Stimulation of the ipsilateral optic papilla resulted in a much more discrete activation of hyperstriatal tissue, lying deep within the anterior portion of the contralaterally responsive area.

The waveform and vertical sequence of field potentials recorded from electrode penetrations in the chicken Wulst differed from those obtained from the pigeon by Parker and Delius (1972). These authors, investigating flash evoked potentials in the pigeon Wulst, recorded a complex field potential waveform located on the HA/HIS border, consisting of at least three positive and two negative peaks with a



total duration of 100ms. They also observed two reversals of polarity of the potential as the recording electrode was advanced from HIS to HD, and from HD into HV. They suggested these factors to indicate multi-layer terminations. However, no similar complexities of waveform or reversals of polarity were found in the present study. Instead, the waveforms of the graded, negative waves recorded from the chicken resemble those recorded from the pigeon by Perisic et al (1971) in response to electrical stimulation of the optic papilla, those recorded from the pigeon by Mihailovic et al (1974) in response to electrical stimulation of the dorsolateral thalamus, and those recorded from the chicken embryo in response to flash stimuli by Sedlacek (1970). Perisic et al (1971) also recorded field potentials in response to flash stimuli in the pigeon - although smaller, the potentials were identical to those obtained in response to electrical stimulation.

There is, at present, no report in the literature of visual cells being isolated from the anterior regions of HV, where Parker and Delius (1972) recorded large flash evoked potentials. Flash evoked field potentials were also recorded from this area in the chicken embryo by Sedlacek (1970). Brown and Horn (1977) have recorded flash evoked multiple unit responses from the chicken HV, but the responsive area lies posterior to the area indicated by Parker and Delius (1972). No evoked responses were found in the chicken anterior HV (ie. that portion of HV lying beneath the responsive areas of IHA and HA) by the present

study - more posterior regions of HV were not investigated.

It should be noted that Parker and Delius (1972) recorded field potential differences between the two poles of a concentric electrode, rather than between a microelectrode and an indifferent electrode. However, pilot recordings obtained from the chicken, using a semi-micro concentric recording electrode, furnished identical, simple waveforms to those obtained with the microelectrodes. The use of different preamplifiers and filters (Parker and Delius recorded with a time constant of 1 second and a high frequency cut-off at 250Hz) could of course account for the differences between waveforms. They do not indicate whether they used a 50Hz filter during recording - 50Hz notch filters used in the present study were found to attenuate the evoked potential, and to cause the appearance of a second negative wave lying on the rising phase of the original wave. However, such considerations do not resolve the conflict between the results indicating a visually silent chicken anterior HV, and those indicating a visually responsive pigeon anterior HV.

The results presented in Section D describe a topographic relationship between the superior-inferior axis of the contralateral retina and the anterior-posterior axis of the Wulst of the chicken (see Chapter D3.2). Direct stimulation of the superior levels of the contralateral optic papilla resulted in maximal evoked field potentials within the most anterior regions of the responsive area of the Wulst. As the

stimulus electrode was positioned at successively more inferior levels of the optic papilla, the location of the maximal evoked field potentials was found to lie in successively more posterior regions of the responsive Wulst. As the optic papillae receive ganglion cell axons in a radial fashion, these results suggest that the superficial retina is represented in the anterior Wulst, whilst the inferior retina is represented in more posterior regions of the Wulst.

Reports in the literature of avian retino-Wulst or thalamo-Wulst topography are contradictory, and do not establish a conclusive or consistent pattern of the representation of the retina upon the Wulst. Two studies include investigation of the chicken. Adamo and King (1967), recording flash evoked potentials from the Wulst of adult chickens, report the responses to show "a diffuseness and a lack of localisation". Miceli et al, (1975) followed the retrograde transport of horseradish peroxidase (HRP) injected into the Wulst of the pigeon, chicken, duck, herring gull and jackdaw. Although only discussing the data obtained from the pigeon in detail, these authors report that they found no essential differences between the species investigated. They found no conclusive evidence of a topographical rostro-caudal relationship between the Wulst and dorsolateral thalamus in all cases. However, they suggest that this may be attributed to either the limited region of the Wulst investigated, and/or the relatively wide diffusion of HRP in the rostro-caudal plane. Hunt and Webster (1972),

however, studying retrograde degeneration in the pigeon thalamus following lesion of the Wulst, report the thalamic degeneration to shift rostro-caudally as the position of the lesion is changed in the same plane.

The only physiological data relating to the topography of the pigeon retino-Wulst projection are provided by Revzin (1969a). He recorded from single cells in the Wulst which responded to visual stimulation, and reported that the retinal projection upon HIS "seemed" to be topographically organised. Unfortunately, no further details are given. Recording single visual units from the Wulst of the burrowing owl, however, Revzin (1969b) did manage to establish a topographic relationship between the retina and Wulst of this species. Thus, the inferior retina was projected to the anterior parts of the Wulst, whereas lateral points in the visual field were projected to medial Wulst areas. Different results, though, were obtained from the barn owl by Pettigrew and Konishi (1976a). Again, studying single unit responses in the Wulst, these authors describe a topographic organisation of the retinal projection upon the Wulst similar to that found in the chicken by the present study. Thus, the area of the contralateral visual field sampled by the superficial retina was represented upon the anterior Wulst, whilst the area sampled by the inferior retina was represented upon the posterior margin of the Wulst. However, they also describe a similar relationship to exist between the nasal retina and the medial Wulst, and between the temporal retina and the lateral Wulst.

No evidence was found in the present study for such a representation of the two margins of the lateral axis of the retina across the lateral axis of the chicken Wulst. Instead, a complex dorsoventral lamination of the retinal projections to the Wulst was revealed by the results presented in Chapters D4 and D5. It is at present unknown whether the spatiotemporal pattern of the dorsoventral lamination of potentials is due exclusively to hyperstriatal interneuron circuitry or collaterals, to a separation of thalamic efferents to the Wulst, or indeed, to some combination of these.

The present study provides evidence for a field within HA which could be the site of the integration of information available from both eyes. Direct stimulation of the ipsilateral optic papilla resulted in much smaller field potentials than did stimulation of the contralateral eye. These ipsilateral responses were located just dorsal to the HA/IHA border, and consisted only of a single, slow field potential. The location of the ipsilateral response was observed to overlap the ventral region of HA responsive to stimulation of the contralateral posterior retina. Furthermore, the latency ranges of the ipsilateral response and the posterior, dispersed HA contralateral responses, located in ventral HA, were similar (see Chapter D4.3, and Figure D17). These results suggest that there is a small area of the ventral HA, located in the anterior Wulst, that could subserve the processing of binocular information from the small frontal visual field overlap in the chicken. (The binocular visual field of the chicken subtends an angle of 26 degrees - the pigeon is

believed to be similar; Benner, 1938). One of the main objectives of the experiments described in the following section was to investigate the presence of cells in the chicken Wulst which would respond to stimulation of both the contralateral and ipsilateral eye.

SECTION E : ELECTRICALLY EVOKED SINGLE UNITS

CONTENTS OF SECTION ECHAPTER E1 : INTRODUCTIONCHAPTER E2 : METHODS

E2.1 : STIMULATION

E2.2 : RECORDING

E2.3 : DATA ANALYSIS

CHAPTER E3 : SINGLE UNIT POTENTIALS

E3.1 : TOTAL SAMPLE POPULATION

E3.2 : MONOCULAR RESPONSES

E3.3 : BINOCULAR RESPONSES

E3.4 : CORRELATION OF UNIT AND FIELD POTENTIALS

E3.5 : SUMMARY

CHAPTER E4 : DISCUSSION



LIST OF ILLUSTRATIONS FOR SECTION E

- FIGURE E1 : SAMPLE POPULATION OF UNITS
- E2 : FIRST SPIKE LATENCY RANGE (ms)
- E3 : CONTRALATERAL UNIT RESPONSES
- E4 : IPSILATERAL UNIT RESPONSES
- E5 : FREQUENCY ATTENUATION OF CONTRALATERAL UNIT  
POTENTIAL
- E6 : INDEPENDENT BINOCULAR UNIT RESPONSE
- E7 : COINCIDENT BINOCULAR UNIT RESPONSE
- E8 : CONTRALATERAL FIELD AND UNIT POTENTIALS
- E9 : IPSILATERAL FIELD AND UNIT POTENTIALS
- E10: INDEPENDENT BINOCULAR FIELD AND UNIT POTENTIALS
- E11: CORRELATION OF CONTRALATERAL FIELD AND UNIT  
POTENTIALS
- E12: CORRELATION OF IPSILATERAL FIELD AND UNIT  
POTENTIALS
- E13: CORRELATION OF BINOCULAR FIELD AND UNIT  
POTENTIALS
- E14: PERCENTAGE OF CELL TYPES ISOLATED FROM CHICKEN,  
PIGEON AND BARN OWL WULST

CHAPTER E1 : INTRODUCTION

Perisic et al (1971), recording electrically evoked visual units from the pigeon Wulst, identified three unit populations: units located in dorsal HA that responded only to stimulation of the contralateral optic papilla; binocular units located in ventral HA responding to both contralateral and ipsilateral stimulation; and units located in ventral HA, and in HIS and HD, which responded only to stimulation of the ipsilateral optic papilla. Pettigrew and Konishi (1976a), recording visually evoked units from the Wulst of the barn owl, identified a further class of cells requiring simultaneous stimulation of the contralateral and ipsilateral eye - they classified these cells as 'binocular disparity units'; that is, cells providing information about the horizontal retinal disparity of an object in visual space, necessary for stereoscopic vision.

The experiments reported in this section were carried out to obtain data from unitary responses in the chicken for a comparison with the unit data reported in the literature for other avian species.

Single unit responses to electrical stimulation of the contralateral and ipsilateral optic papillae were recorded from the visually responsive areas of the Wulst in 90-110g chickens. Only units identified as cells by the usual criteria (biphasic waveform, duration greater than 1mS) are

included in this analysis. These experiments were carried out in order to obtain an estimate of the percentage of cells responding to either contralateral or ipsilateral stimulation, to investigate the presence of binocular cells, and to confirm that the evoked field potentials described in Section D were obtained from areas containing visually responsive cells.

## CHAPTER E2 : METHODS

### E2.1 STIMULATION

Stimulus procedures were identical to those used to evoke field potentials, as described in Section D, Chapter D2.1. Direct stimulation of the superior optic papillae was used in all the experiments reported below.

### E2.2 RECORDING

Unit potential recordings were made via glass microelectrodes with a tip diameter of  $0.5-2.0\mu$  (measured on a scanning electron microscope), and with a tip resistance between 5 and 17 Megohm at 60Hz (measured according to the method of Stone, 1973). The electrodes were filled under vacuum with a 2% solution of pontamine sky blue in 0.5M NaAcetate (Hellon, 1971). The tip resistance after pulling was typically as high as 60 Megohm. This resistance was reduced by gently brushing the tip with a glass rod or finger tip under microscopic guidance.

Recordings were made using the same equipment as described in Section D, Chapter D2.2. Each potential was first recorded with a filter bandwidth setting of 100Hz-10KHz in order to observe the waveform and latency of the response. The unit potential was then recorded with a bandwidth setting of 10Hz-10KHz in order to obtain a visual

correlation between the latency of the unit potential and the slow wave field potential activity at that depth. The relatively high resistance of the electrodes used in these experiments to obtain isolated unit potentials often necessitated the use of a 50Hz notch filter whilst recording with the wide bandwidth setting - although it was possible to record field potential activity under these conditions, the waveform, being of 10-20ms duration, was often distorted and attenuated.

The recording electrode was advanced in 2 $\mu$  steps during these experiments, whilst the optic papillae were constantly stimulated with single pulses at a frequency of 0.3Hz.

### E2.3 DATA ANALYSIS

Isolated unit potentials were converted to TTL logic pulses by the use of the upper and/or lower windows of a discriminator unit (Digitimer Spike Processor, D130). These pulses were then transferred to the Neurolog Averager which computed post stimulus time histograms (PSTHs). A 100 or 50ms time sweep, bin width 0.4 or 0.2ms was used, and 8 or 16 stimulus presentations given to generate each PSTH. The microprocessor provided on-line numerical printouts of the PSTHs, and these were used for accurate latency measurements. The PSTHs, together with trigger pulses and the raw potential waveform recorded under both bandwidth conditions, were stored on magnetic tape. They were subsequently played back through a dual beam storage oscilloscope (Tektronix D13) and

photographed.

## CHAPTER E3 : SINGLE UNIT POTENTIALS

### E3.1 TOTAL SAMPLE POPULATION

The majority of units identified as cells responded to contralateral and/or ipsilateral optic papilla stimulation with one or two action potentials. Very occasionally, multiple responses of up to ten spikes were recorded to a single stimulus presentation. The cells were all recorded from the anterior portion of the Wulst previously found to be the location of field potential responses to electrical stimulation of the eye (see Section D, Chapter D3.4).

Figure E1 gives the number, percentage and types of response recorded in these experiments. Percentages are given to the nearest whole number. The somewhat diffuse nature of the projection, especially to the dorsal regions of the Wulst, was reflected by the large number of isolated units (44%) which failed to respond to the direct stimulation of the optic papillae. Cells were classified as monocular, responding to stimulation of either the contralateral or ipsilateral optic papilla, or as binocular if they showed a response to stimulation of both papillae. The binocular cells have been separated into two subclasses on the basis of the latency difference between the contralateral and ipsilateral responses : 'independent' binocular cells had an ipsilateral response latency consistently longer than the latency of the contralateral response; 'coincident' binocular cells had identical response latencies to both

FIGURE E1 SAMPLE POPULATION OF UNITSA TOTAL CELLS ISOLATED

	VISUAL	NO RESPONSE	TOTAL
N	123	97	220
%	56	44	100

B VISUAL CELLS ISOLATED

	MONOCULAR		BINOCULAR	
	CONTRA	IPSI	INDEPENDENT	COINCIDENT
N	104	4	10	5
%	85	3	8	4

FIGURE E2 FIRST SPIKE LATENCY RANGE (mS)

MONOCULAR		BINOCULAR	
CONTRA	IPSI	CONTRA	IPSI
9-54	16-157	10-96	20-153



contralateral and ipsilateral stimulation. It should be noted that this latter group of cells did not require simultaneous stimulation of both optic papillae to elicit responses. (The effects of simultaneous stimulation of both optic papillae were not investigated due to equipment limitations).

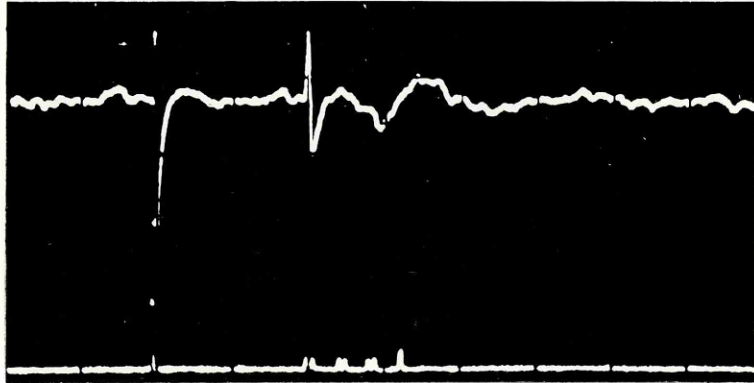
Ipsilateral units were very difficult to isolate, reflecting the small amplitude of the localised ipsilateral field potential, and showed a very large range of first spike latency. The first spike latency ranges of the different classes of cells are given in Figure E2.

### E3.2 MONOCULAR RESPONSES

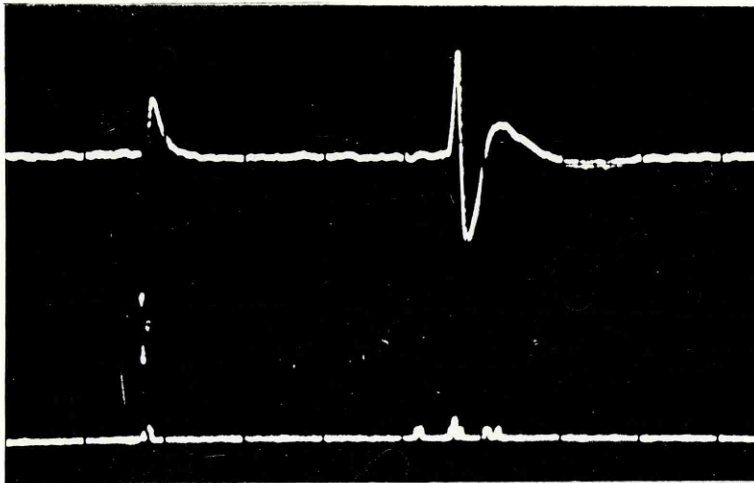
Figure E3 shows a single response (upper trace) and PSTH (lower trace) for each of four cells responding exclusively to stimulation of the contralateral optic papilla, and illustrates the typical biphasic waveform of units classified as cellular responses. The photographs have been retouched only to compensate for the failure of the oscilloscope storage screen to completely follow the fast risetimes of the spikes. The stimulus artifact can be seen on each trace, occurring 10ms after the start of the oscilloscope sweep. Spike amplitudes were typically between 0.2 and 5.0mV. The small positive-negative deflections following the biphasic spike are due to a distortion of the coincident field potential by the recording bandwidth and 50Hz notch filter employed in these recordings.

FIGURE E3 CONTRALATERAL UNIT RESPONSES

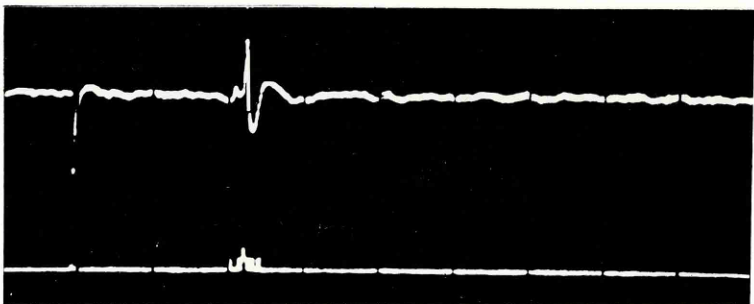
A 1208-31-EN



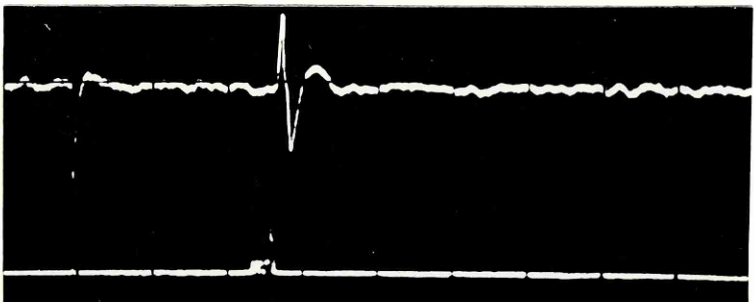
B 1109-31-EN



C 1209-21-HN



D 1209-21-LN



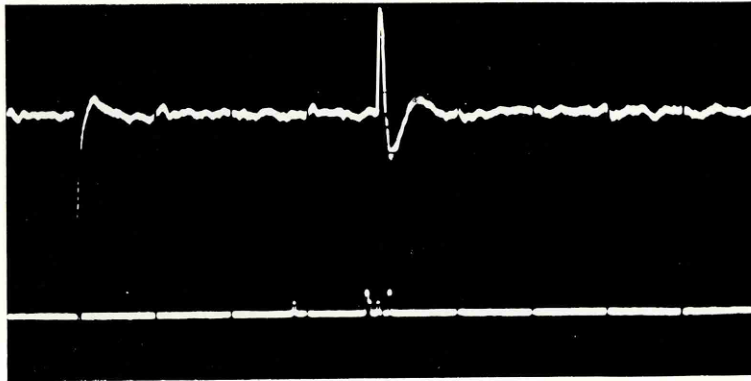
Contralateral units were isolated in both the superficial and deep regions of the hyperstriatum shown to be visually responsive by the field potential studies described in Section D. Figure E3A shows a cell recorded from the HA/IHA border, having a first spike latency of 10.5mS. The records shown in Figures E3B, C, and D were obtained from more superficial areas of HA, and have first spike latencies of 17.3, 20.9 and 28.0mS respectively.

Figure E4 shows a single response and PSTH for two cells responding exclusively to stimulation of the ipsilateral optic papilla. Ipsilateral cells were obtained from regions located between the superficial and deep contralateral areas. (The correlation of unit and field potential locations is discussed in Chapter E3.4).

All cellular responses showed the same order of frequency attenuation exhibited by the evoked field potentials. Figure E5 shows the waveform and PSTHS for 16 stimulations of a contralaterally responsive cell at stimulus rates of 0.3 and 1.0Hz, illustrating the reduced responsiveness of the cell at the higher stimulus frequency.

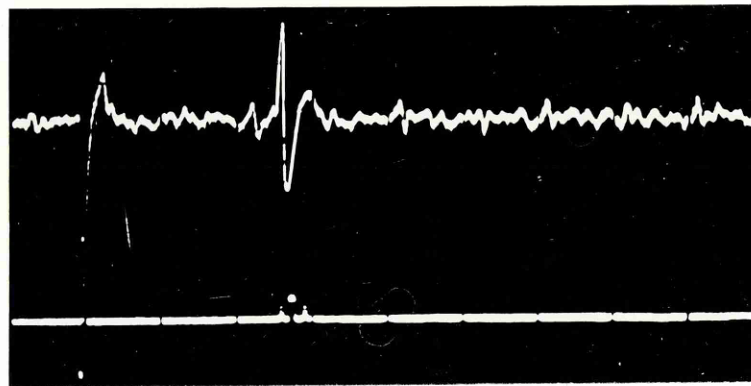
### E3.3 BINOCULAR RESPONSES

Figure E6A shows the response and PSTH of an independent binocular cell to stimulation of the contralateral optic papilla. This cell is an example of those responding with more than one spike to some stimulus presentations.

FIGURE E4 IPILATERAL UNIT RESPONSESA 1209-21-ON

0.5mV

10mS

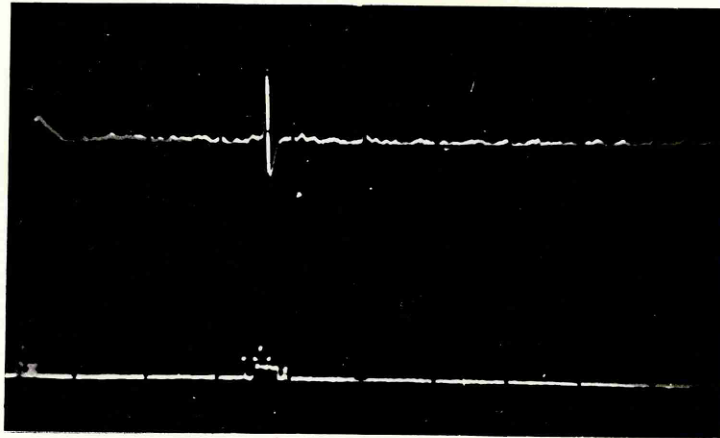
B 1209-21-SN

0.25mV

10mS

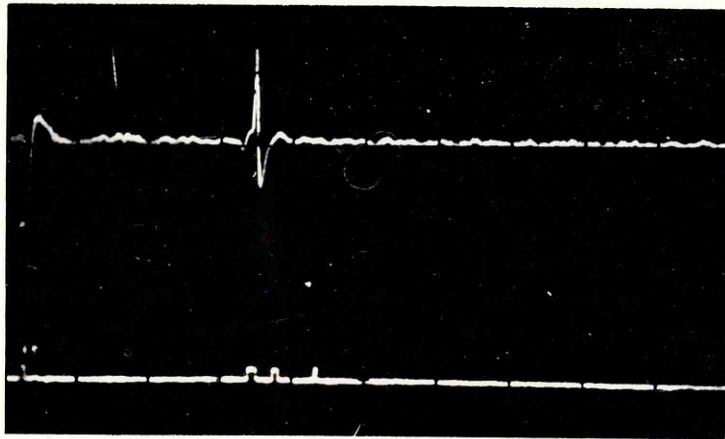
FIGURE E5 FREQUENCY ATTENUATION OF CONTRALATERAL  
UNIT POTENTIAL 1905-11-BN

A STIMULUS FREQUENCY 0.3Hz



RESPONSES TO 16 STIMULI - 16

B STIMULUS FREQUENCY 1.0Hz



RESPONSES TO 16 STIMULI - 6

Figure E6B shows the response and PSTH of the same cell to ipsilateral stimulation. It can be seen from a comparison of the PSTHs that the latency of the ipsilateral response is consistently longer than that of the contralateral response.

Responses of a coincident binocular cell are shown in Figure E7. Comparison of the contralateral and ipsilateral PSTHs indicates an identical response latency to both contralateral and ipsilateral stimulation. Binocular responses were obtained from the ventral HA. The number of binocular and ipsilateral cells isolated (see Figure E1) was too small to determine whether the two groups of cells were located in different areas of the ventral HA. The binocular responsive area, therefore, is assumed to be coincident with the ipsilaterally responsive area.

#### E3.4 CORRELATION OF UNIT AND FIELD POTENTIALS

Excellent correlation between both the localisation and the latency of unit responses and the localisation and latency of the field potentials described in Section D was obtained in these experiments. Figure E8 shows the responses of four contralateral cells, recorded using a wide bandwidth to give a simultaneous representation of the incident slow wave field potential activity at the respective recording points. The response illustrated in Figure E8A was recorded without a 50Hz notch, and shows the unit response to lie on the falling edge of the negative contralateral field potential. Figures E8B, C, and D illustrate responses recorded with a

FIGURE E6 INDEPENDENT BINOCULAR UNIT RESPONSE 1209-21-NN

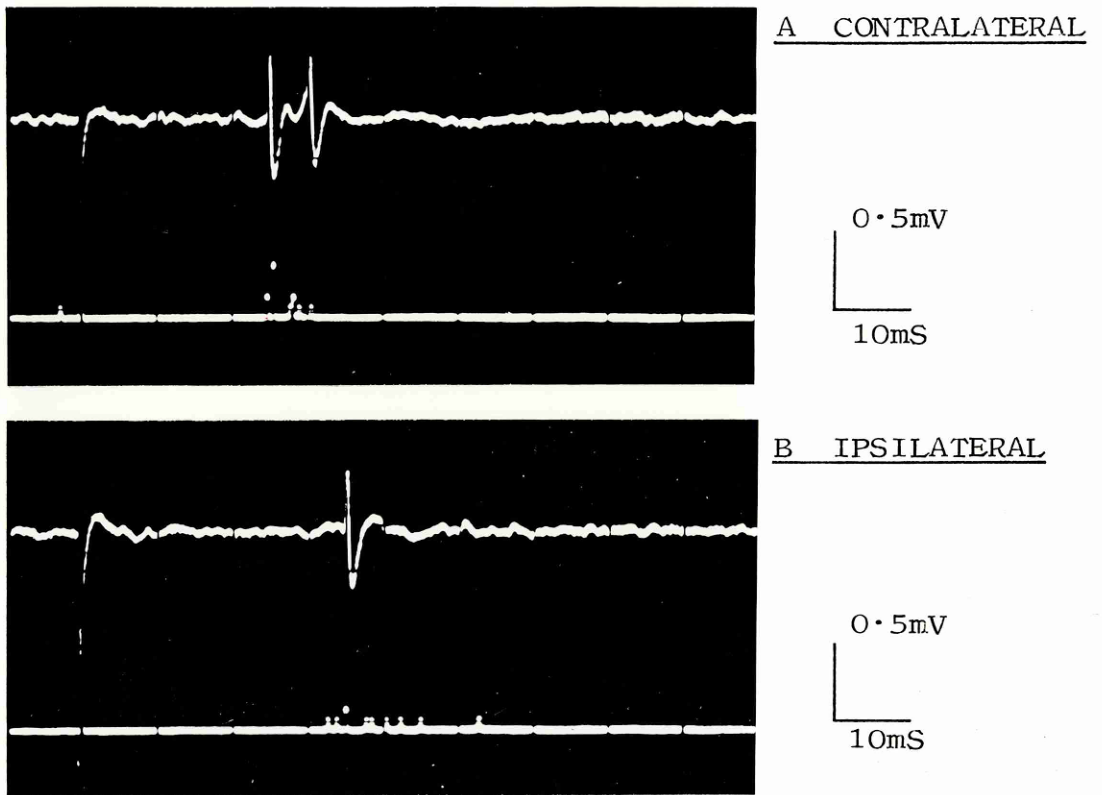


FIGURE E7 COINCIDENT BINOCULAR UNIT RESPONSE 1209-21-RN

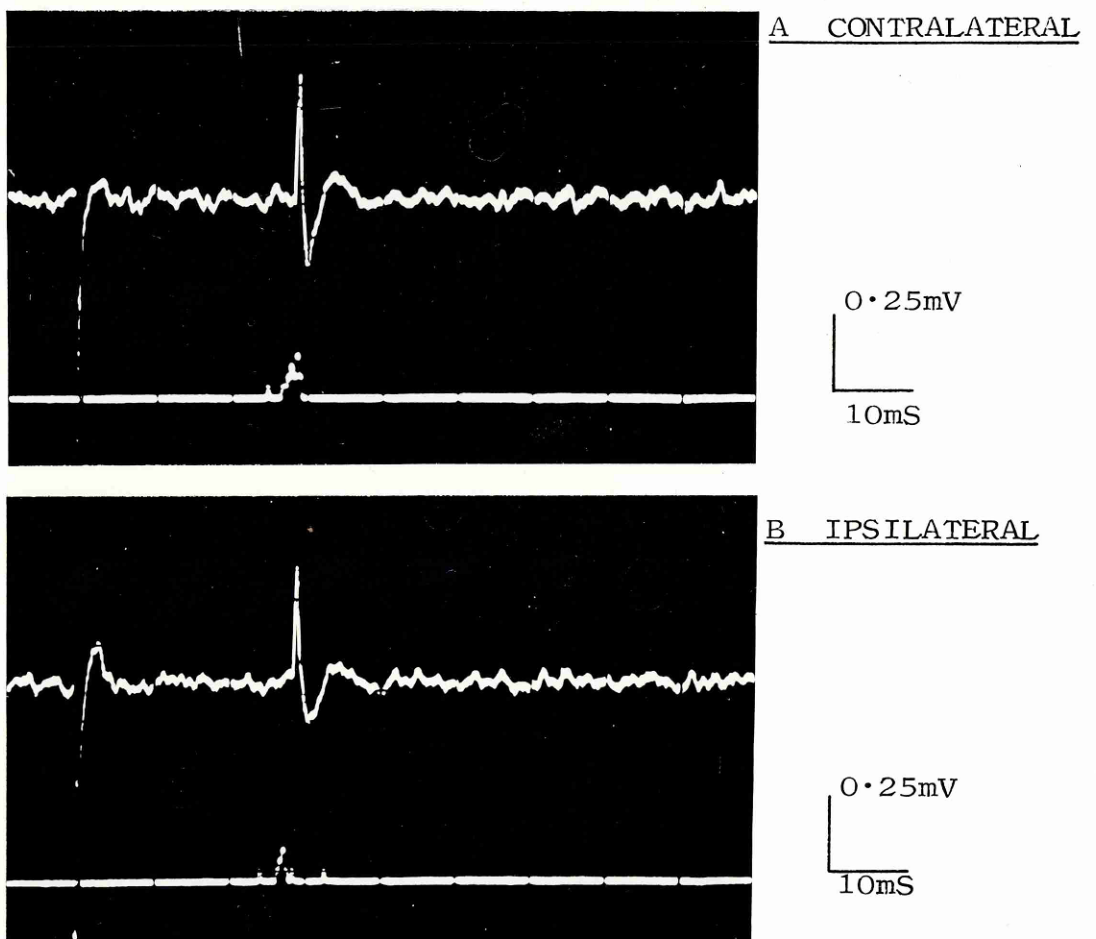
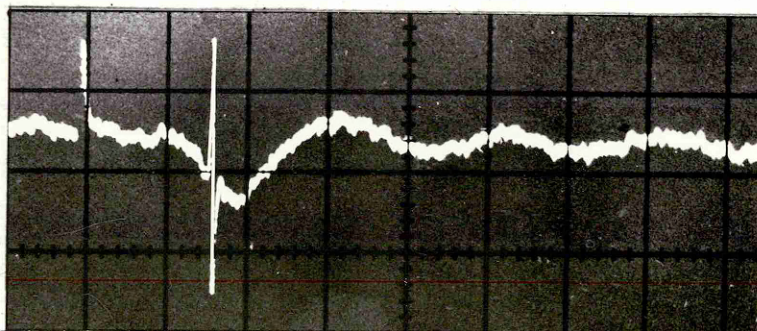
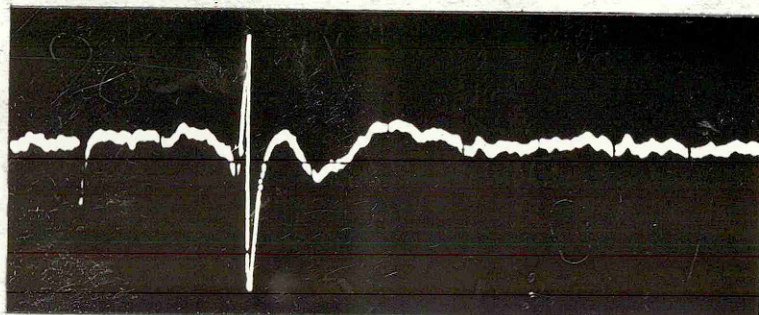
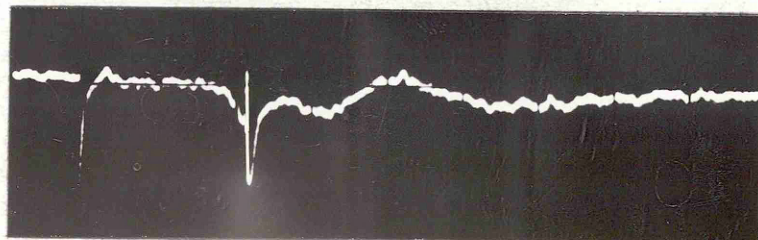
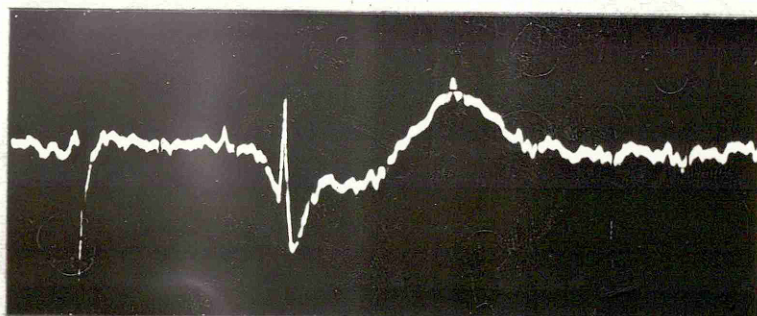


FIGURE E8 CONTRALATERAL FIELD AND UNIT POTENTIALSA 1109-31-DN0.4mV  
10mSB 1209-21-HN0.4mV  
10mSC 1209-21-JN0.5mV  
10mSD 1209-21-LN0.25mV  
10mS



50Hz notch in the circuit, showing subsequent attenuation and distortion of the negative wave immediately after the unit potential. However, all three unit responses clearly lie within the timecourse of the contralateral field potential. Figure E9 shows the unit and field potential responses of an exclusively ipsilateral cell - again, distortion and attenuation of the field potential by the filters is evident, but the unitary response can be seen to lie on the small negative wave of the ipsilateral field potential.

Figure E10 shows the wide bandwidth recording of the responses of an independent binocular cell to contralateral and ipsilateral stimulation, again showing the occurrence of the spike potentials upon the negative slow waves.

Examination of the range of first spike latencies of both monocular and binocular unit responses (see Figure E2) shows that a number of units were isolated whose latency range was longer than that of the evoked field potentials (see Figure D17). This was especially true of ipsilateral responses, which showed a large spread of response latencies across the small population sampled. The variation of unit latencies with respect to the evoked field potential is shown by the next two figures, which illustrate the results obtained from a single penetration which sampled all four classes of unitary response.

Figure E11A shows the field potential waveforms recorded

FIGURE E9 IPSILATERAL FIELD AND UNIT POTENTIALS 1209-21-SN

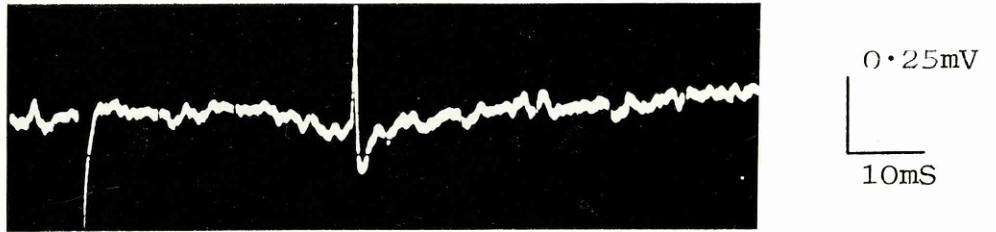
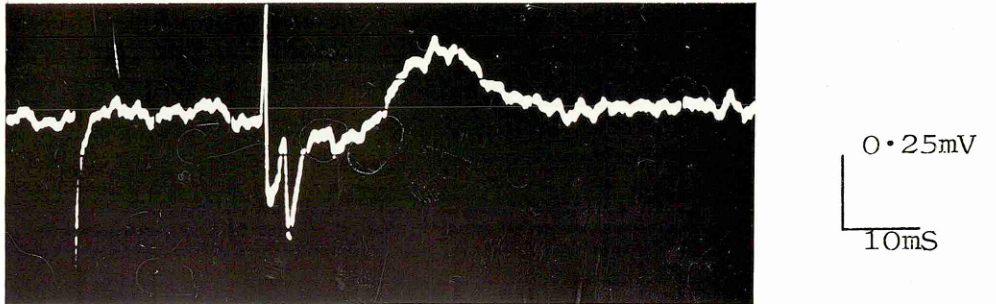
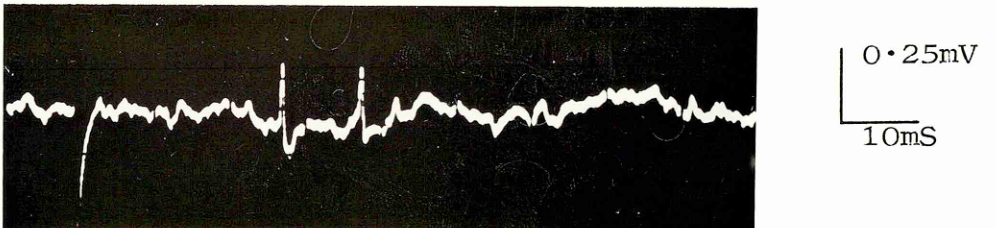


FIGURE E10 INDEPENDENT BINOCULAR FIELD AND UNIT  
POTENTIALS 1209-21-NN

A CONTRALATERAL

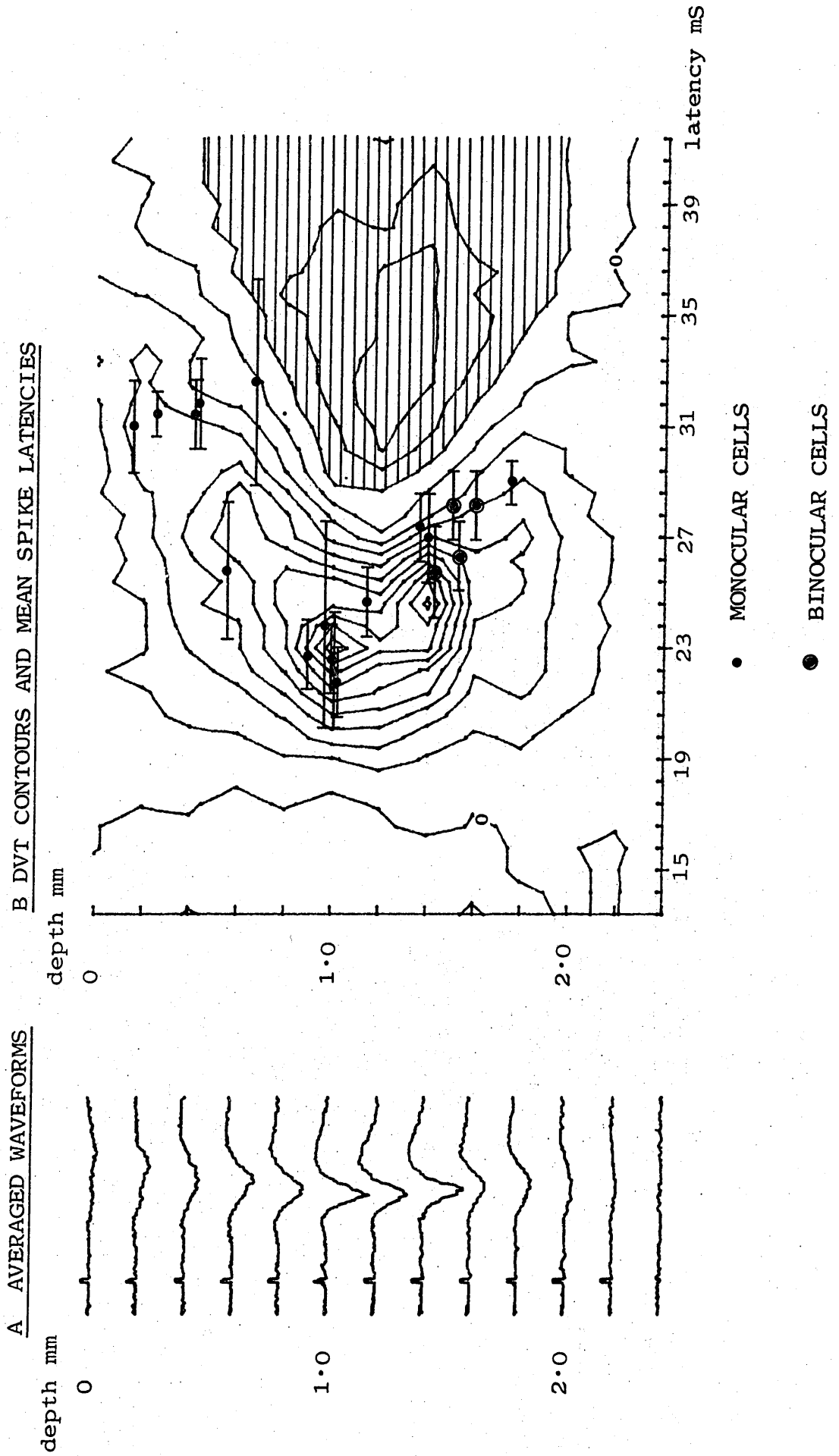


B IPSILATERAL



to contralateral stimulation. This penetration, made at orientation H1, samples only the late, superficial contralateral field potential located in HA. The electrode was advanced in  $2\mu$  steps to isolate unit responses, but at every 0.2mm the recording bandwidth was changed to obtain a record of the slow wave field potential response. The resistance of the electrode was relatively high, in order to obtain unit responses, and hence the waveforms are relatively 'spiky'. This is especially true of the waveforms recorded at 1.0 and 1.4mm below the brain surface - both of these field potentials show a unitary deflection on the negative wave peak. These deflections are reflected by the two apparent maxima present in the DVT contour plot (Figure E11B), located at 1.0 and 1.4mm. The mean spike latencies of contralateral responses recorded in this electrode penetration have been plotted upon the DVT contours. The latency of both exclusively contralateral responses, and of the contralateral response of binocular units, are shown. The standard deviation for each mean latency has been added as an index of the variability of each response. It can be seen that both the mean spike latencies and the variability of all the responses correlate very well with the spatiotemporal distribution of the evoked field potential negativity. Note that the binocular cells lie fairly deeply, between 1.4 and 1.8mm. The equivalent data from the same penetration to stimulation of the ipsilateral optic papilla are presented in Figure E12. A typically much smaller sample of units was isolated. Again, both monocular and binocular responses are plotted against the DVT contours. The depth

FIGURE E11 CORRELATION OF CONTRALATERAL UNIT AND FIELD POTENTIALS

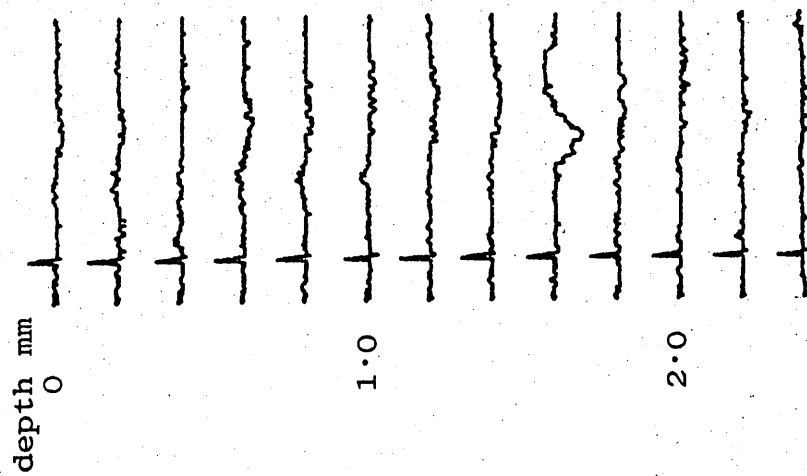


localisation of both classes of response correlate excellently with the depths of the field potential. Only two units, however, show latencies that lie within the temporal distribution of the field potential, the other four showing longer latencies typical of many of the ipsilateral units isolated.

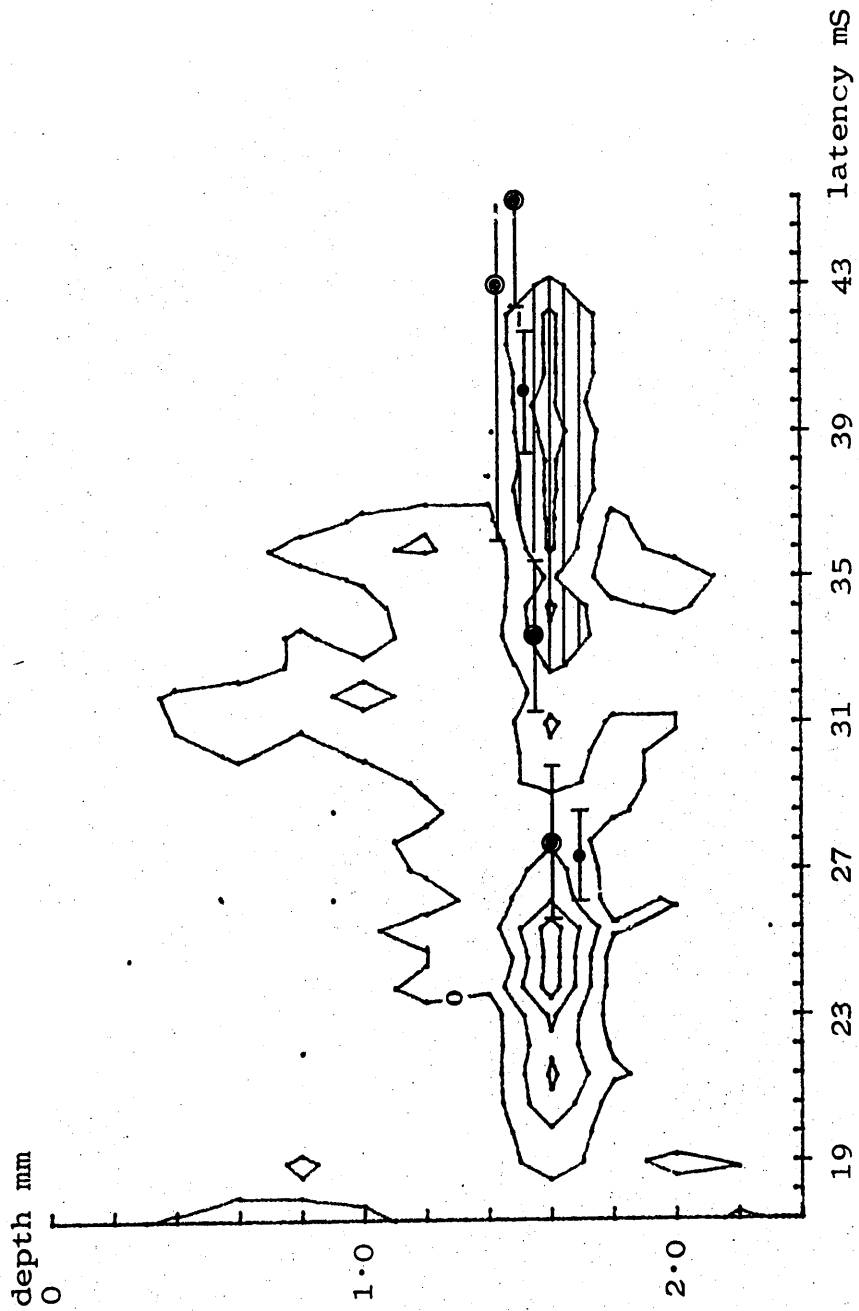
Finally, Figure E13 shows a combined plot of the second voltage contour of the contralateral and ipsilateral field potentials, together with the superimposed mean spike latency and standard deviation of the responses of the binocular cells from this sample. The contours show the relative position of the ipsilaterally responsive area to the superficial contralaterally responsive area sampled by this electrode penetration. The standard deviations indicate only one of the four binocular cells to show coincident contralateral and ipsilateral latencies, the other three cells showing typically varying degrees of temporal separation between the contralateral and ipsilateral responses.

FIGURE E12 CORRELATION OF IPSILATERAL UNIT AND FIELD POTENTIALS

A AVERAGED WAVEFORMS



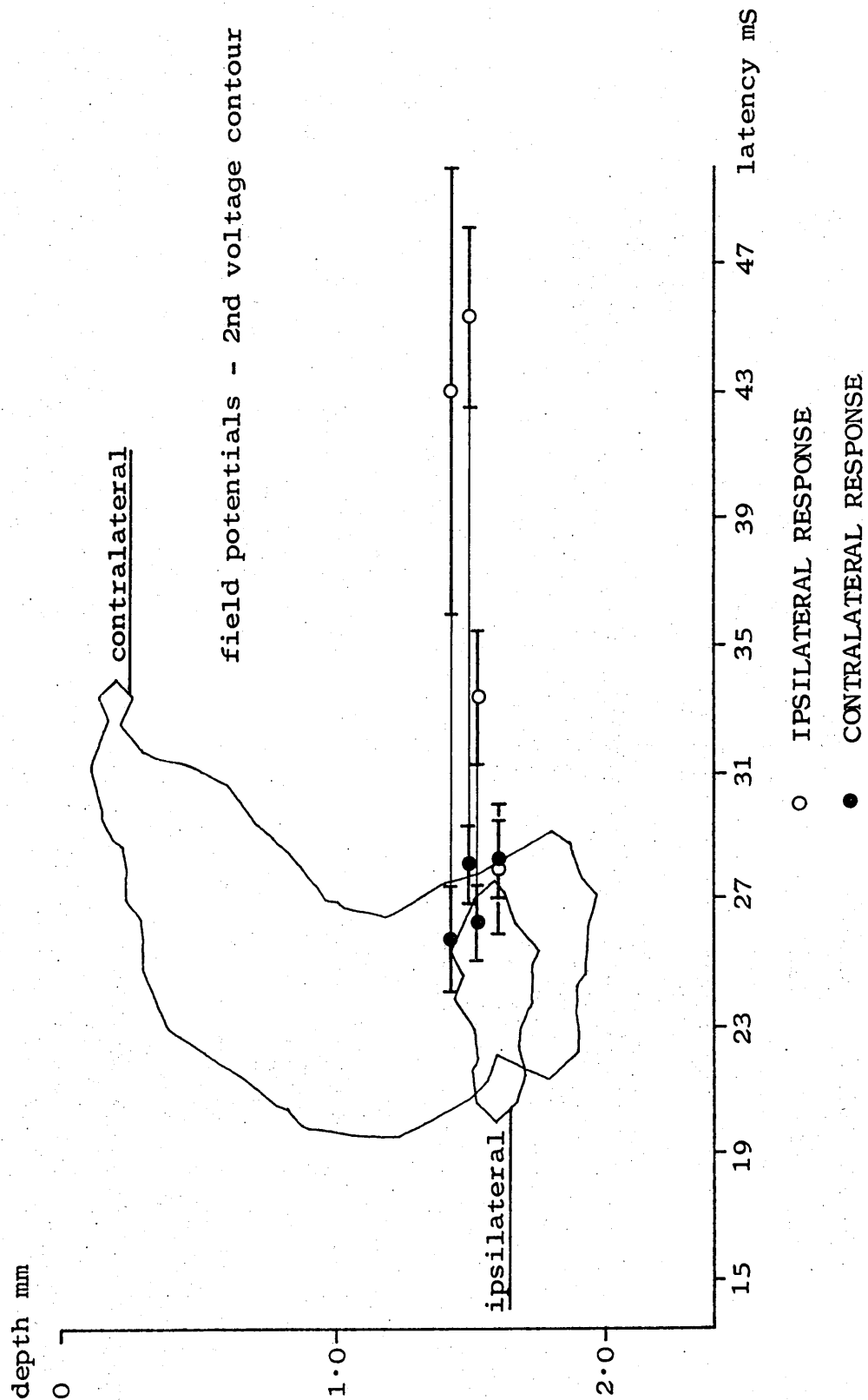
B DVT CONTOURS AND MEAN SPIKE LATENCIES



• MONOCULAR CELLS

• BINOCULAR CELLS

FIGURE E13 CORRELATION OF BINOCULAR UNITS AND FIELD POTENTIALS



### E3.5 SUMMARY OF SINGLE UNIT POTENTIALS

1. The responses of 220 single cells recorded from the Wulst were analysed. 123 (56%) cells responded to electrical stimulation of the optic papillae; 97 (44%) showed no response to the stimulation.
2. Four classes of responsive cell were identified: those responding exclusively to contralateral stimulation (85%); those responding exclusively to ipsilateral stimulation (3%); those responding to stimulation of both optic papillae with consistently different contralateral and ipsilateral response latencies (independent binocular, 8%); and those responding to stimulation of both optic papillae with identical contralateral and ipsilateral response latencies (coincident binocular, 4%).
3. Contralateral cells were located throughout HA and in IHA. Ipsilateral and binocular cells were located in ventral HA.
4. Examples of all four classes of cell could be recorded within the spatiotemporal limits of the negative field potentials described in Section D. First spike latency ranges were : monocular contralateral 9-54mS; monocular ipsilateral 16-157mS; binocular contralateral 10-96mS; binocular ipsilateral 20-153mS.
5. The first spike latency ranges indicated that a population of responsive cells existed whose latency exceeded that of the major negative deflection of the field potentials.



## CHAPTER E4 : DISCUSSION

The results obtained from the analysis of evoked single unit responses show the field potentials reported in Section D to have been obtained from hyperstriatal areas containing cells responsive to electrical stimulation of the optic papillae. From a total sample of 220 cells, 123 (56%) were found to respond to optic papilla stimulation. The large negative field potentials reported in Section D indicated a fairly synchronous burst of activity within the Wulst following electrical stimulation of the eye. However, although many evoked single units could be recorded at times coincident with the negative field potential, units with latencies longer than those of the field potentials could also be reliably driven by the stimulation (see Chapter E3.4). These results are interpreted to indicate

1. that there is a large population of synchronously active visual units within the Wulst that gives rise to the reproducible field potentials;
2. that there are also hyperstriatal and/or thalamic interneurons which introduce delays of the responses of some units;
3. the organisation of the visual input to the Wulst involves a 'concentrated' thalamo-receptive area (ie. IHA - see Section D) associated with a more 'diffuse' responsive cellular field (ie. HA - see Section D).

A large proportion (44%) of the cell sample isolated by the experiments reported in Section E failed to respond to

stimulation of the optic papillae. Revzin (1969a), recording from visual cells in the pigeon Wulst, similarly remarks upon the high proportion of non-visual cells found throughout the visually responsive area. In both the pigeon and the chicken, therefore, the visual projection to the Wulst is revealed by single unit sampling to be generally somewhat diffuse - the visually responsive population of neurons is not congregated in an exclusively visual area (except perhaps IHA/GL), but rather is dispersed amongst other cells of unknown affinities. Various reports in the literature indicate the Wulst to show afferent and efferent relationships other than those involved with the visual system. Adamo and King (1967) report evoked field potentials recorded from the chicken Wulst to auditory stimulation; Cohen and Pitts (1967) elicited head movements in the pigeon by stimulation of areas of the HA and superficial corticoid layer of the Wulst. Cardiac and respiratory changes were also noted in the pigeon by the latter authors subsequent to stimulation of these areas. The presence of multi-modal units in the Wulst has not yet been investigated.

Four classes of visual cell were identified in the present study: those responding exclusively to contralateral stimulation (85%); those responding exclusively to ipsilateral stimulation (3%); those responding to both contralateral and ipsilateral stimulation, and showing independent response latencies (8%); and those responding to both contralateral and ipsilateral stimulation with coincident latencies (4%).

Both ipsilateral and binocular cells were difficult to isolate, as indeed was the small, localised ipsilateral field potential - as such, the percentage sample of ipsilateral and binocular units may well be an underestimate of the population size. However, both field and unit potential studies reveal the ipsilateral and binocular inputs to the chicken Wulst to be very small when compared to the contralateral input. Figure E14 reproduces the data given in Figure E1B, and also compares the results obtained by the present study with those obtained by other workers investigating the pigeon and barn owl. Percentages are given to the nearest whole number.

FIGURE E14 PERCENTAGE OF CELL TYPES ISOLATED FROM CHICKEN, PIGEON AND BARN OWL WULST.

REFERENCE	MONOCULAR		BINOCULAR	
	contra	ipsi	independent	coincident
PRESENT STUDY (CHICKEN)	85	3	8	4
PERISIC ET AL, (1971) (PIGEON)	53	26	21	-
PETTIGREW AND KONISHI, (1976a) (BARN OWL)	9	8	72	simultaneous
				10

Perisic et al (1971) isolated a larger proportion of ipsilateral and binocular cells in the pigeon than found by the present study in the chicken, but did not identify any

binocular cells with coincident contralateral and ipsilateral response latencies. Comparison of the data obtained from the barn owl by Pettigrew and Konishi (1976a) with that obtained from the chicken and pigeon (Figure E14) shows a massive increase in the percentage of binocular cells found in the owl Wulst. Reflecting the large overlap of the contralateral and ipsilateral visual fields in the owl, the large binocular population was found to include cells requiring simultaneous stimulation of both eyes to elicit a response. They classified these cells as 'binocular disparity-selective': each cell showed a distinct preference for the degree of relative retinal alignment of the two images of the stimulus.

Although the spatiotemporal pattern of contralateral and ipsilateral field potentials in the chicken indicates the possibility of the integration of binocular information in the Wulst (see Section D), it is difficult to assess exactly what information some of the independent group of binocular cells are processing - the ipsilateral response latencies of some of these cells were up to 60ms longer than the equivalent contralateral latencies. Even larger populations of this group of cells were found in the pigeon and owl. However, the coincident group of chicken binocular cells, having identical contralateral and ipsilateral response latencies, may be comparable to the binocular disparity group of cells isolated by Pettigrew and Konishi (1976) in the owl HA, even though the chicken cells did not require simultaneous stimulation in order to respond.

Assuming that the visual input to the chicken thalamus is completely crossed (see Section A, Chapter A2.1), then the appropriate delay in the contralateral pathway of the coincident binocular cells, required to match the delay due to the longer ipsilateral pathway, could be due either to thalamic or hyperstriatal circuitry. As the contralateral response latency of the coincident binocular cells lies within the superficial, late contralateral field potential range (see Figures E11 and E13), then it is possible that this contralateral delay is due to transmission via interneurons between IHA and the regions of HA which exhibit the late responses. Furthermore, the longer ipsilateral response latencies of the independent binocular group are presumably due to extra thalamic delays over and above the delay due to the longer ipsilateral pathway - however, although the field potential studies indicate only one area of ipsilateral activity in the Wulst, in ventral HA near the HA/IHA border (see Section D, Chapter D4), it is of course possible that there is circuitry, not being revealed in the small ipsilateral field potentials, contributing to the very long delay of some of the independent binocular ipsilateral responses.

SECTION F : OVERVIEW

The field potential and single unit responses presented and discussed in Sections D and E of this thesis provide a comprehensive description of the spatial organisation and extent of the visual projection area in the Wulst of the young chicken. The retino-Wulst projection was found to be topographically organised - the inferior retina projected to posterior regions of the Wulst, whereas the superior retina projected to anterior regions of the Wulst. As discussed in Section D, Chapter D6, this relationship is identical to that found by Pettigrew and Konishi (1976a) in the barn owl. These authors also describe a topographic relationship between the nasal retina and medial Wulst, and between the temporal retina and lateral Wulst. No evidence was found in the present study for such a relationship between the lateral axis of the retina and the Wulst in the chicken. Instead, anterior (nasal) and posterior (temporal) regions of the retina were found to be represented at different locations along a vertical axis through the Wulst. This spatial arrangement contributed to a complex dorsoventral lamination of monocular and binocular visual inputs to the hyperstriatal laminae of the Wulst - these results are summarised below.

Contralateral responses were localised throughout all but the most ventral regions of HA, and in IHA. Ipsilateral responses were located in ventral HA, just dorsal to the HA/IHA border, and overlapping the ventral portion of the contralaterally responsive region of HA. Binocular responses were also located in this ventral region. No visual evoked responses were obtained from HISm, or the anterior regions of HD and

HV which lie beneath the visually responsive areas of HA and IHA.

Within this lamination of inputs, the contralateral responses were found to show further complexities of organisation. Firstly, two latency populations of response were identified. The earliest responses recorded were always located in IHA and on the HA/IHA border. These responses were interpreted as representing the first activity within the hyperstriatal complex to occur after electrical stimulation of the eye, and to thus indicate that IHA is the major thalamo-receptive lamina of the Wulst. (However, it should be remembered that the present results cannot eliminate the possibility that HA also receives a direct thalamic input). Later responses were found subsequently to spread laterally and posteriorly throughout dorsal regions of HA, and to indicate the presence of collateral and/or interneuron circuitry within the HA visual projection area.

Secondly, a topographical relationship was established between the anterior-posterior (nasal-temporal) axis of the retina and the dorsoventral axis of the Wulst. Stimulation of both anterior and posterior retina resulted in early responses in IHA and late responses in HA - however, the late HA responses to stimulation of the posterior retina were always located ventrally to the late HA responses which followed stimulation of the anterior retina. Posterior and anterior early responses were located in similar regions of IHA, although the posterior IHA response was occasionally



recorded dorsally to the anterior IHA response.

The dorsoventral lamination of the monocular and binocular inputs to the chicken Wulst is very different to that reported for the pigeon. Perisic et al (1971) recorded field and unit potentials from the pigeon Wulst in response to electrical stimulation of the contralateral and ipsilateral optic papillae. They found the potentials to follow the spatial organisation shown in Figure F1D - the present results from the chicken are summarised in Figure F1F. Contralateral responses were recorded from the pigeon dorsal HA, whilst ipsilateral responses were located in ventral HA, throughout HIS, and in dorsal regions of HD. Ventral HA areas, therefore, were shown to receive input from both eyes, and to contain binocular cells responding to stimulation of both optic papillae, as well as exclusively ipsilateral cells. A larger proportion of ipsilateral (26%) and binocular (21%) cells were isolated by Perisic et al (1971) than were isolated by the present study (ipsilateral 3%, binocular 12%; see Section E), and these authors were able to distinguish between the locations of the ipsilateral and binocular unit populations. Thus, the exclusively ipsilateral cells were located ventral to the binocular region of HA. (The ventral region of the chicken HA is shown in Figure F1F to be responsive to binocular '+' ipsilateral stimulation, indicating that no distinction has been made between the locations of the two response populations).

However, no distinction is made between early and late

responses by Perisic et al (1971), and thus the location of a specific thalamo-receptive region in the pigeon Wulst is unclear from this study. Although HA appears to show a similar spatial organisation of responses in the pigeon and chicken from a comparison of these two studies, it should be remembered that the chicken contralateral region of HA only exhibits late, 'secondary' responses. Furthermore, no ipsilateral responses were obtained from the chicken intercalated nucleus, or from HD.

It may, however, be premature to make any definitive statement about the differences between the results reported for the pigeon by Perisic et al (1971), and the results found by the present study of the chicken. A true inter-species difference in the organisation of the retino-Wulst projection may exist. The general pattern of contralateral-binocular-ipsilateral inputs to the pigeon Wulst has been confirmed anatomically by Miceli et al (1975), who investigated the retrograde transport of HRP injected into areas of the Wulst (although they could not distinguish HA from HIS, or HD from HIS and HA, due to HRP spread from the injection sites). However, the pattern of inputs described by Perisic et al (1971) is not in accord with other reports in the literature. Hunt (1974) found no anatomical evidence for the overlap of contralateral and ipsilateral inputs to the pigeon HA that could account for the binocular field - he does suggest, however, that intra-telencephalic collaterals may exist to provide such a field. Unfortunately, a detailed analysis of the neural connectivity within the

Wulst of any avian species is lacking. Furthermore, Hunt and Webster (1972), studying retrograde degeneration of the thalamus following Wulst lesions, found the pigeon HIS to receive a bilateral input (see Figure F1A - although Hunt (1974) restricts this bilateral region to the granule layer of HIS), whereas Perisic et al (1971) found HIS to be responsive only to ipsilateral stimulation. (These latter authors do not identify the granule layer).

Similarly, Karten et al (1973), using the Fink-Heimer method to study terminal degeneration in the pigeon Wulst following lesions of OPT, found the granule layer (and HD to a lesser extent) to receive a bilateral input from OPT, but HA to receive no primary visual thalamic input (see Figure F1B). It should be noted that Karten et al (1973) could only interpret the degeneration patterns in the pigeon in the light of results obtained from the burrowing owl in the same study (see Figure F1C). They also refer to the granule layer of the pigeon as IHA, to denote its correspondence with the owl thalamic terminal field (IHAIN and IHAEX).

It would therefore seem prudent to await further studies of the electrophysiology of the pigeon Wulst, especially of the intercalated nucleus, and a study of the thalamo-hyperstriate organisation in the chicken, before concluding major differences between the thalamofugal projections of these two species.

Conversely, comparison of the present results obtained from

the chicken with those obtained from the barn owl by Pettigrew and Konishi (1976a) reveals some similarities between the organisation of the thalamofugal pathway in these two species. Figure F1E presents a summary of the spatial organisation of the cells described by Pettigrew and Konishi (1976a). Recording single unit responses to visual stimulation of both eyes, they found cells in the superficial Wulst to be binocular, and to have complex receptive field properties, requiring precise conditions of stimulus orientation, direction and velocity. These stimulus requirements and receptive field properties became 'simpler' in deeper parts of HA. Cells recorded from IHA, however, were monocular, and could be mapped into simple antagonistic regions. They also isolated cells with similar properties to those in IHA from the dorsolateral thalamus (OPT); this strongly suggests that IHA is the thalamo-receptive layer of the barn owl Wulst, and that 'higher' levels of processing occur in the more superficial HA. (Anatomical support is provided for this hypothesis by Karten et al (1973), who found OPT of the burrowing owl to project mainly to IHA, but not to HA). Furthermore, IHA receives a monocular input in both the barn owl and the chicken, whilst HA receives a binocular input.

Interestingly, the exclusively contralateral input to the barn owl hyperstriatum was located in IHA<sub>in</sub>, whilst the exclusively ipsilateral input was located in IHA<sub>ex</sub>, lying dorsal to IHA<sub>in</sub>. An identical pattern of inputs was found in the chicken, although no equivalent bilaminar

organisation of IHA could be observed in Nissl preparations of the chicken Wulst. However, the absence of a prominent cellular lamination corresponding with the ipsilaterally responsive area of the chicken hyperstriatum may simply reflect the small size of the ipsilateral projection to this region. Hence, the layer termed IHA in the present study may be both structurally and functionally equivalent to the owl IHA<sub>in</sub>. Similarly, an indistinct layer of cells, lying dorsal to the chicken IHA/HA border and receiving a primary thalamic ipsilateral input, may be equivalent to the owl IHA<sub>ex</sub>.

From studies of the chicken, pigeon and owl thalamofugal pathway, then, is it possible to discern a common plan of the organisation of this pathway in birds? The summary of results presented in Figure F1 indicates the difficulties involved in attempting to answer this question. It should be noted that the lack of visual input to HA suggested by Figures F1B and C is presumably due to the nature of the anterograde degeneration methods used by Karten et al (1973) - the results cannot preclude a 'secondary' visual terminal field in HA (but note that a primary thalamic projection to pigeon HA was revealed by the retrograde degeneration studies of Hunt and Webster (1972), as shown in Figure F1A). However, the various reports also do not provide a consistent picture of the primary visual thalamic terminations in the avian Wulst. A functional correspondence seems to exist between the owl IHA and the chicken granular layer termed IHA in the present study - it is difficult to identify the equivalent pigeon nucleus, however, due to the conflicting anatomical

FIGURE F1 : SUMMARY OF THE SPATIAL ORGANISATION OF VISUAL  
INPUTS TO THE AVIAN WULST

(IN=intercalated nucleus)

ANATOMICAL STUDIES

PHYSIOLOGICAL STUDIES

A Hunt and Webster (1972)

D Perisic et al (1971)

PIGEON

PIGEON



HA	CONTRALATERAL
IN	IPSILATERAL + CONTRALATERAL
HD	IPSILATERAL + CONTRALATERAL

HA	CONTRALATERAL binocular IPSILATERAL
IN	IPSILATERAL
HD	IPSILATERAL

B Karten et al (1973)

E Pettigrew & Konishi (1976a)

PIGEON

BARN OWL

HA	-
IN	IPSILATERAL + CONTRALATERAL
HD	IPSILATERAL + CONTRALATERAL

HA	binocular
IN	IPSILATERAL CONTRALATERAL
HD	-

C Karten et al (1973)

F Present study

BURROWING OWL

CHICKEN

HA	-
IN	IPSILATERAL + CONTRALATERAL
HD	IPSILATERAL + CONTRALATERAL

HA	CONTRALATERAL binocular + IPSILATERAL
IN	CONTRALATERAL
HD	-



= suggested primary thalamic input

and physiological reports in the literature (eg. Karten et al (1973), Figure F1B, and Perisic et al (1971), Figure F1D). On anatomical grounds alone, assuming a common plan with the chicken and barn owl, the thalamo-receptive area of the pigeon Wulst should be located in the granule layer of the intercalated nucleus associated with LFM (as suggested by Karten et al (1973)). At present, there exists no experimental physiological evidence for this hypothesis, and therefore it should not be assumed that any single species is either typical or representative of the avian class.

The finding in the present study that the contralateral input to the chicken Wulst is distributed between at least two separate cellular populations, located in IHA and HA respectively, receives indirect confirmation from a study by Brown and Horn (1977). They recorded multiple unit responses, to flash stimuli, from the Wulst of one day old chickens, and compared the results obtained from a group of dark-reared animals with those from a group of visually-experienced animals. The environmental manipulation was found to affect responses recorded from HA, the dark-reared chickens showing a significantly smaller number of responsive sites in HA than the visually-experienced group. However, lack of visual experience did not affect the responses in deeper parts of the Wulst, in the "hyperstriatum intercalatus" and HD - both groups showed similar responses, described as "very brisk and more consistent than those in HA", in these laminae.

These results suggest an organisation of the chicken Wulst that is very reminiscent of the pattern of the visual inputs to the chicken Wulst suggested by the present study - thalamic input to the deep lying IHA, with further processing in the superficial HA. Furthermore, the results of Brown and Horn (1977) indicate the responsiveness of HA to be dependent upon visual experience. They suggest that the effects could be the result of "increased synaptic effectiveness". It is unclear whether the whole of the area of HA shown by the present study to receive visual input is affected by visual experience, as Brown and Horn only made one electrode penetration in the anterior Wulst of each chicken. The critical period within which such modifications of responsiveness can occur is unknown.

A complete understanding of the functional and structural relationships indicated by the present study within the retino-Wulst projection of the chicken requires much further investigation. The immediate tasks would require an investigation of the cytoarchitecture of the hyperstriatal complex, and both anatomical and physiological studies of thalamo-hyperstriate relationships in the chicken.

Whether the cells of the superficial HA of the chicken Wulst parallel those of the owl, and show more complex stimulus requirements than those of IHA, is unknown. However, single cell recordings made in the early stages of this study did reveal the superficial HA cells of the chicken to show marked preferences for stimulus direction and velocity, and



it was not possible to map the receptive fields of these cells into antagonistic areas. Cells from the chicken IHA region have not yet been sampled using visual stimulation.

The field and unit potential results reported in this thesis indicate that an area of the chicken ventral HA shows the capacity for the processing of binocular visual information. Whether the posterior retina of the chicken shows any structural specialisation related to the frontal binocular field, as in the pigeon (Bingelli and Paule, 1969), remains to be investigated. Further clarification of the nature of the chicken's binocular capacity will require single unit studies of the characteristics of cells whose receptive fields lie in the frontal visual field.

SECTION G : REFERENCES

REFERENCES

- ADAMO, N.J. AND KING, R.L. (1967): Evoked responses in the chicken telencephalon to auditory, tactile and visual stimulation. *Exp. Neurol.* 17: 498-504
- BAGNOLI, B., FRANCESCONI, W. AND MAGNI, F. (1977): Visual Wulst influences on the optic tectum of the pigeon. *Brain Behav. Evolut.* 14: 217-237
- BATESON, P.P.G., HORN, G. AND ROSE, S.P.R. (1975): Imprinting: correlations between behaviour and incorporation of <sup>14</sup>C uracil into chicken brain. *Brain Research* 84: 207-220
- BAYLE, J.D., RAMADE, F. AND OLIVER, J. (1974): Stereotaxic topography of the brain of the quail. *J. Physiol. (Paris)* 68(2): 219-241
- BENNER, J. (1938): Untersuchungen über die Raumwahrnehmung der Hühner. *Z. Wissensch. Zool.* 151: 382
- BILGE, M. (1971): Electrophysiological investigations on the pigeon's optic tectum. *Q. J. Exp. Physiol.* 56: 242-249
- BINGELLI, R.L. AND PAULE, W.J. (1969): The pigeon retina: quantitative aspects of the optic nerve and ganglion cell layer. *J. Comp. Neurol.* 137: 1-18
- BLÜMCKE, S. (1961): Vergleichend experimentell-morphologische Untersuchungen zur Frage einer retino-hypothalamischen Bahn bei Huhn, Meerschweinchen und Katze. *Z. Zellforsch.* 67: 469-513
- BRADLEY, P. AND HORN, G. (1978): Afferent connections of the hyperstriatum ventrale in the chick brain. *J. Physiol.* 275: 53P

- BRAUTH, S.E. AND KARTEN, H.J. (1977): Direct accessory optic projections to the vestibular cerebellum: a possible channel for oculomotor control systems. *Exp. Brain Res.* 28: 73-84
- BROWN, M.W. AND HORN, G. (1978): Effects of visual experience on unit responses in hyperstriatum of chick brain. *J. Physiol.* 275: 55P
- BURGER, R.E. AND LORENZ, F.W. (1960): Artificial respiration in birds by unidirectional air flow. *Poultry Sci.* 39: 236-237
- COHEN, D.H. AND KARTEN, H.J. (1974): The structural organisation of the avian brain. In: I.J. GOODMAN AND M.W. SCHEIN (eds), "Birds, brain and behaviour". Academic Press, New York.
- COHEN, D.H. AND PITTS, L.H. (1967): The hyperstriatal region of the avian forebrain: somatic and autonomic responses to electrical stimulation. *J. Comp. Neurol.* 131: 323-336
- COWAN, W.M. (1970): Centrifugal fibres to the avian retina. *Br. med. Bull.* 26: 112-118
- COWAN, W.M., ADAMSON, L. AND POWELL, T.P.S. (1961): An experimental study of the avian visual system. *J. Anat.* 95: 545-563
- COWAN, W.M. AND POWELL, T.P.S. (1963): Centrifugal fibres in the avian visual system. *Proc. roy. Soc. B.* 158: 232-252
- DE BRITTO, L.R.G., BRUNELLI, M., FRANCESCONI, W. AND MAGNI, F. (1975): Visual response pattern of thalamic neurons in the pigeon. *Brain Research* 97: 337-343
- DE LONG, G.R. AND COULOMBRE, A.J. (1965): Development of the retinotectal topographic projection in the chick embryo. *Exp. Neurol.* 13: 351-363

- DISBREY, B.D. AND RACK, J.H. (1970): "Histological laboratory methods." E. and S. Livingstone, Edinburgh.
- EBBESSON, S.O.E. (1972): A proposal for a common nomenclature for some optic nuclei in vertebrates and the evidence for a common origin of two such cell groups. *Brain, Behav. Evol.* 6: 75-91
- GOTHARD, E. (1898): Quelques modifications au procédé de Nissl, pour la coloration élective des cellules nerveuses. *C.r. Séanc. Soc. Biol.* 5: 530
- HAMDI, F.A. AND WHITTERIDGE, D. (1954): The representation of the retina on the optic tectum of the pigeon. *Quart. J. Exp. Phys. Cog. Med. Sci.* 39: 111-119
- HELLON, R.F. (1971): The marking of electrode tip positions in nervous tissue. *J. Physiol.* 214: 12P
- HIRSCHENBERGER, W. (1967): Histologische Untersuchungen an den primären visuellen Zentren des Eulengehirnes und der retinal Repräsentation in ihnen. *J. für Ornith.* 108 187-202
- HOLDEN, A.L. (1966): Two possible visual functions for centrifugal fibres to the retina. *Nature* 212: 837-838
- HOLDEN, A.L. (1968a): The field potential profile during activation of the avian optic tectum. *J. Physiol.* 194: 75-90
- HOLDEN, A.L. (1968b): Types of unitary response and correlation with the field potential profile during activation of the avian optic tectum. *J. Physiol.* 194: 91-104
- HOLDEN, A.L. (1968c): Antidromic activation of the isthmo-optic nucleus. *J. Physiol.* 197: 183-198

- HOLDEN, A.L. (1968d): The centrifugal system running to the pigeon retina. *J. Physiol.* 197: 199-219
- HOLDEN, A.L. AND POWELL, T.P.S. (1972): The functional organisation of the isthmo-optic nucleus in the pigeon. *J. Physiol.* 223: 419-447
- HORN, G., ROSE, S.P.R. AND BATESON, P.P.G. (1973): Monocular imprinting and regional incorporation of tritiated uracil into the brains of intact and 'split-brain' chicks. *Brain Research* 56: 227-237
- HUBER, G.C. AND CROSBY, E.C. (1929): The nuclei and fibre paths of the avian diencephalon, with a consideration of telencephalic and mesencephalic connections. *J. Comp. Neurol.* 48: 1-225
- HUGHES, G.M. (1963): "Comparative physiology of vertebrate respiration". Heinemann Educational Books Ltd., London.
- HUNT, S.P. (1974): A study of forebrain visual areas in the pigeon. Unpublished PhD thesis. University College, London.
- HUNT, S.P. AND WEBSTER, K.E. (1972): Thalamo-hyperstriate interrelations in the pigeon. *Brain Research* 44: 647-651
- JASSIK-GERSCHENFELD, D., TEULON, J., ROPERT, N. AND BAROIS, A. (1975): Visual receptive field properties of single cells in the nucleus dorsolateralis anterior of the pigeon. *Exp. Brain Res.* 23(Supp): 99
- JASSIK-GERSCHENFELD, D., TEULON, J. AND ROPERT, N. (1976): Visual receptive field types in the nucleus dorsolateralis anterior of the pigeon's thalamus. *Brain Research* 108: 295-305
- KAPPERS, C.U.A., HUBER, G.C. AND CROSBY, E.L. (1936): "The comparative anatomy of the nervous system in vertebrates including man." MacMillan (1960 reprint, Hafner, New York)

- KARTEN, H.J. (1965): Projections of the optic tectum in the pigeon. *Anat. Rec.* 151: 369
- KARTEN, H.J. (1969): The organisation of the avian telencephalon and some speculations on the phylogeny of the amniote telencephalon. *Ann. N.Y. Acad. Sci.* 167: 164-179
- KARTEN, H.J. (1971): Efferent projections of the Wulst of the owl. *Anat. Rec.* 169: 353
- KARTEN, H.J. AND FINGER, T.E. (1976): A direct thalamo-cerebellar pathway in pigeon and catfish. *Brain Research* 102: 335-338
- KARTEN, H.J. AND HODOS, W. (1967): "A stereotaxic atlas of the brain of the pigeon (Columba livia).". John Hopkins University Press, Baltimore.
- KARTEN, H.J. AND HODOS, W. (1970): Telencephalic projections of the nucleus rotundus in the pigeon (Columba livia). *J. Comp. Neurol.* 140: 35-52
- KARTEN, H.J., HODOS, W., NAUTA, W.J.H. AND REVZIN, A.M. (1973): Neural connections of the visual Wulst of the avian telencephalon. Experimental studies in the pigeon (Columba livia) and owl (Speotyto cunicularia). *J. Comp. Neurol.* 150: 253-278
- KARTEN, H.J. AND NAUTA, W.J.H. (1968): Organisation of retinothalamic projections in the pigeon and owl. *Anat. Rec.* 160: 373
- KARTEN, H.J. AND REVZIN, A.M. (1966): The afferent connections of the nucleus rotundus in the pigeon. *Brain Research* 2: 368-377
- KIMBERLY, R.P., HOLDEN, A.L. AND BAMBOROUGH, P. (1971): Response characteristics of pigeon forebrain cells to visual stimulation. *Vision Res.* 11: 475-478

- KNOWLTON, V.Y. (1964): Abnormal differentiation of embryonic avian brain centres associated with unilateral anopthalmia. *Acta. anat.* 58: 222-251
- LA VAIL, J.H. AND LA VAIL, M.M. (1972): Retrograde axonal transport in the central nervous system. *Science* 176: 1416-1417
- LA VAIL, J.H., WINSTON, K.R. AND TISH, A. (1973): A method based on retrograde intra-axonal transport of protein for identification of cell bodies or origin of axons terminating within the central nervous system. *Brain Research* 58: 470-471
- LUMB, W.V. AND JONES, E.W. (1973): "Veterinary anesthesia." Lea and Febiger, Philadelphia.
- MCGILL, J.I. (1964): Organisation within the central and centrifugal pathways in the avian visual system. *Nature* 204: 395-396
- MCGILL, J.I., POWELL, T.P.S. AND COWAN, W.M. (1966a): The retinal representation upon the optic tectum and isthmo-optic nucleus in the pigeon. *J. Anat.* 100: 1-33
- MCGILL, J.I., POWELL, T.P.S. AND COHEN, W.M. (1966b): The organisation of the projection of the centrifugal fibres to the retina in the pigeon. *J. Anat.* 100: 35-49
- MEIER, R.E. (1973): Autoradiographic evidence for a direct retino-hypothalamic projection in the avian brain. *Brain Research* 53: 417-421
- MEIER, R.E., MIHAILOVIC, J. AND CUENOD, M. (1974): Thalamic organisation of the retino-thalamo-hyperstriatal pathway in the pigeon (*Columba livia*). *Exp. Brain Res.* 19: 351-364



- MEIER, R.E., MIHAILOVIC, J., PERISIC, M. AND CUENOD, M.  
(1972): The dorsal thalamus as a relay in the visual pathways of the pigeon. *Experientia* 28: 730
- MICELI, D., PEYRICHOUX, J. AND REPERANT, J. (1975): The retino-thalamo-hyperstriatal pathway in the pigeon. *Brain Research* 100: 125-131
- MIHAILOVIC, J., PERISIC, M., BERGONZI, R. AND MEIER, R.E.  
(1974): The dorsolateral thalamus as a relay in the retino-Wulst pathway in pigeon (Columba livia). *Exp. Brain Res.* 21: 229-240
- MILES, F.A. (1970): Centrifugal effects in the avian brain. *Science* 170: 992-995
- MILES, F.A. (1971): Visual responses of centrifugal neurons to the avian retina. *Brain Research* 25: 411-415
- MILES, F.A. (1972a): Centrifugal control of the avian retina I. Receptive field properties of retinal ganglion cells. *Brain Research* 48: 65-92
- MILES, F.A. (1972b): Centrifugal control of the avian retina II. Receptive field properties of cells in the isthmo-optic nucleus. *Brain Research* 48: 93-113
- MILES, F.A. (1972c): Centrifugal control of the avian retina III. Effects of electrical stimulation of the isthmo-optic tract on the receptive field properties of retinal ganglion cells. *Brain Research* 48: 115-129
- MILES, F.A. (1972d): Centrifugal control of the avian retina IV. Effects of reversible cold block of the isthmo-optic tract on the receptive field properties of cells in the retina and isthmo-optic nucleus. *Brain Research* 48: 131-145
- MORI, S. (1973): Analysis of field response in optic tectum of the pigeon. *Brain Research* 54: 193-206

- MORI, S. AND MITARAI, G. (1974): Late field responses in optic tectum of the pigeon. *Brain Research* 65: 525-528
- NAUTA, W.J.H. AND KARTEN, H.J. (1970): A general profile of the vertebrate brain with sidelights on the ancestry of cerebral cortex. In: F.O. SCHMITT (ed), "Neurosciences 2nd study programme." Rockefeller University Press, New York.
- OKSCHE, A. (1970): Retino-hypothalamic pathways in mammals and birds. In: J. BENOIT AND I. ASSENMACHER (eds), "La photorégulation de la reproduction chez les oiseaux et les mammifères. Coll. int. C.N.R.S. 172." C.N.R.S., Paris.
- O'LEARY, J.L. AND BISHOP, G.H. (1943): Analysis of potential sources in the optic lobe of duck and goose. *J. Cell. Comp. Physiol.* 22: 73-87
- PAGE, K.M. (1965): A stain for myelin using solochrome cyanin. *J. med. Lab. Technol.* 22: 224
- PARKER, D.M. AND DELIUS, J.D. (1972): Visual evoked potentials in the forebrain of the pigeon. *Exp. Brain Res.* 14: 198-209
- PEACOCK, H.A. (1966): "Elementary microtechnique". Edward Arnold, London.
- PERISIC, M., MIHAJLOVIC, J. AND CUENOD, M. (1971): Electrophysiology of contralateral and ipsilateral visual projections to the Wulst in pigeon (Columba livia). *Int. J. Neurosci.* 2: 7-14
- PETTIGREW, J.D. AND KONISHI, M. (1976a): Neurons selective for orientation and binocular disparity in the visual Wulst of the barn owl (Tyto alba). *Science* 193: 675-678
- PETTIGREW, J.D. AND KONISHI, M. (1976b): Effect of monocular deprivation on binocular neurons in the owl's visual Wulst. *Nature* 264: 753-754

- POLYAK, S.L. (1941): "The retina." University of Chicago Press, Chicago.
- POWELL, T.P.S. AND COWAN, W.M. (1961): The thalamic projection upon the telencephalon in the pigeon (Columba livia). J. Anat. 95: 78-109
- REVZIN, A.M. (1969a): A specific visual projection area in the hyperstriatum of the pigeon. Brain Research 15: 246-249
- REVZIN, A.M. (1969b): Some characteristics of a visual projection area in the hyperstriatum of the owl (Speotyto cunicularia). Fed. Proc. 28: 395
- REVZIN, A.M. (1970): Some characteristics of wide-field units in the brain of the pigeon. Brain Behav. Evol. 3: 195-204
- REVZIN, A.M. AND KARTEN, H.J. (1967): Rostral projections of the optic tectum and the nucleus rotundus in the pigeon. Brain Research 3: 264-276
- ROBERT, F. AND CUENOD, M. (1969a): Electrophysiology of the intertectal commissures in the pigeon. I. Analysis of the pathways. Exp. Brain Res. 9: 116-122
- ROBERT, F. AND CUENOD, M. (1969b): Electrophysiology of the intertectal commissures in the pigeon. II. Inhibitory interaction. Exp. Brain Res. 9: 123-136
- ROGERS, L.J. AND MILES, F.A. (1972): Centrifugal control of the avian retina V. Effects of lesions of the isthmo-optic nucleus on visual behaviour. Brain Research 48: 147-156
- ROSE, S.P.R., HAMBLEY, J. AND HAYWOOD, J. (1974): Neurochemical approaches to developmental plasticity and learning. Paper for Asilomar Conference "Neural mechanisms of learning and memory." June, 1974.

- SALZEN, E.A., PARKER, D.M. AND WILLIAMSON, A.J. (1975): A forebrain lesion preventing imprinting in domestic chicks. *Exp. Brain Res.* 24: 145-157
- SAUNDERS, J.T. AND MANTON, S.M. (1969): "A manual of practical vertebrate morphology." Clarendon Press, Oxford. (4th edition, revised by S.M. Manton and M.E. Brown)
- SEDLACEK, J. (1970): The optic projection in brain hemispheres of chick embryo. *Physiologia Bohemoslovaca* 19: 197-204
- SOMA, L.R. (1971): "Textbook of veterinary anesthesia." Williams and Wilkins.
- STOKES, T.M., LEONARD, C.M. AND NOTTEBOHM, F. (1974): The telencephalon, diencephalon and mesencephalon of the canary, *Serinus canaria*, in stereotaxic coordinates. *J. Comp. Neurol.* 156: 337-374
- STONE, J. (1973): Sampling properties of microelectrodes assessed in the cat's retina. *J. Neurophys.* 36: 1071-1079
- STONE, J. AND FREEMAN, J.A. (1971): Synaptic organisation of the pigeon's optic tectum: a Golgi and current source-density analysis. *Brain Research* 27: 203-221
- STURKIE, P.D. (1965): "Avian physiology." Cornell University Press, New York.
- THOMAS, R.C. AND WILSON, V.J. (1965): Precise localisation of Renshaw cells with a new marking technique. *Nature* 206: 211-213
- VAN TIENHOVEN, A. (1970): Neurophysiological approach to photosexual relationships in birds. In: J. BENOIT AND I. ASSENMACHER (eds), "La photorégulation de la reproduction chez les oiseaux et les mammifères. Colloque int. C.N.R.S. 172." C.N.R.S., Paris.

- VAN TIENHOVEN, A. AND JUHASZ, L.P. (1962): The chicken telencephalon, diencephalon and mesencephalon in stereotaxic coordinates. *J. Comp. Neurol.* 118: 185-187
- VONEIDA, T.H. AND MELLO, N.K. (1975): Interhemispheric projections of the optic tectum in pigeon. *Brain, Behav. Evol.* 11: 91-108
- WEBSTER, K. (1974): Changing concepts of the organisation of the central visual pathways in birds. In: R. BELLAIRS AND E.G. GRAY (eds), "Essays on the nervous system." Oxford University Press, Oxford.
- YOUNGREN, O.M. AND PHILLIPS, R.E. (1978): A stereotaxic atlas of the brain of the three-day-old chick. *J. Comp. Neurol.* 181: 567-600